

**A novel approach for investigating the tendinous and capsular layers of
the rotator cuff complex: A biomechanical study**

by

Jessica Y Cronjé

Submitted in fulfilment of the requirements for the degree:

M.Sc. Anatomy

The School of Medicine, Faculty of Health Sciences, University of Pretoria, South Africa

Supervisor: Dr N Keough

Co-Supervisor: Mrs N Mogale

Department of Anatomy

Faculty of Health Sciences

University of Pretoria

Study Advisor: Dr MA de Beer

Department of Orthopaedics

Life Groenkloof Medical Centre

2019

Declaration of Originality

University of Pretoria

The Department of Anatomy places great emphasis upon integrity and ethical conduct in the preparation of all written work submitted for academic evaluation.

While academic staff teaches you about referencing techniques and how to avoid plagiarism, you too have a responsibility in this regard. If you are at any stage uncertain as to what is required, you should speak to your lecturer before any written work is submitted.

You are guilty of plagiarism if you copy something from another author's work (e.g. a book, an article or a website) without acknowledging the source and pass it off as your own. In effect you are stealing something that belongs to someone else. This is not only the case when you copy work word-for-word (verbatim), but also when you submit someone else's work in a slightly altered form (paraphrase) or use a line of argument without acknowledging it. You are not allowed to use work previously produced by another student. You are also not allowed to let anybody copy your work with the intention of passing it off as his/her work.

Students who commit plagiarism will not be given any credit for plagiarised work. The matter may also be referred to the Disciplinary Committee (Students) for a ruling. Plagiarism is regarded as a serious contravention of the University's rules and can lead to expulsion from the University.

The declaration which follows must accompany all written work submitted while you are a student of the Department of Anatomy. No written work will be accepted unless the declaration has been completed and attached.

Full names of student: Jessica Yvonne Cronjé

Student number: u17381322

Topic of work: A novel approach for investigating the tendinous and capsular layers of the rotator cuff complex: A biomechanical study

Declaration

1. I understand what plagiarism is and am aware of the University's policy in this regard.
2. I declare that this MSc Dissertation (e.g. essay, report, project, assignment, dissertation, thesis, etc.) is my own original work. Where other people's work has been used (either from a printed source, Internet or any other source), this has been properly acknowledged and referenced in accordance with departmental requirements.
3. I have not used work previously produced by another student or any other person to hand in as my own.
4. I have not allowed, and will not allow, anyone to copy my work with the intention of passing it off as his or her own work.

SIGNATURE



Table of Contents

Declaration of Originality	i
List of Figures	v
List of Tables	vii
Abstract	1
Acknowledgements	2
Chapter 1: Introduction and Problem Statement.....	3
1.1. Introduction	3
1.2. Problem Statement.....	4
Chapter 2: Aim, Objectives, and Outline.....	6
2.1. Aim	6
2.2. Objectives	6
2.3. Dissertation Outline.....	6
Chapter 3: Literature Review.....	7
3.1. History of the Rotator Cuff.....	7
3.2. Anatomy of the Rotator Cuff Complex	9
3.2.1. The Subacromial Bursa	10
3.2.2. Subacromial Bursitis	11
3.3. Rotator Cuff Histopathology	11
3.3.1. Critical Zone.....	13
3.3.2. Pathogenesis	13
3.4. Rotator Cuff Biomechanics	14
3.4.1. Material Property Testing.....	14
3.4.2. Structural Property Testing	15
3.5. Mechanisms of Failure	17
3.5.1. Intrinsic Factors.....	17
3.5.2. Extrinsic Factors.....	18

3.6.	Tear Classifications of the Rotator Cuff.....	20
	Chapter 4: Manuscripts on Biomechanical Principles	22
4.1.	Manuscript 1 Title – Biomechanical principles of the measure of stiffness of the tendinous and capsular layers of the rotator cuff complex: Elastic modulus	22
4.1.1.	Abstract	22
4.1.2.	Introduction	22
4.1.3.	Materials and Methods	25
4.1.4.	Results	28
4.1.5.	Discussion	35
4.1.6.	Conclusion.....	37
4.1.7.	References	38
4.2.	Manuscript 2 Title – Biomechanical principle of the load capacity of the tendinous and capsular layers of the rotator cuff complex: Peak load	41
4.2.1.	Abstract	41
4.2.2.	Introduction	41
4.2.3.	Materials and Methods	43
4.2.4.	Results	45
4.2.5.	Discussion	52
4.2.6.	Conclusion.....	54
4.2.7.	References	54
	Chapter 5: Synopsis	58
5.1.	Findings for Chapter 2	58
5.2.	Limitations.....	59
5.3.	Future direction.....	60
5.4.	Clinical relevance	60
5.5.	Conclusion	60
	Chapter 6: References for Chapters 1 and 3	62
	Chapter 7: Annexures	71

7.1.	Annexure 1: Ethics approval letter	71
7.2.	Annexure 2: Letter of permission from the National Tissue Bank.....	72
7.3.	Annexure 3: Ethics renewal for 2019 approval letter.....	74
7.4.	Annexure 4: Copyright permission letter concerning Figure 3.2 of image contained in article by Clark and Harryman, 1992.....	76
7.5.	Annexure 5: Graphic representation for individual elastic modulus findings in Chapter 4, Section 4.1.4.....	78
7.6.	Annexure 6: Graphic representation for capsular and tendinous comparisons within a sample, in Chapter 4, Section 4.1.4.....	98
7.7.	Annexure 7: Graphic representation for capsular comparisons and tendinous comparisons of single rotator cuff segments, in Chapter 4, Section 4.1.4.....	108

List of Figures

Figure 3.1. Drawing of a tear in the capsular layer of the RC of an elderly person by Alexander Monro, 1788.....	7
Figure 3.2. Five histological layers of the RC insertion onto the humerus by Clark and Harryman, 1992.....	12
Figure 3.3. Basic setup of Instron 1342 at Council for Scientific and Industrial Research (CSIR) in Pretoria, Gauteng.....	16
Figure 4.1.1. Proximal humerus showing sharp dissection through the fascial plane connecting the tendinous (*) and capsular (†) layers of the SC of a right arm. <i>S/P – Superior/Proximal; AL – Anterolateral; AM – Anteromedial; I/D – Inferior/Distal</i>	25
Figure 4.1.2. (A) Shows the humeral shaft clamped (*) and mounted on the fixed base plate, with the tendinous strip of the SS clamped (***) and mounted to the load cell. (B) Shows the DIC cameras (†) mounted on a stand and aimed at the testing area of the Instron with two accompanying lights (††).....	26
Figure 4.1.3. DIC tracker definition analysis.....	27
Figure 4.1.4. DIC results for the tendinous layer of an IS strip where (A) is the reference image taken and (B) is the image representing deformation, in the blue area indicated by the red arrows of the TEMA software.....	28
Figure 4.1.5. Linear regression of elastic modulus and sample thickness for tendinous (T) and capsular (C) layers of SS, IS, and SC, displayed as R^2 values.....	31
Figure 4.1.6. SS tendinous layer (dots) observed to have a greater elastic modulus than SS capsular layer (crosses) observed throughout SS testing.....	32
Figure 4.1.7. IS tendinous layer (dots) observed to have a greater elastic modulus than IS capsular layer (crosses) in 6 of 7 tests of IS.....	32
Figure 4.1.8. SC tendinous layer (dots) observed to have a greater elastic modulus than SC capsular layer (crosses) in 6 of 8 tests of SC.....	33
Figure 4.1.9. Representation of variation between IS capsular layers of eight individuals.....	34

Figure 4.1.10. Representation of variation between IS tendinous layers of eight individuals	34
.....	
Figure 4.2.1. Clamp on the left designed to hold the humerus around the shaft during testing, holes in clamp allow for screw placement to hold the humerus in place. Clamp on the right designed to hold onto capsular and tendinous strips between the teeth, with added sandpaper to prevent clamp tearing of strips	44
Figure 4.2.2. Start screen for Bluehill software used to record the load (in Newtons) and extension (in mm) for each test of the tendinous and capsular RC components	45
Figure 4.2.3. Linear regression of peak load and sample thickness for tendinous (T) and capsular (C) layers of SS, IS, and SC, displayed as R ² values	47
Figure 4.2.4. Comparison of the tendinous layer peak load yields for SS, IS, and SC for all samples	49
Figure 4.2.5. Comparison of the capsular layer peak load yields for SS, IS, and SC for all samples	49
Figure 4.2.6. Red oval indicates a full-thickness tear of SSC for sample 002, of a right arm	50
.....	
Figure 4.2.7. On the left the red oval highlights a full-thickness tear of ISC for sample 005, from a left arm; on the right the red oval highlights a partial-thickness tear of IST for sample 013, from a left arm	51
Figure 4.2.8. On the left the red oval highlights full-thickness tearing of SCC near insertion for sample 004, from a left arm; on the right the red oval highlights a full-thickness tear of SCT for sample 002, from a right arm	51

List of Tables

Table 4.1.1. Elastic modulus, approximate yield points, and thickness records obtained from graphs generated during DIC post-processing.....	29
Table 4.2.1. Peak load records (in Newtons) obtained during tensile testing using Bluehill 2 software coupled to Instron 1342.....	46
Table 4.2.2. Tendon thickness (in mm) obtained prior to tensile testing.....	46
Table 4.2.3. T-test for significance of mean values between RC components and between all capsular and tendinous layers respectively.....	48
Table 4.2.4. Tear formation distance from insertion onto proximal humerus (in mm).....	50

Abstract

Rotator cuff (RC) muscle insertion was previously thought to consist of singular, individual tendons inserting onto predefined areas on the greater and lesser tuberosities. However, more recent publications describe the RC muscle tendons as forming a singular insertion across the tuberosities, consisting of both tendinous and capsular portions. Orthopaedic surgeons are now considering these two layers in their surgical approach and treatment plans; therefore this study aimed to test and compare the elastic modulus and maximum load to failure for both tendinous and capsular layers taken from supraspinatus (SS), infraspinatus (IS) and subscapularis (SC). Fourteen ($n = 14$) fresh/frozen arms were used in this study. Each RC muscle was reverse dissected and trimmed to a 2 x 2cm strip, which was separated into its two layers, still attached to the humerus. An Instron 1342 with a 1kN load cell was used to place the samples under tensile testing till failure (Newtons/N). Accompanying Integrated Design Tools (IDT) NX8-S2 cameras captured images for full-field strain measurements with the Image Systems TEMA software package through digital image correlation (DIC). SS, IS, and SC tendinous layers yielded higher average elastic moduli readings (72.34 MPa, 67.04 MPa, and 59.61 MPa respectively) compared to their capsular components (27.38 MPa, 32.45 MPa, and 41.49 MPa respectively). Likewise, the tendinous layers for SS, IS and SC all showed higher average loads to failure (252.74 N, 356.27 N and 385.94 N, respectively) when compared to the capsular layers (211.21 N, 168.54 N and 281.74 N, respectively). These biomechanical differences need to be taken into account during surgical repair owing to the fact that, should these layers be repaired as one singular structure, it may place the weaker less elastic, capsular layer under more strain, possibly leading to either re-tear complications or reduced postoperative healing and functionality. Thus, based on the results, it is recommended that surgeons consider and repair each layer independently for better postoperative biomechanical integrity.

Key words: Rotator cuff, RC, elastic modulus, modulus of elasticity, extension, peak load, tension, biomechanics, biomechanical, supraspinatus, SS, infraspinatus, IS, subscapularis, SC, tendinous, tendon, capsular.

Acknowledgements

First and foremost, I thank God for guidance, strength, patience, and persistence. When I see in human anatomy how everything works together so perfectly, with all its complexities, I know that I witness creations by a Higher Power. To God be the glory.

Thank you to my supervisors, Dr Natalie Keough and (soon to be Dr) Nkhensani Mogale, who remained patient with my “deadlines” and for being generally supportive and inspiring. You motivated me to be a better researcher, aim higher, and aspire to live a full and balanced life. Thank you most for renewing my passion for human anatomy. Thank you also for your time and guidance, I appreciate you both! Thank you to Shavana for being my co-pilot and putting up with my space-brained moments. Without you everything about Masters would have been a lot more intimidating.

Thank you to Chris McDuling and Dr Abrie Oberholster, without the two of you testing would not only *not* have been possible, but it would not have been as much fun. Thank you for your enthusiasm, your time, and your expertise! Thank you also to Dr de Beer for putting the ball in motion for this study and for going against the current because of what you knew was right. Thank you for operating on my living specimen, so far so good. I also want to thank Mrs Myleen Oosthuizen for your invaluable assistance in locating articles and obtaining copyright.

I would like to thank my family for your undying love and ability to listen to me tell you about the human shoulder a bazillion times. Thank you for all of your support, inspirational phone calls to not give up, write-time snacks, and availability when I needed aid. Julle weet wie julle is ;) xx.

I dedicate this dissertation to my parents without whom I would not exist and this study would have been written by someone else. On a serious note, dankie Ma en Pa, julle het vir my die wêreld oop gemaak, my ondersteun deur drie grade, my verdra in my sywurm tye, en nog lief gebly vir my (hoop ek). Dankie dat julle my motiveer om beter te doen as wat ek dink ek kan, en vir die voorbeeld van vrygewigheid en liefdadigheid. Dankie ook aan my Boetie vir jou stille ondersteuning en jou hulp wanneer ek met my rekenaar sukkel of net ‘n koffietjie wou vang. Ek is lief vir julle.

I want to acknowledge and thank those individuals who donated their bodies so that through their generosity we are able to create better medical practices and make the world a better place, one limb at a time.

Chapter 1: Introduction and Problem Statement

1.1. Introduction

The rotator cuff (RC) unit is composed of interconnected tendinous and capsular layers which act to stabilize the humerus and aid in rotation of the arm around the shoulder joint (Standring, 2016; Pauzenberger *et al.*, 2018). The four muscles (supraspinatus, infraspinatus, subscapularis, teres minor) involved in forming the RC unit originate on the scapula and extend towards the proximal aspect of the humerus as interdigitating tendinous fibres interlinking with the deeper positioned capsular layer (Clark and Harryman, 1992; Halder *et al.*, 2000a; Vosloo *et al.*, 2017).

Due to the simplified representation and lack of clarity in textbooks and atlases concerning the structure of the RC unit, medical practitioners often forget that the tendons are interlinked not only with each other, but also with their underlying capsular layer (Tank, 2013; Drake *et al.*, 2014; Moore *et al.*, 2014; Netter, 2014). The tendinous layer, sometimes referred to as the fibrous endoskeleton of the RC unit, acts as a common insertion point and is also the point where the RC muscles blend (interdigitate) together (Halder *et al.*, 2000a). The capsular layer, or articular capsule, is divided in three sections based on the fibre directions; the inner and outer fibre divisions run from the glenoid to the humerus and the middle division runs in the sagittal plane. The articular capsule constitutes the deep layer of the RC and covers the area from the glenoid labrum up to the humerus (Nimura *et al.*, 2012; Mochizuki *et al.*, 2016).

The two layers vary considerably in their biomechanical function and tensile properties. Looking at the biomechanical functions of the tendinous layer, the RC muscles produce high tensile forces which pull the humeral head into the glenoid fossa of the scapula. The supraspinatus muscle acts to stabilise the glenohumeral joint (GHJ) by compressing the shoulder from a superior aspect and subsequently elevates the shoulder. The infraspinatus muscle stabilises the shoulder by controlling anterior/posterior and posterosuperior movement. The subscapularis muscle, said to be a passive stabilizer, resists displacement anteriorly and inferiorly (Halder *et al.*, 2000a; Standring, 2016). Teres minor makes up the final component of the RC muscles and functions weakly to adduct and minorly rotate the arm laterally. Because of the minimal effects, teres minor will not be included in the current study and won't be further discussed.

Few studies have investigated the biomechanical properties of the capsular layer even though this layer, to an extent, serves as the footprint of the tendinous layer due to their interdigitation (Nimura *et al.*, 2012; Vosloo *et al.*, 2017; Pauzenberger *et al.*, 2018). The capsular layer inserts as a thick cover onto the humerus, with some parts being thinner based on their attachment area, and aids in the production of synovial fluid (Halder *et al.*, 2000; Drake *et al.*, 2014). The capsular layer contributes towards joint stability and assists with abduction of the arm (Drake *et al.*, 2014).

A lack of clarity concerning the anatomy and biomechanical properties of the RC has led to many surgeons operating on the torn RC as though the tendinous and capsular layers were biomechanically similar, and repairing them as such. By observing and evaluating the exact location of the RC tear, and being familiar with the varying biomechanical properties of the tendinous and capsular layers and treating them as individual structures, could lead to better post-operative outcomes. For instance, in many cases the RC tear is mended by binding the two layers, which leads to a functional change in the layers and ultimate motive ability of the limb (Dean *et al.*, 2012). A considerable number of individuals who have been for RC surgery have poor post-operative success. Often the tendons do not heal sufficiently, general pain is eminent, a lack of full functional regain of the extremity is experienced, and in extreme cases some patients have been reported with osteonecrosis of the humeral head following arthroscopic repair (Fealy *et al.*, 2006; Gamradt *et al.*, 2010; Vosloo *et al.*, 2017).

Therefore, the purpose of this project was to produce biomechanical evidence on the differences between the capsular and tendinous layers with a primary focus on modulus of elasticity and load to failure. Evidence of this nature should provide surgeons with the means to consider repairing the tendinous and capsular layers of the RC separately in order to promote better quality of life, better post-operative healing, and decrease the percentage of patients needing to return for a similar surgery due to the lack of correct healing of the RC.

1.2. Problem Statement

Most human anatomy manuals depict the rotator cuff (RC) to be four separate muscles and tendons that insert onto predefined areas of the lesser and greater tuberosities of the humerus. The same manuals also do not emphasise the fact that the capsular and tendinous layers of the RC display varying biomechanical properties, often overlooked by surgeons. Surgeons repairing RC tears therefore place sutures through both layers with no consideration of the

varying biomechanical properties of the interdigitated, yet individual layers. This study therefore looked to address this problem by providing high-quality, evidence-based outcomes for the need to repair the tendinous and capsular layers separately.

Chapter 2: Aim, Objectives, and Outline

2.1. Aim

The aim of this study was to biomechanically investigate the tendinous and capsular layers of the rotator cuff (RC) complex in a novel way.

2.2. Objectives

This was an observational study where the gross anatomy was observed and noted with regard to attachment, interdigitation, and the biomechanical properties (load to failure/peak load, and modulus of elasticity) of the supraspinatus (SS), infraspinatus (IS), and subscapularis (SC) muscles' tendinous and capsular layers. These were tested and compared in a South African fresh tissue sample.

The objectives of this study were to:

- Observe the anatomical insertions and interdigitations of the supraspinatus (SS), infraspinatus (IS), and subscapularis (SC) muscles by reverse dissection of fresh shoulder human specimens.
- Test the peak load (N) and modulus of elasticity (MPa) of each of the three RC muscles' tendinous and capsular layers (i.e. SS tendinous with IS tendinous; SS tendinous with SC tendinous; IS tendinous with SC tendinous etc.).

2.3. Dissertation Outline

The current research is arranged to maintain a golden thread, while concurrently concentrating the focus of each section on its central theme. Chapter 3 follows and deals with a broad body of significant literature needed to accentuate the importance of the study and its findings. Chapter 4 contains the study methods, materials, and findings in the form of two articles – each containing a biomechanical feature as focal point, though linked to each other by statistical findings. Chapter 5 then provides a synopsis for the entire dissertation. Finally, references and annexures can be found in Chapter 6 and 7, respectively.

Chapter 3: Literature Review

3.1. History of the Rotator Cuff

The first literature to the author's knowledge that mentions a tear in the rotator cuff (RC) complex was by Alexander Monro in 1788. Monro labels a drawing (Figure 3.1) and comments that the tear "a hole with ragged edges" he observed in the capsular layer of an elderly person, was one he had not noticed in any other shoulder he had seen until that time (Monro, 1788).

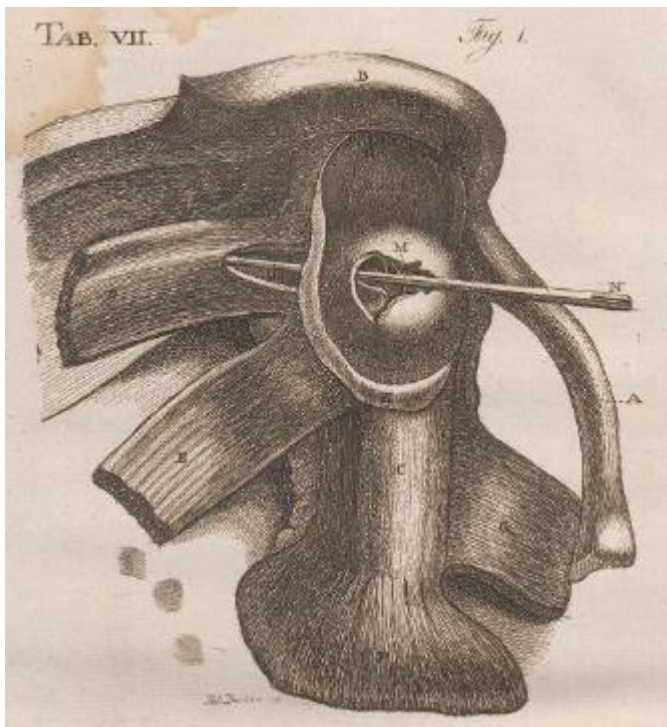


Figure 3.1. Drawing of a tear in the capsular layer of the RC of an elderly person by Alexander Monro, 1788.

Nearly half a century later an article addressing the presence of RC tears was published in the London Medical Gazette by John G Smith. In his article Smith discusses seven cases of shoulder pathology, making mention of the integration of the tendons of the RC muscles into their capsular layer (Smith, 1834).

Approaching the end of the 19th century a certain capsular tear operation was introduced by Gerster (1884). The term 'capsulorrhaphy', meaning simply the surgical repair of a capsule via a small incision, was used to describe the operation performed by Gerster, where he excised certain portions of the damaged capsule of the shoulder and then sutured it closed. This method

of operation brought to light again the fact that the RC complex consisted of two layers (Gerster, 1884). The reason these mentions by Smith (1834) and Gerster (1884) are so significant are because, up until this point, and even 50 years later, shoulder surgery of any kind was not a developed speciality and made little impression on the interests of the medical community. Codman (1934) in his book “The shoulder: Rupture of the supraspinatus tendon and other lesions in or about the subacromial bursa”, makes it clear in the preface that, other than himself and a handful of other surgeons, few doctors in the early 1900’s had any love for shoulder operations (Codman, 1934).

Codman (1934) proceeds to mention Gray, “It is not necessary to specify which Gray or even to state the title of his book... (he) bequeathed a real legacy to almost every English-speaking doctor who has studied medicine since his time”. Of course, he was speaking of Henry Gray, a name all medical students are still familiar with today from their textbooks “Gray’s Anatomy”. Gray released his first book, “Anatomy: Descriptive and surgical”, which would serve to immortalize his name (Gray, 1858). “Anatomy: Descriptive and surgical” became attractive at the time for its illustrations and logical topic format. In this book, he describes the RC more from a component view point than a structural perspective, with the aim to clearly define the muscles and their boundaries. However, in this description the knowledge that these muscles interdigitate with each other and their capsular layer as they near the humerus is lost to the reader.

Codman (1934) in his book, somewhat criticises Gray (1858) for his vague descriptions on aspects of the shoulder. Codman does, however, defend Gray, mentioning to the audience that no man can understand a field completely if he is not an expert in that field. A noteworthy quote by Codman is that “Most medical books are scarcely more enduring than shooting stars”. Though this may be less true today, new discoveries are still brought to light almost daily. Those in the medical field should be wary and read constantly as new knowledge tests old practices and, as with the capsular layer of the RC, new practices test whether surgeons are familiar with established knowledge.

Although Codman (1934) and many other authors (Gerster, 1884; McLaughlin, 1944; Clark and Harryman, 1992; Longo *et al.*, 2011; Dean *et al.*, 2012; Nimura *et al.*, 2012; Pauzenberger *et al.*, 2018) kept emphasising the importance of the capsular layer and the elaborate interdigitation, other anatomy manuals (Tank, 2013; Drake *et al.*, 2014; Moore *et al.*, 2014; Netter, 2014) which give short descriptions of origins and insertions or images of bony

insertions of muscles, have remained the foundation for medical practitioners to study anatomy from. However, the latest edition of Gray's Anatomy has started to explore in more detail the complete and complex unit of the RC, and mentions briefly that interdigitation exists between the tendinous and capsular layers (Standring, 2016).

3.2. Anatomy of the Rotator Cuff Complex

According to the latest edition of Gray's Anatomy, the RC muscles (supraspinatus, infraspinatus, subscapularis, and teres minor) originate on the scapula and taper towards their partially interdigitated insertion with the capsular layer on the humerus (Standring, 2016). In truth, the entire RC structure is interdigitated, and the RC unit inserts across the lesser and greater tuberosities of the humerus as two wide and overlapping layers: a tendinous and a capsular layer (Clark and Harryman, 1992; Edwards *et al.*, 2016; Vosloo *et al.*, 2017). These layers are the main stabilising factors of the very mobile glenohumeral joint (GHJ) (Cowan and Varacallo, 2018).

The supraspinatus muscle (SS) originates on the medial 2/3 of the supraspinous fossa of the scapula and courses towards its insertion, together with the articular capsule, onto the greater tuberosity of the proximal humerus. The SS is classified as a circumpennate muscle and has a thick belly medially that tapers into a tough tendon, which will interdigitate with the other RC muscles and capsular layer. The superficial fibres of the tendinous extremities of this muscle run longitudinally and the deep fibres run obliquely; these oblique fibres are the manner in which the muscle interdigitates with adjacent muscles. Functionally, SS serves to initiate abduction of the shoulder (initial 15°), prevent superior and posterior displacement of the humerus and also helps to retract the arm in these directions. SS is the only RC muscle that doesn't aid in rotation of the humerus. SS is innervated by efferent branches of the suprascapular nerve (originating from the C4-6 spinal nerves), which also branches to innervate infraspinatus (IS). Blood is supplied to SS via the dorsal scapular and suprascapular (which also supplies IS) arteries (Halder *et al.*, 2000; Nimura *et al.*, 2012; Moore *et al.*, 2014; Standring, 2016).

The IS originates on the medial 2/3 of the infraspinous fossa of the scapula, as well as from the infraspinous fascia. The fibres taper from their origin into a thick tendon that passes inferior to the lateral end of the scapular spine from where it continues to insert with the articular capsule, onto the greater tuberosity of the proximal humerus. The IS is also classified as a circumpennate muscle with fibres running similarly to those of SS. Functionally, IS serves to

stabilise the humeral head and aids is the main lateral rotator of the shoulder joint. It has been suggested that the superior fibres of IS may assist with the abduction function of SS due to their interdigitated connection, however, this has yet to be tested. Blood is supplied to IS via the dorsal scapular and the circumflex scapular arteries (which also supplies subscapularis: SC) (Halder *et al.*, 2000a; Halder *et al.*, 2000b; Nimura *et al.*, 2012; Standring, 2016).

Subscapularis (SC) originates from the subscapular fossa of the scapula and the tendinous intramuscular septa. The fibres taper into a flat tendon which interdigitates anteriorly with the articular capsule and surrounding RC muscles, specifically the SS. The SC is classified as a multicircumpennate muscle as it is composed of numerous intramuscular tendons. SC also forms the floor of the bicipital sheath. Functionally SC is a strong adductor of the GHJ while aiding in medial rotation of the humerus about the GHJ and has been said to be a passive stabilizer (Halder *et al.*, 2000c; Nimura *et al.*, 2012; Standring, 2016). SC is innervated by upper and lower subscapular nerves, which originate from posterior cords of the brachial plexus (C5-7) (Moore *et al.*, 2014; Standring, 2016). Blood is supplied to SC through the subscapular and suprascapular arteries, in addition to the circumflex scapular artery. Naidoo *et al.* (2014) found that, in some cases, SC is also supplied by thoracodorsal, lateral thoracic, and posterior circumflex humeral arteries.

The RC muscles together work to stabilise the shoulder at the GHJ. Together this complex unit provides the majority of the motion capability of the arm, such as abduction, adduction, and medial and lateral rotation. In order to function effectively, these layers must remain well lubricated, which is the responsibility of the subacromial bursa.

3.2.1. The Subacromial Bursa

The subacromial bursa, approximately 10-15mm in height, can be found in the subacromial space under the coracoid process, coracoacromial ligament, acromion, and acromioclavicular joint (Cowan and Varacallo, 2018). The subacromial bursa has been found to play a vital role in the healing process of RC tears as it is a source of blood vessels, fibroblasts, and in some cases synovial cells (Uthoff and Sarkar, 1991). This fibrovascular region of the subacromial bursa has been labelled the falciform edge and surgeons were encouraged to remove it in the past as they thought the tissue too weak to hold stitches, however, we now know this region to be one of repairing tissue and to be important in the healing process (Uthoff and Sarkar, 1991; Ishii *et al.*, 1997). Other than lubrication and healing, this bursa has been found to be particularly important when it comes to the detection of RC tears. When inflammation,

hypertrophy, oedema, and/or necrosis affect the subacromial bursa, pain linked to RC tears is experienced (Chillemi *et al.*, 2016). The most common epidemiology which could cause the listed aetiologies is repetitive overhead motions of the arm, common in athletes and manual labourers. When the subacromial bursa becomes pathological, the term subacromial bursitis is used to describe the changes associated with the inflammation process.

3.2.2. Subacromial Bursitis

Inflammation of the subacromial bursa has been described in three phases: acute, chronic, and recurrent. Acute bursitis is seen as local inflammation with thickened synovial fluid, physically experienced as painful movement of the arm, especially overhead. Chronic bursitis is more severe and means that inflammation of the bursa endures for such a long period of time that weakness and even rupture of surrounding structures (such as the SS tendon) occurs. Recurrent bursitis affects the shoulder when individuals suffer from repetitive trauma, which could be from routine physical activities, or when individuals suffer from rheumatoid arthritis. Inflammation due to subacromial impingement, overuse, trauma, or infection (to name a few) causes the synovial cells of the bursa to produce more fluid and collagen. The fluid produced can be rich in fibrin which then leads to haemorrhage, described as bursitis (Hirji, Hunjun, and Choudur, 2011). Inflammation is a normal part in the healing process and occurs in two parts: inflammation is introduced in response to initial tissue damage, and is then stopped by anti-inflammatory macrophages towards the end of the healing process. However, when inflammation becomes chronic, damaged tissue is negatively impacted at a cellular level (Longo *et al.*, 2011; Abraham *et al.*, 2017). The following section will describe the normal histology and the cellular changes that take place when a RC tear is present.

3.3. Rotator Cuff Histopathology

The histological composition of the RC can be examined using techniques such as immunohistochemistry, reverse transcription polymerase chain reaction, and enzyme linked immunosorbent assays (Dean *et al.*, 2012). Clark and Harryman (1992) were the first authors who histologically found that the RC muscles consist of five distinct histological layers (Figure 3.2):

1. Layer one is the thin (1mm), most superficial layer. It comprises out of large arterioles and obliquely oriented fibres from the coracohumeral ligament, which extend to the greater tuberosity between the SC and SS muscles, to blend with the periosteum.

2. Layer two is found deep to layer one and ranges between 3-5mm in thickness. Arterioles from layer one pass into layer two by moving between muscle fascicles. Tightly packed, parallel fibres can be seen in this layer as large bundles, which have a diameter of about 1-2mm. These bundles extend from the bellies of the SS and IS muscles to the humerus.
3. Layer three is approximately 3mm thick and contains smaller blood vessels than seen in the two layers superficial to it. The larger arteries from layers one and two tend to run in an interval between layers two and three. The tendinous structure of layer three has smaller, non-uniformly oriented, loosely packed fascicles when compared with those seen in layer two.
4. Layer four is the thinnest layer (less than 1mm) and contains only capillaries running adjacent to the extra-articular surface of the joint capsule of the shoulder. This layer consists of loose connective tissue with thick collagen fibre bands, which also border the extra-articular surface of the joint capsule of the shoulder.
5. Layer five is the deepest layer (the capsule) and ranges from 1.5-2mm in thickness; no blood vessels have been noted in this layer. Layer five is formed by continuous and interwoven collagen fibrils which run from the glenoid labrum to the humerus, inserting as Sharpey fibres.

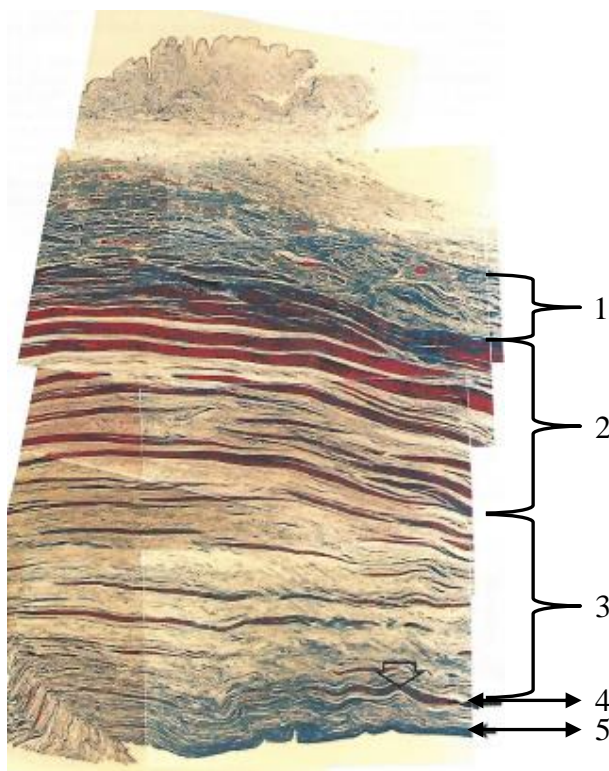


Figure 3.2. Five histological layers of the RC insertion onto the humerus by Clark and Harryman, 1992.

The SS and IS can be observed to intersect approximately 15mm before their joint insertion onto the humerus, and this interdigitation is observed most distinctly in the third histological layer. The SC can be observed to blend with the IS posteriorly and with SS anteriorly. The combined insertion of SS, IS, and SC onto the humeral tuberosities can be histologically observed as a fibrocartilaginous zone (Benjamin *et al.*, 1986; Clark and Harryman, 1992). Just proximal to this fibrocartilaginous zone we find what was first described by Codman in 1934 as the “critical portion” and later the “critical zone” (Codman, 1934; Maffulli and Furia, 2012).

3.3.1. Critical Zone

The critical zone is the tendon area most partial to tearing; it can be found about 10-15mm from the humeral insertion, or between the fibrocartilage and proper tendon transition regions (Itoi *et al.*, 1995; Pandey and Willems, 2015; Naidoo *et al.*, 2016). The transition regions (proper tendon, fibrocartilage, mineralised fibrocartilage, bone) differ in the amount and type of collagen present, contributing to varying tissue compositions. As RC disease sets in, a larger amount of type III collagen and hypovascularity in the critical zone have been noted (Codman and Akerson, 1931; Itoi *et al.*, 1995; Levy *et al.*, 2008; Pandey and Willems, 2015; Naidoo *et al.*, 2016). Structural changes developing when an individual has a RC tear are due to the body’s attempts at healing the defect.

3.3.2. Pathogenesis

Remodelling, which is active even in healthy tissue, becomes accelerated when there is a sign of disease or injury, such as a RC tear. Remodelling is evident in the form of decreased levels of pentosidine, which is a non-protein biomarker of advanced glycation end-products (AGEs); meaning low pentosidine levels indicate higher AGE levels (Sejersen *et al.*, 2015). When this process is accelerated, more collagen III is generated leading to pathological tissue appearing less mature than normal tissue. Although collagen III has been said to be a precursor of collagen I, the main component in healthy RC tissue, it is less organised and the affected tissue is left with a matrix that is mechanically unstable (Dean *et al.*, 2012; Sejersen *et al.*, 2015). Other cellular changes taking place in an attempt to heal a RC tear are increases in fibroblasts, blood supply, and inflammation. However, as the size of the tear increases, the healing attempts are counteracted and the overall matrix changes, which attempt to restore the RC component to its former function, become mechanically weak scar tissue. What used to be large and organised fibrils become smaller disorganised fibrils with weaker biomechanical function (Dean *et al.*, 2012).

3.4. Rotator Cuff Biomechanics

Important biomechanical functions of the RC unit are to aid in arm movement, as well as stabilising the shoulder joint (Yamamoto and Itoi, 2015). At a 90° angle the RC unit, along with the physical properties of the rounded humeral head and concave glenoid fossa, provide compressive forces to stabilise the shoulder (concavity-compression effect) (Lippitt *et al.*, 1993; Yamamoto and Itoi, 2015). During arm movement the SC and the IS act from anterior and posterior positions to generate a balanced torque that resists humeral head translation (Yamamoto and Itoi, 2015).

3.4.1. Material Property Testing

The range of stretching that a soft tissue is capable of undergoing before failing is known as elastic modulus (Elkhatny *et al.*, 2017). This material property of the RC can be observed at both microscopic and macroscopic levels. Microscopically, when a soft tissue is mechanically loaded, researchers have observed the proteins in charge of relaying movement are mainly type I collagen, fibrillin, and elastin (Akhtar *et al.*, 2011). Macroscopically, elastic modulus can be seen as displacement from the resting position (Yeh *et al.*, 2002). Testing the elastic modulus of soft tissue proves difficult due to its anisotropic, viscoelastic, and heterogeneous nature. Recently however, researchers (McCormick and Lord, 2010; Zhou *et al.*, 2016; Mallett and Arruda, 2017) have found the optimal method for testing modulus of elasticity in a soft tissue sample is using digital image correlation (DIC).

DIC enables the calculation of full-field tissue strain by comparing a series of digital photographs at different levels of deformation. The algorithm tracks a number of groups of pixels within a stochastic speckle pattern to measure surface displacement. Combining this information then produces a complete two- or three-dimensional picture of deformation vector fields and strain maps (McCormick and Lord, 2010). To extract elastic modulus from DIC results, a material with a known cross-sectional area is required, that is uniformly loaded, exhibiting homogeneous uniaxial strain (defined as a ratio of total deformation : initial height). To obtain an observable area of tissue, researchers have suggested airbrushing techniques employing water insoluble ink. The airbrushing allows the investigator to apply a random pattern of speckles to moist biomaterial for DIC analysis. The DIC results are processed by TEMA to create strain data points and extensometer strains across the surface of the analysed sample, also known as strain maps (Mallett and Arruda, 2017; <http://www.imagesystems.se/tema/>). TEMA software is a product of Image Systems used for

advanced motion analysis testing. Tracking algorithms of TEMA review images imported from DIC and create quantifiable values for stress and strain experienced by the analysed tissue. The stress and strain values can then be plotted in Excel to produce a graph containing a well of information.

Three main points of interest contained in the produced graph are the proportional limit, the elastic modulus, and the breakpoint of the tissue (Heary *et al.*, 2017). The proportional limit (or yield point) is the point at which tissue has undergone elastic deformation, and after which plastic deformation occurs (Vaidya and Pathak, 2018). The modulus of elasticity is equated by a best-fit line plotted to the slope of the stress-strain graph. Elastic modulus is therefore “Ratio of stress applied to tissue : Strain inherent to stress applied” (Elkakatny *et al.*, 2017). Yield point is the final observation of note gathered from the produced graph and is seen as the point at which a tissue has reached its capacity to withstand strain, and breaks (Vaidya and Pathak, 2018).

3.4.2. Structural Property Testing

Yield point or peak load is of particular importance in identifying the strength of various soft tissue components, and what force can be applied to the tissue before it tears. The standard operating procedure is to use a materials testing system (MTS), such as an Instron, to measure peak load (Halder *et al.*, 2000a; Halder *et al.*, 2000b; Itoi *et al.*, 1995).

Instron is a hydraulic servo-controlled machine used for testing tension and/or compression of a sample (Gouw and Wevers, 1982; Li *et al.*, 2011). The Instron machine consists mainly of a load frame, load cell, upper and lower grip fixtures (with one moveable and one fixed head), a fixed base plate, and a crosshead (Figure 3.3). When conducting a tension test, the tissue sample is clamped in the upper and lower grip fixtures. The upper fixture connects with the load cell and the lower fixture with the base plate of the crosshead. The crosshead is the component of the Instron which moves down, opposite to the stationary upper fixture and load cell (<https://sites.tufts.edu/bray/instrumentation/instron-test-system/>). As the Instron is conducting a tensile test, data points are measured at a predetermined sampling frequency by a desktop computer, connected to the Instron through a frame interface box, running Bluehill. Bluehill is an integrated modular software program which interprets the data generated by the Instron tensile test, creating a record of the load applied (in Newtons) (Illinois Tool Works Incorporated, 2008). Bluehill generates PDF documents containing a table with load and extension data, as well as load vs. extension graphs. In both the table and graph the peak load

obtained before failure is highlighted by Bluehill for easy observation. Once this peak load value has been reached, the Instron may continue to collect data points and transfer them to Bluehill, but a steady decline in the slope of the graphs produced will be noted, and the peak load value will not be obtained again.

This mechanical simulation of RC tearing highlights the fact that trauma to the tendinous or capsular components leads to decreased biomechanical capacity of the injured component to withstand tensile load. Though previous authors have investigated the peak load of RC components in the past, little to no mention has been made of the individual tendinous and capsular layers' differences in load tolerance (Itoi *et al.*, 1995; Halder *et al.*, 2000a; Halder *et al.*, 2000b; Sano *et al.*, 2013). This difference is an important missing link, not only because tears occur in multifactorial ways, but because the different ways in which they occur create different tear types, found in different layers of the RC complex, alternatively affecting the overall biomechanical strength.

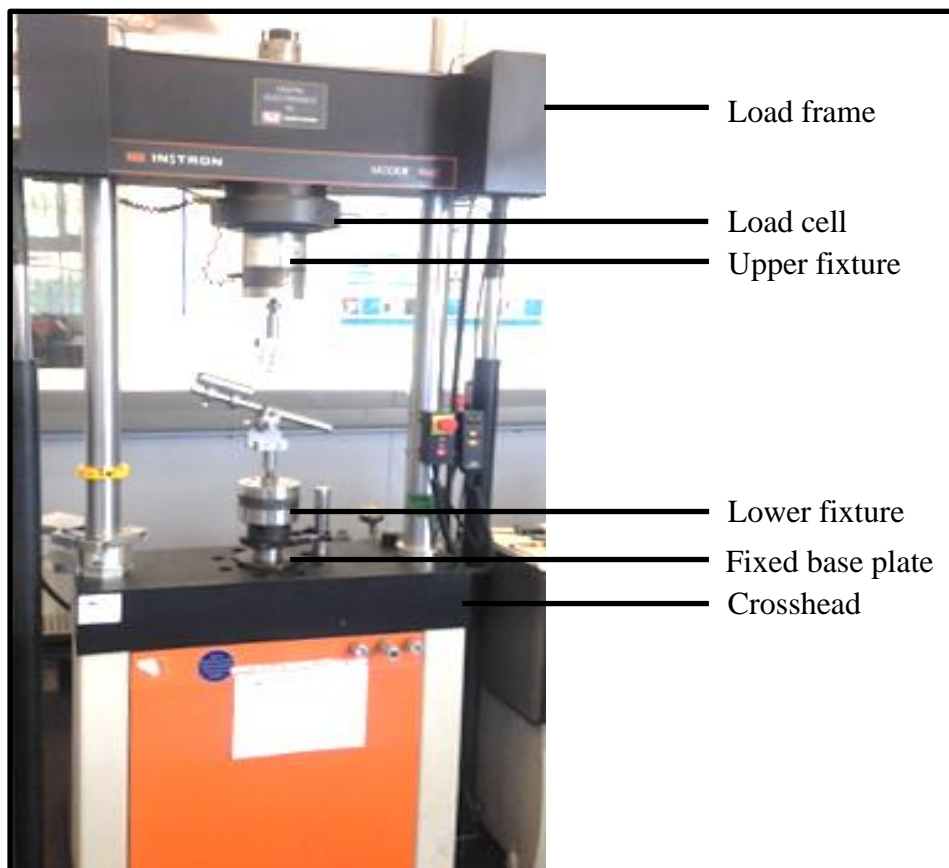


Figure 3.3. Basic setup of Instron 1342 at Council for Scientific and Industrial Research (CSIR) in Pretoria, Gauteng.

3.5. Mechanisms of Failure

RC tears are, in most cases, painful and occur when there is a regeneration failure as a result of intrinsic and extrinsic factors (Codman and Akerson, 1931; Lewis, 2010; Factor and Dale, 2014; Yamamoto and Itoi, 2015). Intrinsic factors lead to degeneration within the tendon and extrinsic factors lead to impairment, secondary to tendon degeneration (Codman and Akerson, 1931; Neer, 1983; Lewis, 2010; Sambandam *et al.*, 2015; Yamamoto and Itoi, 2015).

3.5.1. Intrinsic Factors

Intrinsic factors responsible for RC tears directly involve the RC complex and have been isolated by various researchers into origin theories. The five theories generated are: hyperperfusion theory (hypovascular critical zone described in Section 3.3.1), degenerative theory, degenerative microtrauma theory, extracellular matrix modifications theory, and apoptotic theory (Codman, 1934; Riley *et al.*, 2002; Yuan *et al.*, 2002; Yadav *et al.*, 2009).

The degenerative theory revolves around the concept that RC tears form over a life-span of pathological processes at work in the subacromial bursa. The theory implies that tears present when tendons become diseased and weak. Codman and Akerson described this as “end-results” stating that most RC tears discovered at the time were not the result of major acute traumas, but the accumulation of many micro-traumas (Codman and Akerson, 1931). This theory binds well with the degenerative microtrauma theory that small RC tears are the result of repetitive micro-loading, which then progress into larger tears if untreated (Pandey and Willems, 2015). Degeneration forms a large proponent of RC tears and occurs due to certain repetitive activities, and naturally as we age and is thus also classified as the chronic form of a RC injury (Via *et al.*, 2013). The percentage of individuals with RC tears increases dramatically from the 5th (13%) to 8th (51%) decades of life (Hashimoto *et al.*, 2003; Yamaguchi *et al.*, 2006).

Chronic changes to the RC have been summarized into the extracellular matrix modifications theory. As individuals age, negative changes to their normal RC complex cellular structure occurs such as fibrocartilaginous changes, calcified deposits in the tendons, reduced cellularity, and fatty degeneration or infiltration (Buck *et al.*, 2010; Codman and Akerson, 1931; Hashimoto *et al.*, 2003; Karas, Wang, Dhawan, and Cole, 2011; Nyffeler and Meyer, 2017). Although fatty infiltration is age-related, where it involves half or more of the total muscle fibres, a RC tear is usually noted (Goutallier *et al.*, 1994; Buck *et al.*, 2010). When a tear occurs, fat tissue is deposited among tendon fibres, and is characterised by fibre atrophy and fibrosis (Buck *et al.*, 2010; Osti *et al.*, 2013). Fatty infiltration is perhaps one of the most

significant and well-studied degenerative features, and has been studied in connection with post-operative success after RC tear repair. Goutallier created a five-stage classification system, scoring the amount of fatty infiltration in the muscle fibres, and comparing this with post-operative success. Stage 0 implies no fatty infiltration, stage 1 is observed when there are very few fatty streaks, stage 2 can be seen as almost an equal amount of muscle to fat, stage 3 is an equal amount of muscle and fat, and finally stage 4 presents with more fatty infiltration than original muscle fibres (Goutallier *et al.*, 1994). From stage 2 onwards, fatty infiltration can be associated with a RC tear, and is more likely to be present in older individuals (Ohzono *et al.*, 2017). Fatty infiltration has also been observed to negatively affect collagen turnover in RC tendons, thereby hindering collagen proliferation resulting in tendon degeneration, and may even result in apoptosis (Factor and Dale, 2014).

The apoptotic theory can be linked to the degenerative theories in that there exists a relationship between repetitive stress and the activation of apoptosis in tendon cells, contributing to tissue degeneration (Yuan *et al.*, 2002; Benson *et al.*, 2010; Bedi *et al.*, 2012). The apoptotic theory finds its origin with Yuan *et al.* (2002) who noted that older individuals contain a greater number of apoptotic cells in their tendons than younger individuals. Although the authors state that this may be the result of the presence of a RC tear, because older individuals are more likely to have RC tears, there is a possibility that the increase in these cells are a result of ageing.

The five intrinsic theories form the major proponent of the multifactorial aetiology of RC tears, but are not the only factors responsible for degeneration of RC tendons.

3.5.2. Extrinsic Factors

Extrinsic factors that result in RC complications have been split into three main theories: The multifactorial theory, chronic impingement syndrome theory, and overuse theory (Codman and Akerson, 1931; Neer, 1972; McMaster and Troup, 1993; Lin *et al.*, 2004; Via *et al.*, 2013).

The multifactorial theory is largely associated with degeneration and combines multiple factors that may result in RC tears. Some of the factors include pathology interfering with muscle function (e.g. acromial enthesophyte formation), changes in scapular or humeral kinematics, postural abnormalities, RC muscle performance deficits, a decrease in the ability to extend the pectoralis minor muscle or posterior shoulder, variations to the normal anatomy

(acromion shape), and impingement (Neer, 1983; Seitz *et al.*, 2011; Sambandam *et al.*, 2015; Yamamoto and Itoi, 2015; Weiss *et al.*, 2018).

The chronic impingement syndrome theory is based on the shape and position of the acromion and coracoacromial ligament (Via *et al.*, 2013; Tawfik *et al.*, 2014). The shape of the acromion has been found to be a major contributing factor to the chronic formation of RC tears (Bankart, 1923; Bigliani, Ticker, Flatow, Soslowky, and Mow, 1991; Nyffeler and Meyer, 2017). Bigliani (1991) described three types of acromion shapes and the risk of developing a RC tear associated with each. Type I acromion has a flat inferior surface for the RC tendons to pass beneath, and is rarely associated with RC tears. Type II is slightly inferiorly curved and is sometimes associated with RC tears. Type III acromion has a hooked appearance, is curved further inferiorly than type II, and is most often observed in individuals with RC tears. The type III acromion is most often seen in chronic impingement syndrome and RC tearing (70%) (Via *et al.*, 2013). Impingement of a tendon occurs beneath the acromion and coracoacromial ligament, eventually resulting in an RC tear, and has been described in three stages of intensity (Neer, 1983; Via *et al.*, 2013). Stage one can be observed as oedema and haemorrhage resulting from repetitive overhead motions and is mostly seen in younger individuals. Stage two develops when there is recurrent inflammation causing the bursa to become thick and fibrotic; stage two is therefore simply observed as fibrosis and tendinitis and mostly occurs in middle-aged individuals. Stage three is mainly seen in individuals older than 40 years of age and results when the impingement has lasted for a period sufficient enough to create partial or full thickness tears; chronic impingement can even result in osteological changes such as bone spurs, humeral head ascension, and anterior acromion erosion (Neer, 1983). This third stage of impingement is largely attributed to the overuse of the affected arm. The overuse theory states that RC tears are the result of chronic repetitive motions of the arm that place the RC in frictional contact with surrounding tissue, resulting in a tear (Via *et al.*, 2013).

Although the impingement and overuse theories supply detailed clear-cut causes for superior or bursal-sided RC tears, they don't explain how the more frequently occurring articular-sided tears occur (Pandey and Willems, 2015; Nyffeler and Meyer, 2017). For this reason, Neer's theory that impingement is the primary cause of RC tearing is incorrect, and a combination of factors would appear to make the RC a minefield for sustaining injury. Because of the multifactorial ways in which RC disease can occur, many individuals are affected; up to 30% of the population has been reported visiting surgeons for shoulder pain (Chaudhury *et al.*, 2012; Vosloo *et al.*, 2017). RC tears are diagnosed by physical examination (testing muscle

strength and arm motion), looking at X-rays, ultrasound, and/or MRI. Defining the side, size, and shape of the tear is then paramount to constructing the best repair approach.

3.6. Tear Classifications of the Rotator Cuff

Accurate classification of RC tears should be made in order to understand quality of life and biomechanical deficits individuals with these lesions experience (Akhtar *et al.*, 2011; Gumina and Borroni, 2016). As there are manifold ways in which RC tears occur, many kinds of tears exist. Surgeons have thus formulated different orders of classification systems to describe the various RC tears.

The first classification that should be made is the level at which the tear is found, that is to say (1) bursal-sided, (2) interstitial, or (3) articular-sided. (1) Bursal-sided tears are specific to the more superficial tendinous layer of the RC, near the subacromial-subdeltoid bursa. Bursal-sided tears, although not the most common, have been associated with the greatest amount of pain between the three levels (Fukuda *et al.*, 1987; Lee *et al.*, 2000; McMonagle and Vinson, 2011; Gumina and Borroni, 2016; Saremi, 2016; Pauzenberger *et al.*, 2018). The more intense pain experienced results when this lesion is caused by chronic impingement (Via *et al.*, 2013; Aydin and Karaismailoglu, 2017; Kim *et al.*, 2018). (2) Interstitial-sided tears occur within the mid-substance between the bursal and articular sides of the involved tendon. Interstitial tears have also been called intrasubstance tears, intratendinous tears, and intramuscular cysts, and can occur along with bursal or articular-sided tears. These tears often remain unobserved during arthroscopic surgery due to their interstitial nature, but can be visualised pre-operatively with MRI (McMonagle and Vinson, 2011; Gumina and Borroni, 2016). (3) Articular-sided tears are the most frequently observed and correspond to the capsular side of the RC complex. Authors have found that the articular side of the RC has a stress-failure zone that is half of the bursal side (which has more robust collagen), which could explain the more frequent occurrence of articular-sided tears (Nakajima *et al.*, 1994; Luo *et al.*, 1998; Lee *et al.*, 2000). These individually organised tears can each be described as partial-thickness tears (PTTs), which make up half of the next level of tear classification.

PTTs involve either only the articular or interstitial or bursal layer individually, or the bursal and interstitial or the articular and interstitial layers together. PTTs were first categorised by Ellman (1990) into three degrees of RC involvement. The first degree is described as tears that are up to 3mm thick, the second degree as 3-6mm thick, and the third degree as more than 6mm in thickness of the affected RC section (Ellman, 1990). Ellman created this classification

system based on the assumption that a healthy tendon is 10-12mm thick, which creates some dispute when grading affected tendons, especially those of older individuals (who may have thinner tendons due to attrition and degeneration). Therefore, Gartsman (2001) reclassified this system by stating that the first degree involves less than a ¼ of the thickness of the tendon, the second degree involves less than half of the thickness, and the third degree involves more than half the thickness of the affected tendon (Gartsman, 2001). When articular-sided tears propagate to the bursal side, or vice versa, the tear is described as a full-thickness tear (FFT) (McMonagle and Vinson, 2011). FTTs were sub-classified by DeOrio and Cofield (1984) based on the greatest observed diameter of a tear that completely perforates the thickness of a RC section. Small tears are less than 10mm wide, medium tears are 10-30mm wide, large tears are 30-50mm wide, and massive tears are more than 50mm wide (DeOrio and Cofield, 1984). PTTs precede FTTs and this progression into the next phase of tearing can be predicted by an initial sharp increase in and then disappearance of pain, fatty infiltration and tear propagation in the shoulder region (Melis *et al.*, 2009; McMonagle and Vinson, 2011).

The last order of categorizing RC tears that is of note is the geometric classification system. The geometric system is based on four tear shapes, or types: (1) Crescent, (2) U-shaped, (3) L-shaped, and (4) massive and immobile (Davidson and Burkhart, 2010; Watson *et al.*, 2018). (1) Crescent tears are wide anterior-to-posterior (AP), short medial-to-lateral (ML) with good ML mobility. (2) U-shaped tears spread more medially than crescent tears with the rounded end of the U, on the medial stretch of the tear, reported to be adjacent to the glenoid rim. The U-shaped tear, unlike the crescent, is wider ML, and narrower AP. (3) Where L-shaped tears have been studied, research has shown that one end of this tear is more mobile than the other, which is usually the end surgeons manoeuvre to suture to the bone during repair (Watson *et al.*, 2018). (4) Often where massive, immobile tears have occurred, surgeons cannot intervene to restore the function of the muscle due to the lack of a mobile ML area.

Once a diagnosis has been made based on tear classification, the doctor may advise treatment options such as less invasive arthroscopic or invasive open surgical techniques (Park *et al.*, 2007; Mazzocca *et al.*, 2010; Yamamoto and Itoi, 2015). As the specifications of the RC lesion impact greatly upon choice of surgical approach, it is imperative that surgeons are familiar with tear location, size, and shape. These aspects could also yield information on the aetiology of the tear, as well as the biomechanical principles behind RC injury and eventual failure (Gumina and Borroni, 2016).

Chapter 4: Manuscripts on Biomechanical Principles

4.1. Manuscript 1 Title – Biomechanical principles of the measure of stiffness of the tendinous and capsular layers of the rotator cuff complex: Elastic modulus

4.1.1. Abstract

Elastic modulus is an important biomechanical component, which indicates stiffness or elasticity of a particular material. This study consisted of a sample of 8 fresh tissue human arms obtained from the National Tissue Bank, under the auspices of the Department of Anatomy, University of Pretoria (Ethics reference number: 384/2018). Upon reverse dissection of the RC muscles to their insertion site, 2x2cm segments were retained for analysis. Digital Image Correlation (DIC) was employed to visualise the deformity of the tendinous and capsular portions of each of the three muscles and after post-processing elastic modulus values were obtained. The tendinous layers for SS, IS, and SC yielded observably higher average elastic moduli readings (72.34 MPa, 67.04 MPa, and 59.61 MPa respectively) when compared to their capsular components (27.38 MPa, 32.45 MPa, and 41.49 MPa respectively). These varying elastic moduli for the tendinous and capsular layers should direct surgeons to adapt their techniques, taking into consideration that biomechanical differences between the two layers could be lost if they are not repaired separately.

4.1.2. Introduction

In 2012 a longitudinal survey, conducted from the year 1996 to 2006 on United States patients operated for rotator cuff (RC) repair, was released. The survey found a 141% increase in patients visiting medical practitioners (Colvin *et al.*, 2012) for RC surgery by 2006. RC pathology affects individuals in careers as diverse as hairdressing and professional athleticism and the vast aetiologies contributing to RC tearing makes this condition increasingly prevalent (Mitchell *et al.*, 2005). RC tear reports surge as working environments become more competitive, requiring individuals performing repetitive arm motions in their daily careers to strain their shoulders even more.

Current research on the RC complex and the epidemiology of tear formation focus on describing how individual muscles of the RC complex are affected, neglecting the anatomical and biomechanical complexity of this structure. The anatomy of the (RC) complex has been

described as having 5 histological, and two macroscopic layers (Codman, 1934; Clark and Harryman, 1992; Dean *et al.*, 2012; Vosloo *et al.*, 2017). When a RC tear presents, the mobility, strength, and range of motion of the arm become negatively affected. When surgeons do not take into consideration in their surgical technique that two layers with varying biomechanical characteristics exist, they are responsible for altering the biomechanical capability of the shoulder they are repairing. The capsular layer is especially disregarded by most surgeons, though it may very well display with individual biomechanical characteristics, such as elasticity.

Modulus of elasticity measures the resistance of a material to becoming elastically deformed when a load is applied (Vaidya and Pathak, 2018). The elastic modulus is described as a ratio of “stress applied to material” to “strain associated with applied stress”, and can be calculated with Hooke’s Law ($E = \sigma/\epsilon$) when a rigid homogeneous material is tested (Kent, 2006; Elkatatny *et al.*, 2017). However, the RC complex consists of soft-tissue that is non-homogeneous and therefore requires a modified method for calculating elastic modulus (Mallett and Arruda, 2017). Recent literature details the use of digital image correlation (DIC) in extracting data from photos, calculating full-field deformation, and interpreting this into data points that can be used to construct stress/strain curves from which elastic moduli can be obtained (McCormick and Lord, 2010; Mallett and Arruda, 2017). When viewing these graphs stress is denoted as σ and conveys force applied to the tissue per unit area. Strain is denoted as ϵ and conveys the extension a material undergoes. A steeper σ/ϵ slope with little extension prior to yield demonstrates a stiffer, and therefore more brittle object (Rothenberg *et al.*, 2017). Where the stress/strain values increase at similar rates and reach equally great values, the material can be interpreted to be both stiff and strong, or able to withstand great tensile loading. The toughness of the tissue is measured by viewing the surface area underneath the curve; larger surface areas imply that more energy will be required to break the material (Hayden *et al.*, 1965; Boyer, 1987; Courtney, 1990). A typical elastic modulus data series proceeds at an incline where both stress and strain values increase, reaching a “dipping point” where a brief decline in the slope is seen, followed by a temporary return to the incline trend. This “dipping point” is the yield point of the material being subjected to tensile loading, but should not be confused with the break point, which is the ultimate and total failure of the material (Peloquin *et al.*, 2016). The yield point is important in biomedical technology as it is the value which materials used in reparative operations are compared to, ensuring they have a much greater

yield strength to withstand forces that will act on the affected region post-operatively (Väänänen *et al.*, 2008; Gorash and MacKenzie, 2017).

Very few studies have investigated the idea that the biomechanical properties, such as the elastic modulus, between the capsular and tendinous layers of the RC vary. Those that have delved into these biomechanical differences mainly focus on the SS. Nakajima and co-authors (1994) were among the first to study biomechanical differences in the RC complex. In their study, which focussed on supraspinatus (SS), they found that the capsular layer displayed with a greater elastic modulus value (average of 8.2MPa +/- 0.2SD) when compared to the overlying tendinous layer (average of 7.2MPa +/- 0.3SD). The findings of Nakajima *et al.* were from a cadaveric sample obtained after they had sectioned the SS into thirds, thus the average elastic modulus value obtained is likely not an accurate representation for SS as a whole (Nakajima *et al.*, 1994). Another study on SS was conducted a year later by Itoi *et al.* (1995), where the muscle was again sectioned into thirds to gauge the individual strength of the anterior, middle, and posterior portions, and elasticity contributions. The modulus of elasticity in the particular case was reported at an average of 26.6MPa (SD of 11MPa) for SS (Itoi *et al.*, 1995), yielding vastly different values to those obtained by Nakajima *et al.* (1994).

Recently, Vosloo *et al.* (2018) conducted a biomechanical study on the RC complex and noted that elasticity of the tendinous and capsular layers varied. A personal communication within the dissertation by Vosloo states that the tendinous layer is believed to be more resistant to tensile loading, and therefore able to undergo more elastic deformation, than the capsular layer (MA de Beer 2018, pers. comm.). For the tendinous layers of SS, IS and SC, Vosloo (2018) obtained elastic modulus averages of 15.5 MPa, 11.5 MPa, and 79.3 MPa, respectively. For the capsular layers of SS, IS, and SC average elastic modulus values of 27.4 MPa, 23.5 MPa, and 0.9 MPa were respectively obtained. The instrument used to record these results was an MTS TestSuite™ TW Essential (TWS) Software 4.1.5.736 coupled to an MTS Criterion Model 41 (Vosloo, 2018). Recent studies highlight the use of DIC analysis as being superior in calculating stress and strain tissues undergo during tensile loading, from which elastic modulus values can be obtained. Using DIC should produce a more accurate data yield associated with elastic modulus pertaining to soft tissue samples. The current observational study thus used the TEMA software DIC algorithm to provide a more detailed description and create a better understanding of how the tendinous and capsular layers of the RC components differ in elasticity.

4.1.3. Materials and Methods

Eight (n = 8) fresh frozen human shoulders were obtained from the National Tissue Bank, once ethical clearance had been granted by the University of Pretoria Health Sciences Faculty's Ethics Committee (Annexure 1 and 2; Ethics approval number 384/2018). The shoulders were randomly selected from an adult sample (>18 years), yielding a sample of all white South Africans with age ranging from 44-88 years, equally divided between left and right shoulders. Where pathology was noted, the affected portion of the RC was excluded from testing. Sex, and ancestry were not considered exclusion criteria.

The skin, fat, and translucent fascia was removed along with all muscles of the scapula and proximal humerus, except the SS, IS, and SC. These remaining RC muscles were reverse dissected towards their insertion on the humerus and then sectioned into SS, IS, and SC portions of approximately 20x20mm wide strips. The tendinous and capsular layers were then separated by sharp dissection through the fascial plane between them, to a point where they were indistinguishable from each other (Figure 4.1.1). The end-product of this dissection yielded six strips for testing, one tendinous and one capsular layer for the SS, IS and SC. These strips were treated with standard phosphate buffered saline (PBS) solution throughout testing to maintain moisture levels and keep the strips as close to a natural state as possible. An electric bone saw was used to cut through the humeral shaft approximately 20cm from the most superior point on the humeral head.

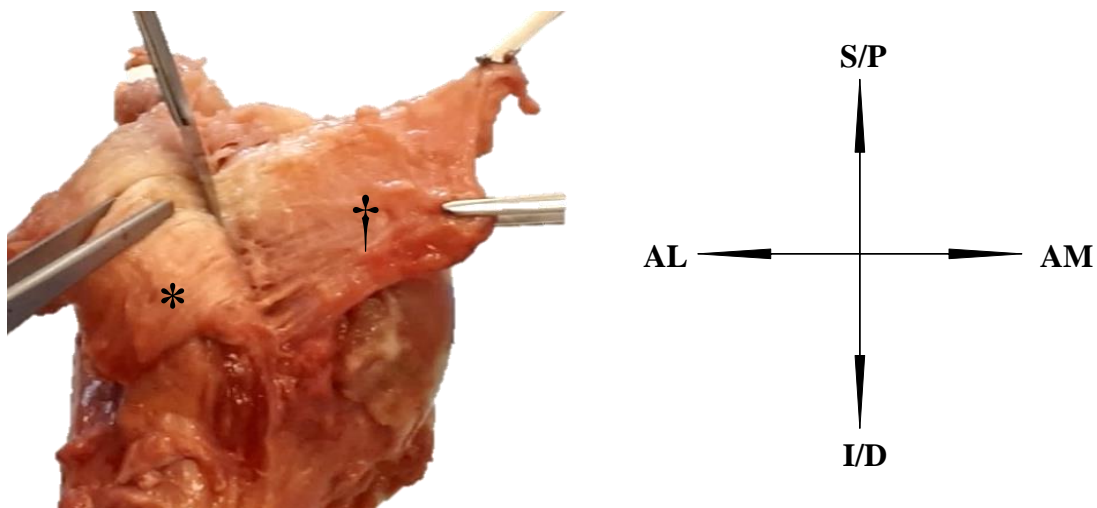


Figure 4.1.1. Proximal humerus showing sharp dissection through the fascial plane connecting the tendinous (*) and capsular (†) layers of the SC of a right arm. *S/P* – Superior/Proximal; *AL* – Anterolateral; *AM* – Anteromedial; *I/D* – Inferior/Distal.

In order to observe the range of elasticity of each strip individually the prepared specimen was separately clamped around the humeral shaft at one end and by the strip at the other end. These clamps were then mounted on a 25kN servo-hydraulic universal testing machine (Instron model 1342), which was programmed with a conformance of ASTM E 4. The clamp holding the humeral shaft was mounted on the lower fixture connected to the fixed base plate, and the clamp clasping the strip end was mounted on the upper fixture connected to the load cell of the Instron, in as near to the anatomical position as possible (Figure 4.1.2.A).

Next, a stereo camera setup of two IDT NX8-S2 cameras was done to capture tensile testing images for digital image correlation (DIC) analysis. 50mm lenses were used at a distance of approximately 435mm from the testing area, obtaining a field view of 120x90mm. To attain symmetric camera orientation, the use of a laser diode was incorporated. In order to eliminate lens distortion and calculate camera orientation the camera setup was calibrated using a square-shaped pattern calibration panel with a pitch distance of 7mm. The yield of this setup was a ten-frame-per-second stereo capturing of the speckle pattern deformation in the RC strip analysed. A CoCo-80X digital signal analyser additionally recorded the displacement and load measurements taken by the Instron. Three-dimensional point tracking and DIC analysis were performed using TEMA motion analysis software. The final setup of testing can be viewed in Figure 4.1.2. This setup and information were provided by Dr Oberholster (AJ Oberholster 2019, pers. comm.).

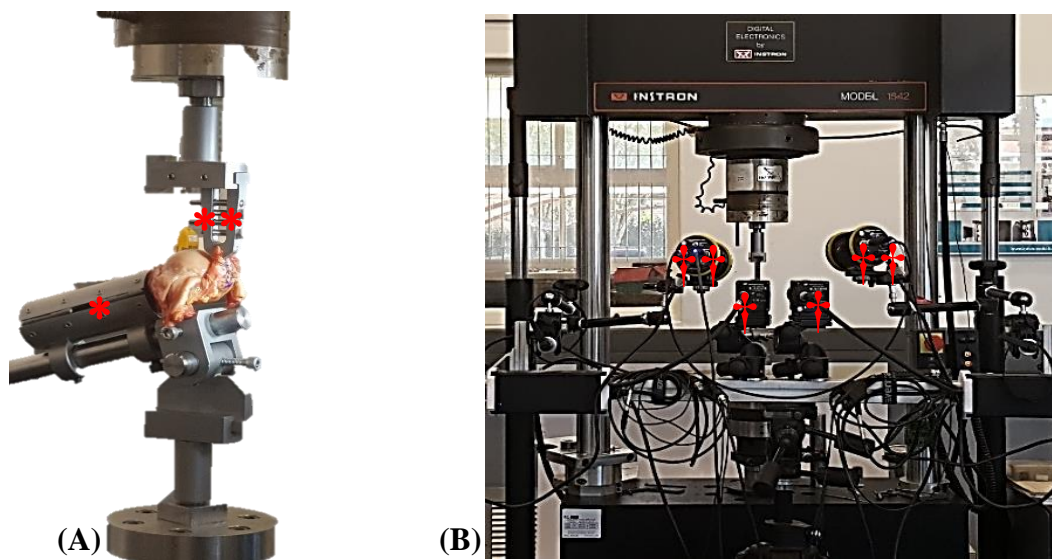


Figure 4.1.2. (A) Shows the humeral shaft clamped (*) and mounted on the fixed base plate, with the tendinous strip of the SS clamped (**) and mounted to the load cell. (B) Shows the DIC cameras (†) mounted on a stand and aimed at the testing area of the Instron with two accompanying lights (††).

To measure the elastic deformation of each strip, markers were placed on the clamps which served as reference points of known size, and the strip being tested was sprayed with water insoluble ink. The strip spraying was done manually using a toothbrush to create random, fine speckles on the surface of the strip facing the camera. The DIC algorithm correlates the random speckle pattern in the images and tracks the displacement of the speckles to calculate and visualise strain.

For each specimen the capsular layer was tested before the tendinous layer and testing of SS, IS, and SC were randomised. Once the specimen was fixed to the Instron and could be mechanically loaded, the cameras were activated and began documenting the strip displacement. A tracker definition was used by DIC conforming the analysis to a 10x10 x:y area, incorporating the width and thickness of the strip, and yielding error reports of the recording accuracy (Figure 4.1.3).

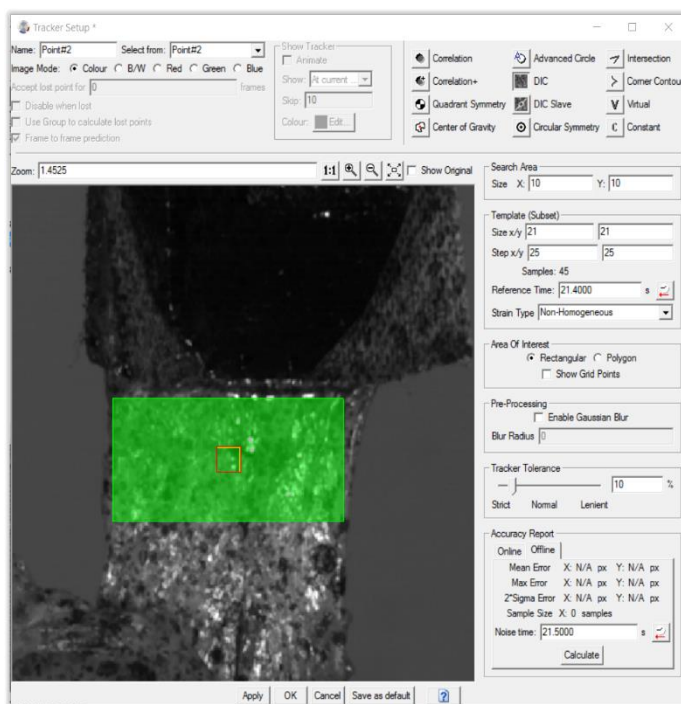


Figure 4.1.3. DIC tracker definition analysis.

As the strip is being mechanically loaded, calculated strains are mapped onto an area of interest focussed on by the cameras. A virtual extensometer is added to this image in line with the clamp holding the strip and the load path, to obtain average engineering strain across the area of interest (Figure 4.1.4).

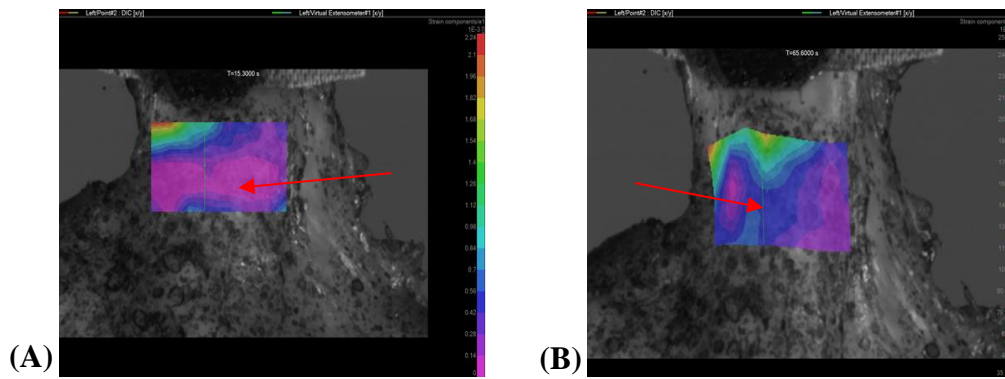


Figure 4.1.4. DIC results for the tendinous layer of an IS strip where (A) is the reference image taken and (B) is the image representing deformation, in the blue area indicated by the red arrows of the TEMA software.

The capsular and tendinous portions of the SS, IS, and SC of each of the samples had been mechanically loaded up to a point of plastic deformation, after which no elastic information could be gathered. These DIC results then underwent post-processing where vertical displacement was calculated and Instron displacement measured. Engineering stress was calculated for each sample using the following equation: $\sigma_{eng} = F/A$ (where F represents load, and A represents cross-sectional area). Young's modulus (or elastic modulus) was then calculated using a linear curve-fitting applied to the generated graphs. Correlation and regression statistics were also included to observe whether thickness held any correlation with elasticity outputs.

4.1.4. Results

Reverse dissection of the RC muscles from their origins to insertion on the humerus revealed that the SS, IS, and SC insert across the humeral tuberosities as interdigitated tendinous and capsular sheets. Approximately 15mm from the insertion onto the humerus the SS, IS, and SC are indistinguishable from one another, save for following the course of their muscular ends into the capsular-tendinous junction. Upon sharp dissection of each section 20mm from the humeral insertion, the tendinous and capsular layers could be visualised as individual layers, connected through parallel fibres or a facial plane (Figure 4.1.1). The tendinous layer was consistently thicker than its capsular counterpart per SS, IS, and SC section, except in one case (SC 014). The majority of the tendinous and capsular layers could be tested; where pathology was noted, the strip was excluded from the final findings.

Table 4.1.1. Elastic modulus, approximate yield points, and thickness records obtained from graphs generated during DIC post-processing

Arm	Layer	Elastic Modulus (MPa)	Yield Point (Strain; Stress(kPa))	Thickness (mm)
004	SST	68.673	(0.079; 3281.935)	05.20
	ISC	31.248	(0.225; 6105.059)	02.10
	IST	82.654	(0.133; 6740)	05.60
	SCC	76.568	(0.191; 8476.557)	03.20
	SCT	32.571	(0.262; 6692.789)	04.70
006	SST	20.894	(0.136; 1449.761)	02.80
	ISC	21.246	(0.210; 2855.471)	01.80
	IST	52.867	(0.178; 3809.552)	03.70
	SCC	24.598	(0.227; 4606.856)	03.20
	SCT	79.514	(0.118; 3234.369)	04.50
007	SSC	11.130	(0.092; 932.238)	03.40
	SST	75.995	(0.088; 4812.952)	04.60
	ISC	42.782	(0.076; 3195.602)	02.60
	IST	38.805	(0.187; 4670.383)	04.00
	SCC	22.583	(0.234; 3745.087)	03.40
	SCT	55.468	(0.044; 2107.152)	06.80
008	ISC	36.552	(0.118; 3562.897)	03.20
	IST	30.478	(0.233; 6370.965)	04.20
	SCC	44.254	(0.154; 5004.433)	02.10
	SCT	84.761	(0.085; 6483.808)	03.80
010	SSC	38.846	(0.177; 6339.768)	01.00
	SST	108.387	(0.107; 5067.690)	03.75
	ISC	41.173	(0.114; 4320.675)	01.50
	IST	47.327	(0.094; 3171.895)	04.00
	SCC	57.497	(0.157; 5218.825)	02.40
	SCT	54.712	(0.100; 3383.150)	04.60
011	ISC	38.318	(0.078; 2800.598)	02.20
	IST	203.806	(0.034; 4672.639)	04.35
	SCC	60.826	(0.202; 8179.384)	02.20
	SCT	45.111	(0.075; 4702.437)	03.50
013	SSC	26.233	(0.074; 1923.489)	02.80
	SST	36.305	(0.070; 2504.884)	05.30
	ISC	5.891	(0.118; 691.783)	02.80
	IST	22.909	(0.231; 4914.533)	04.60
	SCC	22.794	(0.150; 2851.674)	03.00
	SCT	78.120	(0.139; 3390.910)	06.30
014	SSC	39.812	(0.067; 3267.026)	03.00
	ISC	42.390	(0.111; 4509.902)	01.10
	IST	57.479	(0.090; 4737.918)	04.10
	SCC	22.774	(0.140; 1979.171)	04.60
	SCT	46.657	(0.198; 7962.914)	04.10

Table 4.1.1 summarises the elastic modulus, approximate yield point, and thickness of the respective capsular and tendinous layers for each specimen's SS, IS, and SC; the corresponding graphs can be viewed in Annexure 5. Where C follows the muscle abbreviation the capsular

layer has been indicated, and where T follows the muscle abbreviation the tendinous layer has been indicated (e.g. SSC corresponds to the capsular layer for SS, and SST corresponds to the tendinous layer for SS, etc.). The bolded values indicate the highest elastic modulus value obtained for the capsular and tendinous layers for each SS, IS, and SC. Pathology affected six of the segments to be tested, therefore these were excluded. The capsular layers of the RC sections generally yielded lower elastic modulus readings than their tendinous counterpart of the same shoulder, except in 5 of the 19 comparisons. The mean elastic moduli for all capsular and tendinous layers were 27.383 (+/- 12.181 SD) and 72.340 (+/- 29.579 SD) MPa respectively for SS, 32.450 (+/- 12.902 SD) and 67.041 (+/- 58.201 SD) MPa respectively for IS, 41.487 (+/- 21.417 SD) and 59.614 (+/- 18.980 SD) MPa respectively for SC. Yield points are provided to indicate the approximate point past which the RC section underwent plastic deformation and the elasticity readings past this point are observably lower. The yield point can be observed where strain increased more quickly than stress which brought on permanent deformation in the tissue.

The average thickness for all capsular and tendinous layers were 3.067 and 4.330mm respectively for SS, 2.163 and 4.319 respectively for IS, and 3.013 and 4.788 respectively for SC. To evaluate whether the thickness of the sample correlated with the final elastic yield, Pearson's correlation coefficient and linear regression was done. The equation used to calculate Pearson's correlation coefficient reads as follows:

$$r = \frac{[n\sum xy - (\sum x)(\sum y)]}{\sqrt{[n\sum x^2 - (\sum x)^2] \cdot [n\sum y^2 - (\sum y)^2]}}$$

In the equation, r represents Pearson's correlation coefficient, n is the number of pairs of scores, \sum is the sum of, xy is the product of the paired scores where x represents sample thickness and y represents elasticity. Upon inserting the obtained values for sample thickness and corresponding elasticity into the equation, a value of $r = 0.306$ was obtained.

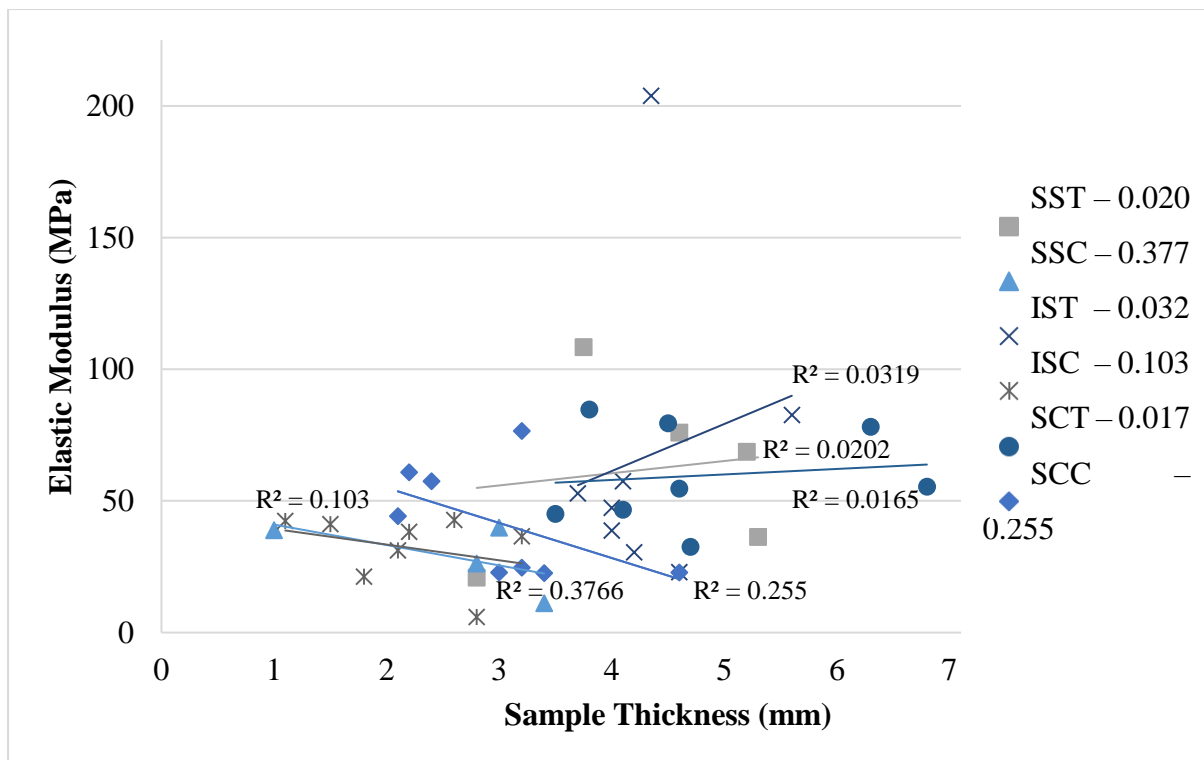


Figure 4.1.5. Linear regression of elastic modulus and sample thickness for tendinous (T) and capsular (C) layers of SS, IS, and SC, displayed as R^2 values.

Next, linear regression values were obtained, as seen in Figure 4.1.5, for both the tendinous and capsular layers of SS, IS, and SC respectively. Graphs were plotted with sample thickness on the x-axis and elastic modulus values on the y-axis, and then linear trend lines were fitted to each graph. Linear regression can be calculated using the following equation:

$$y = b_0 + b_1 \cdot x$$

In the equation, y represents the dependent variable (in this case elastic modulus), b_0 represents the intercept, b_1 represents the slope, and x is the independent variable (sample thickness). According to the graphs, linear regression values were obtained ranging from 0.016 (for SCT) to 0.376 (for SSC).

The graphs that follow are isolated representations of the overall generated graphs for elastic modulus, to avoid repetitiveness. The DIC post-processing yielded stress (kPa) and strain (unitless) values which were plotted against each other to obtain graphs. Linear curve-fitting was applied to the graphs, of which the steepest slope indicated the elastic modulus for that sample.

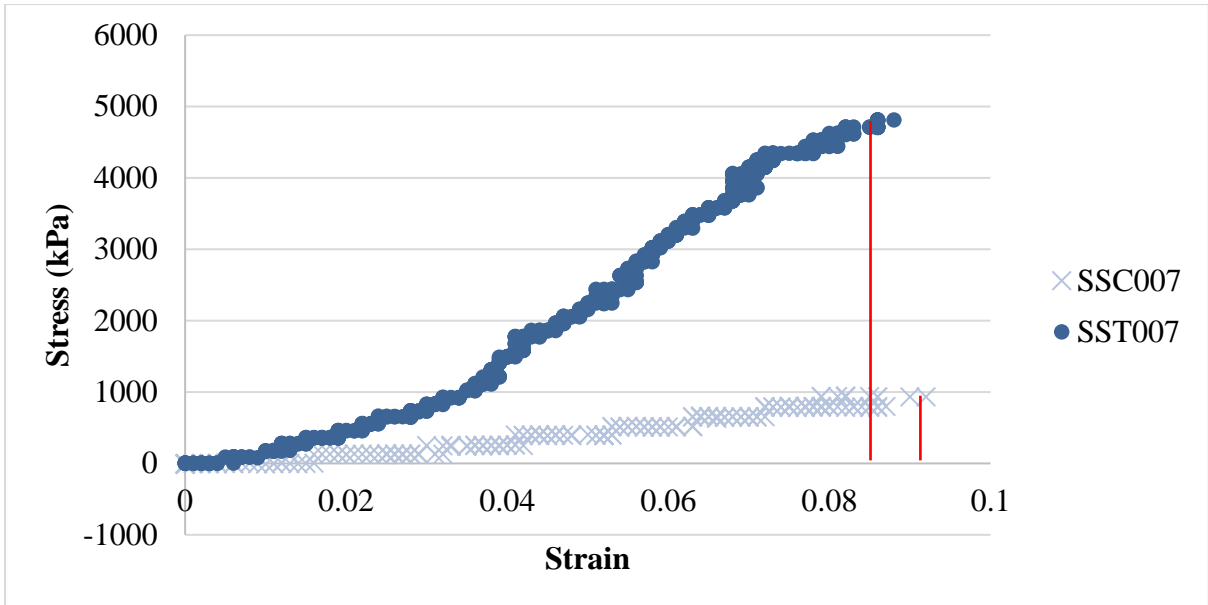


Figure 4.1.6. SS tendinous layer (dots) observed to have a greater elastic modulus than SS capsular layer (crosses) observed throughout SS testing.

Figure 4.1.6 demonstrates a typical Young’s modulus slope where the tendinous portion of SS for sample 007 is indicated in blue with an observably steeper slope than the capsular layer, indicated by grey x’s. Approximate yield points for tendinous and capsular layers varied little in measures of strain, seen between 0.08 and 0.1, but varied more in stress levels observed at almost 5000 kPa for the tendinous portion, but only nearing 1000 kPa for the capsular portion. More varying stress values lead to an observably greater surface area beneath the SST curve.

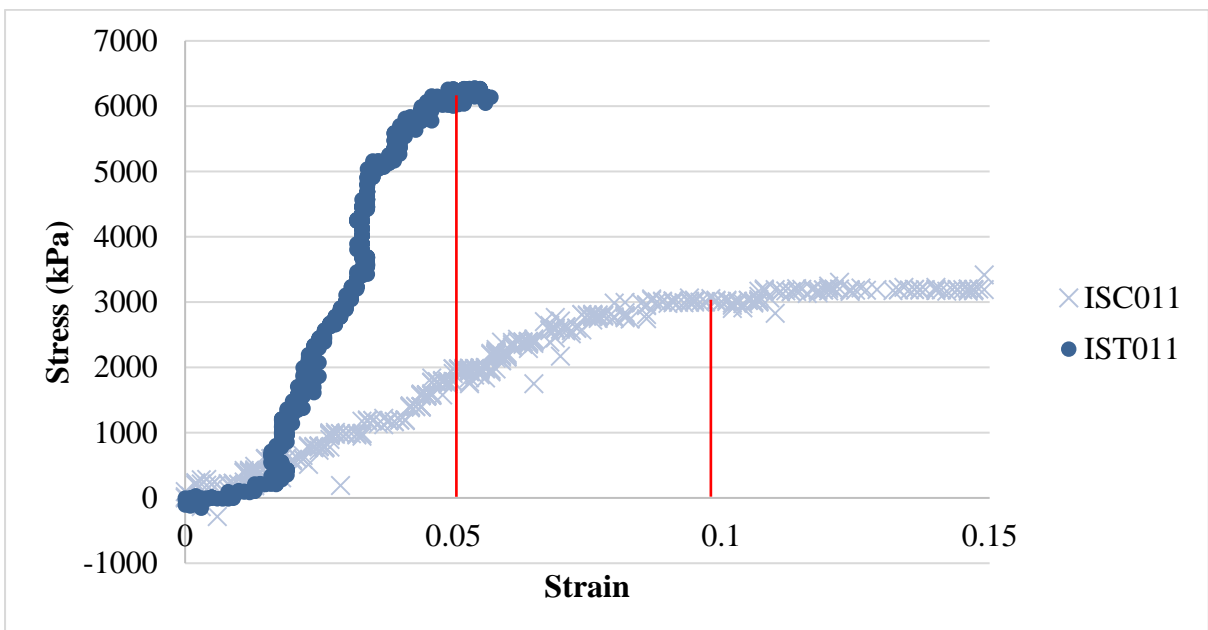


Figure 4.1.7. IS tendinous layer (dots) observed to have a greater elastic modulus than IS capsular layer (crosses) in 6 of 7 tests of IS.

Figure 4.1.7 compares the tendinous (IST) and capsular (ISC) layers of sample IS 011 where the tendinous layer can be seen to have a greater maximum stress but low strain yield, and the capsular layer has a lower stress but higher strain yield. Although the strain and stress yield points for tendinous and capsular layers vary considerably, the surface area beneath the two curves appears to be approximately the same.

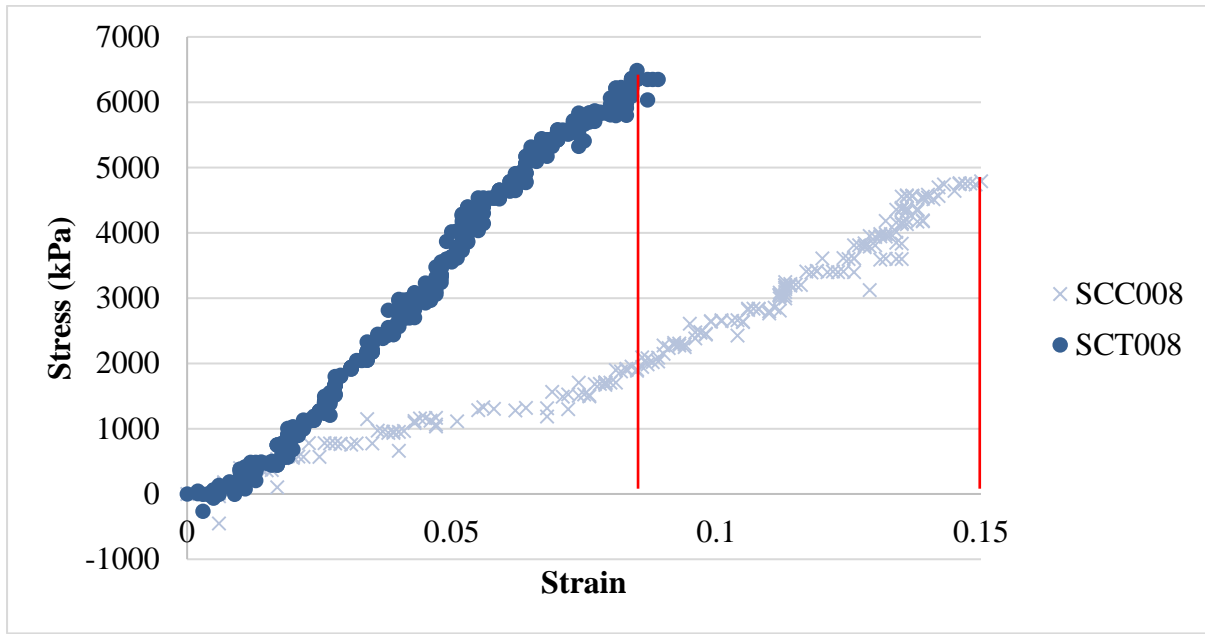


Figure 4.1.8. SC tendinous layer (dots) observed to have a greater elastic modulus than SC capsular layer (crosses) in 6 of 8 tests of SC.

Figure 4.1.8 shows similar findings to the previous figures but with a more parallel, albeit delayed for the capsular portion, stress/strain path. The surface area, depicting tissue toughness, is similar for both layers. The range in stress values for the yield point is narrower (± 1500 kPa) compared to the ranges obtained for SS (± 4000 kPa) and IS (± 3000 kPa) specimens between tendinous and capsular layers.

To view the remainder of the graphs comparing the capsular and tendinous portion for individual shoulders please refer to Annexure 6.

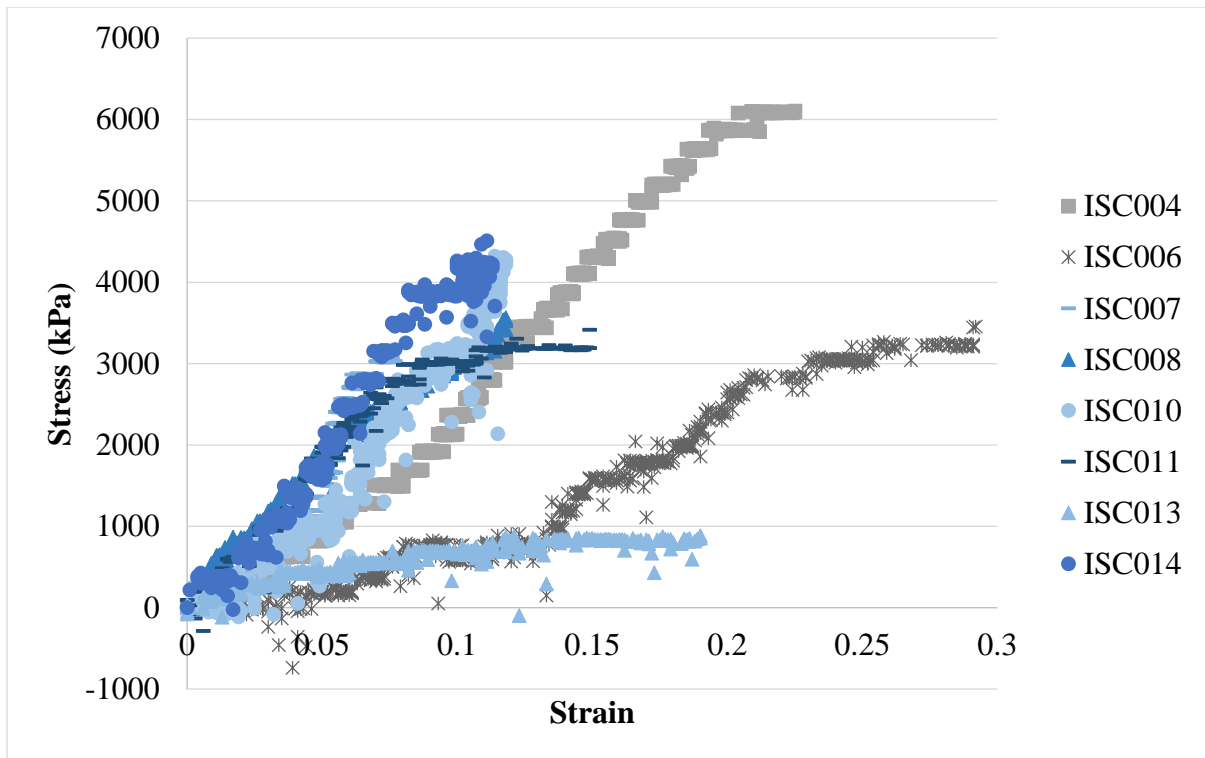


Figure 4.1.9. Representation of variation between IS capsular layers of eight individuals.

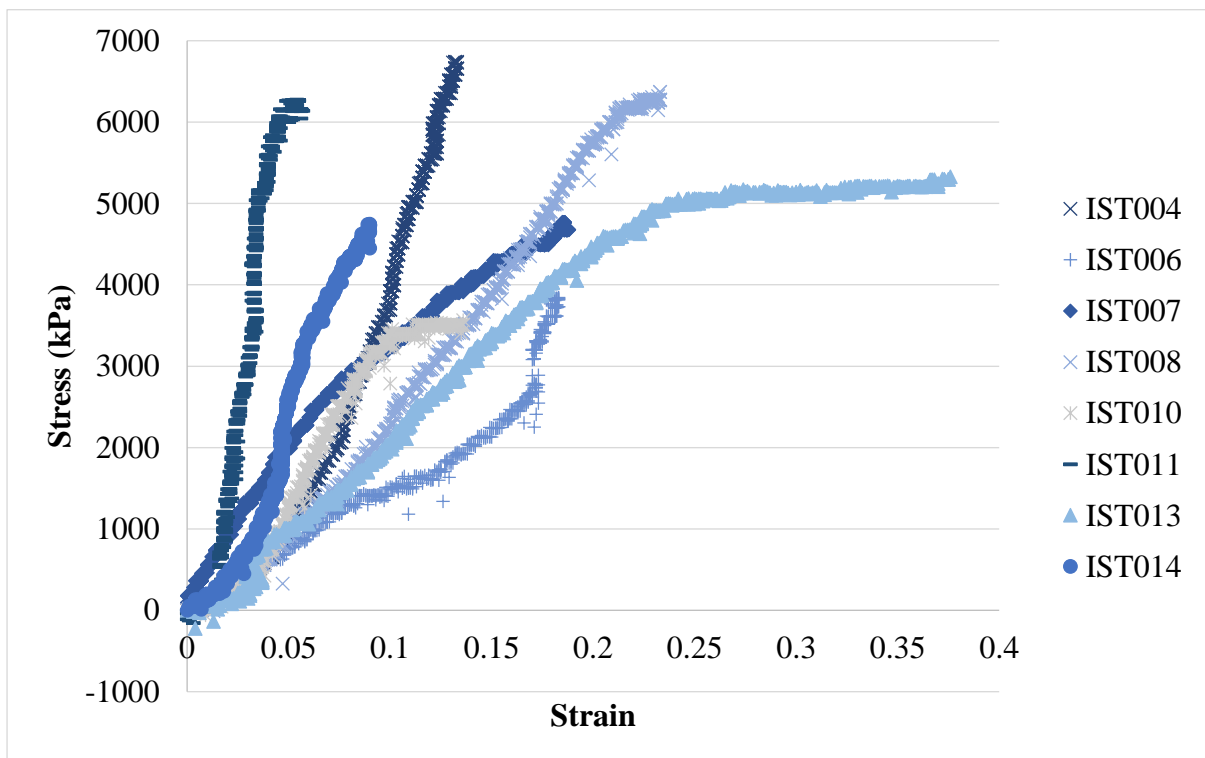


Figure 4.1.10. Representation of variation between IS tendinous layers of eight individuals.

Figures 4.1.9 – 4.1.10 are included to show inter-individual variation of the capsular and tendinous layers respectively for IS. An initial toe-region, where the graphs appear compacted, can be most clearly visualised between 0 and 0.025 strain. All samples appear to follow the

same trend, then begin to vary in strain and stress values after 0.025 strain. The tendinous layer (Figure 4.1.10) follows an observably steeper trend when viewed in comparison with the capsular layer (Figure 4.1.9) for IS. These observations were similar for the SS and SC capsular and tendinous comparisons and can be viewed in Annexure 7.

4.1.5. Discussion

The present manuscript aimed to provide elastic modulus data for both the tendinous and capsular layers of the SS, IS, and SC. The insertion of these muscles was found to be an interconnected, interdigitated complex of tendinous and capsular layers. Parallel fibres (a fascial plane) formed strong but moveable connections between the layers, so that the layers could be observed to ‘slide’ over one another when one or the other layer was pulled.

Other than the existence of these anatomically distinguishable layers, this study verifies the biomechanical variation between the tendinous and capsular layers of the RCs’ SS, IS, and SC respectively, as well as between capsular layers and tendinous layers respectively of various individuals. In Table 4.1.1 distinct differences in the elastic modulus and thicknesses of the tendinous and capsular layers can be observed. The tendinous layers were found to be thicker and also have higher elastic moduli/stiffness in all cases but for the SC capsular layer of 014.

To investigate whether increased thickness of the tendinous and capsular layers contributed to increased elastic moduli values, Pearson’s correlation coefficient and linear regression values were calculated. According to the Pearson’s correlation coefficient value obtained in the current study, 0.306, a weak positive relationship exists between sample thickness and elastic modulus. According to the values obtained in the linear regression analysis seen in Figure 4.1.5, keeping in mind the small sample size, 2-38% of the dependent variable (modulus of elasticity) could be predicted by the independent variable (sample thickness). These results indicate that thickness is not an accurate predictor of elastic modulus for the tendinous or capsular layers of the RC complex. This is to be expected as elastic modulus has been found, in principle, to be independent of sample thickness in other engineering materials tested (Wang *et al.*, 2013). Although no direct correlation could be made between the thickness of the segment and the elastic modulus, the trend of thicker tendon than capsular layer also generally carried through to higher elastic moduli for tendinous than capsular layers.

In Figures 4.1.6-4.1.8 red lines are drawn perpendicular to the x-axes approximately at the yield points to demarcate the surface area under the graph. Figure 4.1.6 was estimated to have

a steeper slope for the tendinous portion (SST) for shoulder 007 than the capsular portion (SSC), but with approximately the same extension values. The surface area beneath both graphs is quite large implying toughness of SST and SSC. The steeper slope of SST implies both strength and ductility, whereas the SSC yields a slope which also indicates ductility, but less strength than SST. The graph visually mimics the average elastic moduli findings for the capsular and tendinous layers of SS throughout testing, seen in the steeper slope for the tendinous portion (average elastic modulus of 72.340 MPa) as compared to the more gracile slope of the capsular portion (average elastic modulus of 27.383 MPa). The slope seen for SSC in Figure 4.1.6 is typically observed where plastic materials have been subjected to slow loads, these materials are thought not to have a 'fracture point'.

Figure 4.1.6 was observed with a drastically steeper slope for the tendinous portion (IST) than the capsular portion (ISC) which had a more gradual incline. The similar surface area beneath both curves imply similar toughness in the tendinous and capsular portions of the tissue. Whereas shoulder 011 IST can be estimated to be a stronger material based on the greater stress yield, ISC would be more ductile and not as strong, based on the greater strain and lesser stress yields. The tendinous portion appears to have a shorter period of plastic deformation before reaching a break point than the capsular portion which can be seen to remain in a state of plastic deformation between 0.1 and 0.15 strain before a break point was reached. The slope seen for IST in Figure 4.1.7 is typical of a brittle material, implying that the tested material acts like bone. However, IST did not follow a completely linear path for stress/strain values, consistent with non-homogeneous, viscous materials.

Figure 4.1.8 depicting shoulder 008 shows similar surface areas for both the capsular (SCC) and tendinous (SCT) portions of SC. It is expected that their toughness is similar, but that these layers differ in strength and ductility. Whereas SCT would be stronger due to the greater stress values, SCC would be more ductile, due to the greater strain values. This smaller stress yield range could indicate that SC capsular portion is more resistant to stress forces than the capsular portions of SS and IS. For the remaining SC stress/strain graphs seen in Annexure 6, more variability was noted than for SS and IS. Shoulder 010 could be found with almost the same findings as shoulder 008, which has been discussed. Shoulders 006, 007, and 011 were observed to have greater surface area beneath the capsular layer (SCC) than the tendinous layers (SCT). 006 and 011 are expected to have tougher SCC compared with SCT as the surface area is less beneath the tendinous portions, and also stronger and more ductile capsular layers than tendinous layers due to greater stress/strain yields. Shoulder 007 tendinous layer can be

interpreted to be tougher than that of shoulders 006 and 011, but still mechanically less ductile and possibly weaker than the capsular layer. The observational findings from Figures 4.1.6-4.1.8 indicate that the tendinous portions of the RC complex show generally stronger characteristics than their more ductile capsular counterparts, and that the RC is an anatomically tough structure.

In reference to Figures 4.1.9-4.1.10 which display variation between all analysed capsular and tendinous layers for IS, individual variation at this anatomical level can clearly be seen. Though the respective capsular and tendinous layers from different individuals originally follow the same course, once they reach stress values around 1000 kPa and strain values around 0.05 they begin to branch out. The values plotted up to 1000kPa and 0.05 strain can be described as the toe-region. The toe-region dictates that the fibres within the respective capsular and tendinous portions were loaded from a point where they were crimped up to a point at which they straightened out. Once the fibres of the tendinous or capsular layer were completely straightened, a more accurate depiction of the individual segment's stress/strain path could be visualised. The tendinous layers for IS (Figure 4.1.10) display with generally steeper slopes compared to the capsular layers (Figure 4.1.9). This steeper trend indicates tougher material property of the tendinous layer compared to the capsular layer which follows a more plastic material property trend. Upon comparing all tendinous and capsular layers respectively for SS and SC, similar findings were noted, and can be viewed in Annexure 7.

When comparing the results obtained in the present study with those observed by Vosloo *et al.* (2018) generally higher average elastic modulus values were obtained. The present study demonstrated that the capsular layer consistently displayed with elastic modulus readings lower compared to the tendinous counterpart per component, whereas Vosloo *et al.* (2018) observed the opposite, having more elastic capsular layers compared to tendinous layers, excluding SC. The significant contradictions between results obtained in the present study as compared to Vosloo *et al.* (2018) may be attributed to the use of DIC analysis in the present study, providing real-time deformation and more accurate elastic modulus readings as compared to those obtainable from standard MTS software output.

4.1.6. Conclusion

Previous studies on the RC complex either ignored the existence of the capsular layer or focussed on how much force the tendons could endure. Elastic modulus findings, particularly pertaining to the differences between tendinous and capsular layers of the RC have lacked

comprehensive exploration up to this point. This study detailed biomechanics of the more superficial tendinous and deeper capsular macroscopic layers of the RC with their joint insertion across the humeral tuberosities as two interdigitated sheets. Differences between these layers were noted in thickness as well as elastic moduli. It was noted that thicker samples would not necessarily yield greater elastic modulus values. Both layers were found to be quite tough, but the tendinous portions proved stronger than the capsular portions and could therefore be expected to extend more under tensile loading than the capsular layer. This fact alone should be cause for surgeons to operate on the tendinous and capsular layers as separate structures, as repairing them as one could significantly impact the ductility of the segment. Variation between different individuals' tendinous and capsular portions for RC segments highlight the fact that no two individuals can be operated on in the same way. Surgeons need to be aware of the different anatomical layers and that they respond differently to tensile loading. If these layers are not repaired individually, significant biomechanical loss can be experienced by patients with RC disease. For instance, if the surgeon were to bind the two layers together, the capsular portion could be expected to suffer greatly when exposed to loads usually only conducted through the tendinous portion, as the capsular layer is not as strong. A knowledge of the difference in elastic modulus records for the tendinous and capsular layers could lead surgeons to developing better operative techniques for mending tears found in one or both layers.

4.1.7. References

Boyer, H.F., 1987. Atlas of stress-strain curves. ASM International.

Clark, J., Harryman, D., 1992. Tendons, ligaments, and capsule of the rotator cuff: Gross and microscopic anatomy. *The Journal of Bone and Joint Surgery. American Volume.* 74: 713–725.

Codman, E.A., 1934. Rupture of the supraspinatus tendon and other lesions in or about the subacromial bursa, In: *The shoulder.* R.E. Kreiger.

Colvin, A.C., Egorova, N., Harrison, A.K., Moskowitz, A., Flatow, E.L., 2012. National trends in rotator cuff repair. *The Journal of Bone and Joint Surgery.* 94: 227–233.

Courtney, T.H., 1990. Mechanical behaviour of materials. McGraw-Hill.

Dean, B.J.F., Franklin, S.L., Carr, A.J., 2012. A systematic review of the histological and molecular changes in rotator cuff disease. *Bone and Joint Research.* 1: 158–66.

Elkatatny, S., Mahmoud, M., Mohamed, I., Abdulraheem, A., 2017. Development of a new correlation to determine the static Young's modulus. *Journal of Petroleum Exploration and Production Technology*. 8: 17–30.

Gorash, Y., MacKenzie, D., 2017. On cyclic yield strength in definition of limits for characterisation of fatigue and creep behaviour. *Open Engineering*. 7: 126–140.

Hayden, H.W., Moffatt, W.G., Wulff, J., 1965. *The structure and properties of materials (Volume III): Mechanical behaviour*. Wiley.

Itoi, E., Berglund, L.J., Grabowski, J.J., Schultz, F.M., Growney, E.S., Money, B.F., An, K.-N., 1995. Tensile properties of the supraspinatus tendon. *Journal of Orthopaedic Research*. 13: 578–584.

Kent, M., 2006. *The Oxford dictionary of sports science and medicine*, 3rd ed. Oxford University Press.

Lee, G.B., Kholinne, E., Kwak, J.-M., Sun, Y., Alhazmi, A.M., Jeon, I.-H., 2019. Infraglenoid muscle as an anatomic variation of the anterior rotator cuff. *Case Reports in Surgery*.

Mallett, K.F., Arruda, E.M., 2017. Digital image correlation-aided mechanical characterization of the anteromedial and posterolateral bundles of the anterior cruciate ligament. *Acta Biomaterialia*. 56: 44–57.

McCormick, N., Lord, J., 2010. Digital image correlation. *Materials Today*. 13: 52–54.

Mitchell, C., Adebajo, A., Hay, E., Carr, A., 2005. Shoulder pain: Diagnosis and management in primary care. *British Medical Journal*. 331: 1124–1128.

Nakajima, T., Rokuuma, N., Hamada, K., Tomatsu, T., Fukuda, H., 1994. Histologic and biomechanical characteristics of the supraspinatus tendon: Reference to rotator cuff tearing. *Journal of Shoulder and Elbow Surgery*. 3: 79–87.

Peloquin, J.M., Santare, M.H., Elliott, D.M., 2016. Advances in quantification of meniscus tensile mechanics including nonlinearity, yield, and failure. *Journal of Biomechanical Engineering*. 138: 0210021–02100213.

Rothenberg, A., Gasbarro, G., Chlebeck, J., Lin, A., 2017. The coracoacromial ligament: Anatomy, function, and clinical significance. *The Orthopaedic Journal of Sports Medicine*. 5: 2325967117703398.

Väänänen, P., Nurmi, J.T., Nuutinen, J.P., Jakonen, S., Happonen, H., Jank, S., 2008. Fixation properties of a biodegradable “free-form” osteosynthesis plate. *Oral Surgery, Oral Medicine, Oral Pathology, Oral Radiology and Endodontology*. 106: 477–482.

Vaidya, A., Pathak, K., 2018. Mechanical stability of dental materials, in: Asiri, A.M., Inamuddin, A.M. (Eds.), *Applications of Nanocomposite Materials in Dentistry*. Elsevier Imprint: Woodhead Publishing, pp. 285–305.

Vosloo, M., 2018. The biomechanical properties of the capsular and bursal layers of the rotator cuff complex: A clinical investigation. University of Pretoria.

Vosloo, M., Keough, N., de Beer, M.A., 2017. The clinical anatomy of the insertion of the rotator cuff tendons. *European Journal of Orthopaedic Surgery and Traumatology*. 27: 359–366.

Wang, S., Chen, G., Huang, H., Ma, S., Xu, H., He, Y., Zou, J., 2013. Vapor-phase synthesis, growth mechanism and thickness-independent elastic modulus of single-crystal tungsten nanobelts. *Nanotechnology*. 24: 505705.

4.2. Manuscript 2 Title – Biomechanical principle of the load capacity of the tendinous and capsular layers of the rotator cuff complex: Peak load

4.2.1. Abstract

Peak load is a biomechanical factor which describes the maximal strength, or tension threshold of a particular structure. Fourteen ($n = 14$) fresh tissue arms were obtained from the National Tissue Bank and dissected to a level that only the RC muscles remained attached to the humeral head. Segments measuring 2x2cm were retained for analysis. Bluehill 2 software was connected to an Instron (model 1342) MTS machine to record the peak loads obtained for both layers of SS, IS, and SC of all samples available. The tendinous layers for SS, IS, and SC could withstand greater tensile loads (252.736 N, 356.274 N, and 385.935 N respectively) when compared to their capsular layers (211.212 N, 168.542 N, and 281.736 N respectively). As the results obtained show significant differences exist in the peak loads of various RC components, surgeons should be wary of the capsular layer, which is often overlooked. Should surgeons treat the RC complex as consisting of only one layer they run the risk of damaging inherent structural biomechanics within the shoulder complex. The weaker capsular layer is at particular risk of damage when repaired to adhere to the tendinous layer, as it is not able to withstand the same tensile forces.

4.2.2. Introduction

The human shoulder is able to endure strain and almost constant active movement on a daily basis, being rotated, abducted and adducted at the joint by the rotator cuff (RC) muscles. The RC is made up of the supraspinatus (SS), infraspinatus (IS), subscapularis (SC), and teres minor (TM), which taper towards their insertion onto the proximal humerus as a superficial tendinous and deep capsular layer (Standring, 2016). When these muscles are placed under constant tensile loading or a sudden massive load, the elastic modulus for these segments reaches a yield point and/or break point where permanent structural change can be noted as a RC tear (Pandey and Willems, 2015).

Pain is usually the trigger symptom for most individuals with RC tears to go see a doctor. The pain that individuals with RC tears experience is conveyed to the brain through nerves known as nociceptors (Dubin and Patapoutian, 2010). These nociceptors are sensitive to inflammatory processes in their surrounding tissue. Inflammation is a normal part in the healing

process and occurs in two parts: inflammation is introduced in response to initial tissue damage, and is then stopped by anti-inflammatory macrophages towards the end of the healing process. However, when inflammation becomes chronic, damaged tissue degenerates even further (Abraham *et al.*, 2017). It is therefore fortunate when individuals with RC tears do experience pain, so that they may seek surgical reparation before the disease progresses too far. Unfortunately, RC tears aren't always painful and many individuals with torn shoulder tendons carry on as usual, not noticing their weakening range of arm movement and can remain asymptomatic (Mall *et al.*, 2010; Moosmayer *et al.*, 2013).

RC tears can occur anywhere within the capsular-tendinous structure of the complex due to the different forces and internal/external factors at play. As individuals age their tendons degenerate, which causes a weaker infrastructure more prone to lesions forming. Other intrinsic and extrinsic influences include arm over-use, poor health, and anatomical deviations such as the acromion shape chaffing the tendons beneath it (Codman and Akerson, 1931; Neer, 1972; McMaster and Troup, 1993; Lin *et al.*, 2004; Via *et al.*, 2013). However, the most common location for a RC tear has been noted as being on the capsular side (inside) of the RC complex. Capsular-sided partial thickness tears are more common than bursal-sided tears and when left untreated may spread from the capsular side to the bursal side as a full-thickness RC tear (Nakajima *et al.*, 1994; Luo *et al.*, 1998; Lee *et al.*, 2000). The point at which these tears originate has been postulated to be approximately 10-15mm from the most distal insertional area of the affected segment in a transitional area known as the "critical zone" (Codman, 1934; Itoi *et al.*, 1995; Levy *et al.*, 2008; Pandey and Willems, 2015; Naidoo *et al.*, 2016). When a tensile stress applied on a section of the RC is greater than the strength of that section a RC tear will most likely result in this critical area (Itoi *et al.*, 1995). As this critical zone becomes mostly affected in the capsular portion spreading to interstitial areas which lie deep to the tendinous layer, lesions are frequently overlooked during arthroscopy (McMonagle and Vinson, 2011). Utilising ultrasonography or MRI proves useful in identifying the existence of these deeper tears (Bryant *et al.*, 2002). A surgically relevant ultrasonographic or MRI report should detail the tear shape, location, and size, tendon retraction, and extent of fatty infiltration (Tawfik *et al.*, 2014). Once the relevant parameters surrounding the tear have been noted, invasive techniques are applied to mend RC lesions. The most common surgical approaches involve suturing of torn segments to the bone with suture-anchors, however studies have noted that certain suture-anchors cause bioreactions which lead to bone resorption (Chow and Gu, 2004; Hyatt *et al.*, 2016). Another error encountered in most RC repair surgeries is the general

lack of acknowledgement by surgeons of the existence of the capsular layer. Biomechanical studies have emphasised the anatomical existence of the capsular layer and have investigated the relative strength of this layer in comparison to the tendinous layer, but somewhat as an afterthought.

In 2013 Sano *et al.* analysed the stress distribution within the various RC tendons to study tear patterns. They found that, in the act of abduction, SS can translate a load of 50.1 Newtons (N), IS a load of 63.3 N, and SC a load of 22.5 N. When the arm is externally rotated SS can translate a load of 10.5 N, IS a load of 94.9 N, and SC a load of 15 N (Sano *et al.*, 2013). The peak load translated through SS was recorded in another study to be as much as 652 Newtons (N) (with a standard deviation, SD, of 278.4 N) in maximum contraction (Itoi *et al.*, 1995). Halder *et al.* (2000a) reported in their study that IS has a peak load of 2058.5 N (SD of 688 N) (Halder *et al.*, 2000a). SC has been previously reported with a peak load of 1724 N (SD of 492 N) (Halder *et al.*, 2000b). A general lack of complete testing documentation surrounding these studies leaves room for scepticism as to what the true peak load endurance of the healthy RC muscles' tendinous and capsular portions are, individually.

Peak load differences between the tendinous and capsular layers should be taken into account and lead surgeons to operate on the biomechanically different layers, separately. The current study aimed to provide a statistical and visual account of the existence of these separate layers with separate biomechanical capacities. Notes on the relative location where tears formed were also made strictly based on testing parameters, which do not necessarily relate to in-situ RC pathology, but were included for reference.

4.2.3. Materials and Methods

After approval by the Ethics Committee of the University of Pretoria, Health Sciences Faculty, 14 fresh frozen human shoulders were obtained from the National Tissue Bank (Annexure 1 and 2; Protocol number 384/2018). Random selection yielded a sample of all white South African shoulders from individuals ranging from 44-88 years old, of which 6 were right shoulders and 8 were left shoulders. If pathology affected a portion of the RC, the section was excluded from testing. Sex, and ancestry were not considered exclusion criteria. Lower age limits were set at 25 years as the study focussed on the older population, more subject to developing RC tears.

The skin, fat, and translucent fascia were removed along with all scapular and proximal humeral muscles, except SS, IS, and SC. These remaining RC muscles were reverse dissected towards their insertion on the humerus and then sectioned into SS, IS, and SC portions of approximately 20x20mm wide strips. The tendinous and capsular layers were then sharply dissected from each other through the fascial plane connecting them. The end-product of this dissection yielded six strips per specimen for testing, one tendinous and one capsular layer for the SS, IS, and SC. These strips were treated with standard phosphate buffered saline (PBS) solution throughout testing to keep them moist and as close to a natural state as possible. An electric bone saw was used to cut through the humeral shaft approximately 20cm from the most superior point on the humeral head.

Each of the prepared specimens were then clamped in turn around the humeral shaft at one end and by a strip at the other end in clamps designed by Mr R Verbeek from Elite Surgical, Gauteng (Figure 4.2.1). These clamps were then mounted on a 25kN servo-hydraulic universal testing machine (Instron model 1342), which was programmed with a conformance of ASTM E 4, making it ideal to accurately conduct tensile tests. The clamp holding the humeral shaft was mounted on the lower fixture connected to the fixed base plate, and the clamp clamping the strip end was mounted on the upper fixture connected to the load cell of the Instron. Each strip was clamped in an orientation as near to the anatomical position as was made possible by the testing setup.



Figure 4.2.1. Clamp on the left designed to hold the humerus around the shaft during testing, holes in clamp allow for screw placement to hold the humerus in place. Clamp on the right designed to hold onto capsular and tendinous strips between the teeth, with added sandpaper to prevent clamp tearing of strips.

Tensile testing was randomised between SS, IS, and SC, but in each case the capsular layer was tested before the tendinous layer. Once the specimen was mounted and ready, load was applied in displacement control at a rate of 5mm per minute. The software program which recorded the resultant extension and applied load was Bluehill 2 (Figure 4.2.2). Bluehill 2 tracked the load (in Newtons) and extension (in mm) for each sample, and isolated the peak load before failure.



Figure 4.2.2. Start screen for Bluehill software used to record the load (in Newtons) and extension (in mm) for each test of the tendinous and capsular RC components.

4.2.4. Results

Upon conclusion of the analyses on the six segments (three capsular and three tendinous) for all 14 shoulders, exclusion criteria in the form of pathology left a yield of 70 testable segments of the original 84.

Table 4.2.1. Peak load records (in Newtons) obtained during tensile testing using Bluehill 2 software coupled to Instron 1342

Specimen \ Layer	SSC	SST	ISC	IST	SCC	SCT
001				202.188	88.188	233.528
002	158.378	201.637	81.098	323.498	248.367	250.918
003	292.149	283.408	306.514	309.378	473.729	393.146
004		309.646	210.679	766.948	551.251	580.654
005			279.537	134.709	124.66	428.638
006		167.665	132.319	275.916	257.379	223.261
007	237.42	377.318	172.07	395	231.975	272.888
008			237.167	511.76	213.787	367.415
009	185.043	148.892		184.181	342.345	477.055
010	167.495	338.423	121.242	238.898	269.794	398.409
011			127.47	425.252	420.272	359.41
012	229.225	195.247	210.291	268.239		
013	110.456	215.122	48.551	491.285	215.11	437.459
014	309.527	290	95.567	460.589	225.711	594.378
Mean	211.212	252.736	168.542	356.274	281.736	385.935
SD	68.418	77.303	81.017	166.849	132.608	121.140

Table 4.2.1 summarises the peak load achieved per section for each sample, recorded in Newtons (N). Where the abbreviation of the muscle is followed by a C, the capsular layer has been indicated, and where followed by a T, the tendinous layer has been indicated (e.g. SSC is the capsular layer for SS, SST is the tendinous layer for SS, etc.). Bolded values indicate the greatest peak load achieved throughout testing for each layer of SS, IS, and SC. The peak loads recorded ranged from 48.551 N (IS capsular layer) to 766.948 N (IS tendinous layer). The capsular layers generally reached peak loads lower than their tendinous counterparts of the same shoulder, except in 8 of 33 comparisons. The peak load has been recorded as the maximum load applied to the RC segment before structural failure occurred to an extent that all further readings sampled through the Bluehill software decreased.

Table 4.2.2. Tendon thickness (in mm) obtained prior to tensile testing

Specimen \ Layer	SSC	SST	ISC	IST	SCC	SCT
004		5.20	2.10	5.60	3.20	4.70
006		2.80	1.80	3.70	3.20	4.50
007	3.40	4.60	2.60	4.00	3.40	6.80
008			3.20	4.20	2.10	3.80
010	1.00	3.75	1.50	4.00	2.40	4.60
011			2.20	4.35	2.20	3.50
013	2.80	5.30	2.80	4.60	3.00	6.30
014	3.00	4.75	1.10	4.10	4.60	4.10
Average	2.55	4.40	2.16	4.32	3.01	4.79
SD	1.06	0.96	0.69	0.58	0.81	1.17

Table 4.2.2 summarises some of the sections' thicknesses recorded prior to testing. Logistical constraints and tissue pathology resulted in certain sections not being recorded and tested. To evaluate whether thickness correlated with the peak load per RC segment, Pearson's correlation coefficient and linear regression analyses were conducted. Pearson's correlation coefficient is calculated using the following equation:

$$r = \frac{[n\sum xy - (\sum x)(\sum y)]}{\sqrt{[n\sum x^2 - (\sum x)^2] \cdot [n\sum y^2 - (\sum y)^2]}}$$

In the equation, r represents Pearson's correlation coefficient, n is the number of pairs of scores, \sum is the sum of, xy is the product of the paired scores where x represents sample thickness and y represents peak load. Upon inserting the obtained values for sample thickness and corresponding peak load into the equation, a value of $r = 0.551$ was obtained.

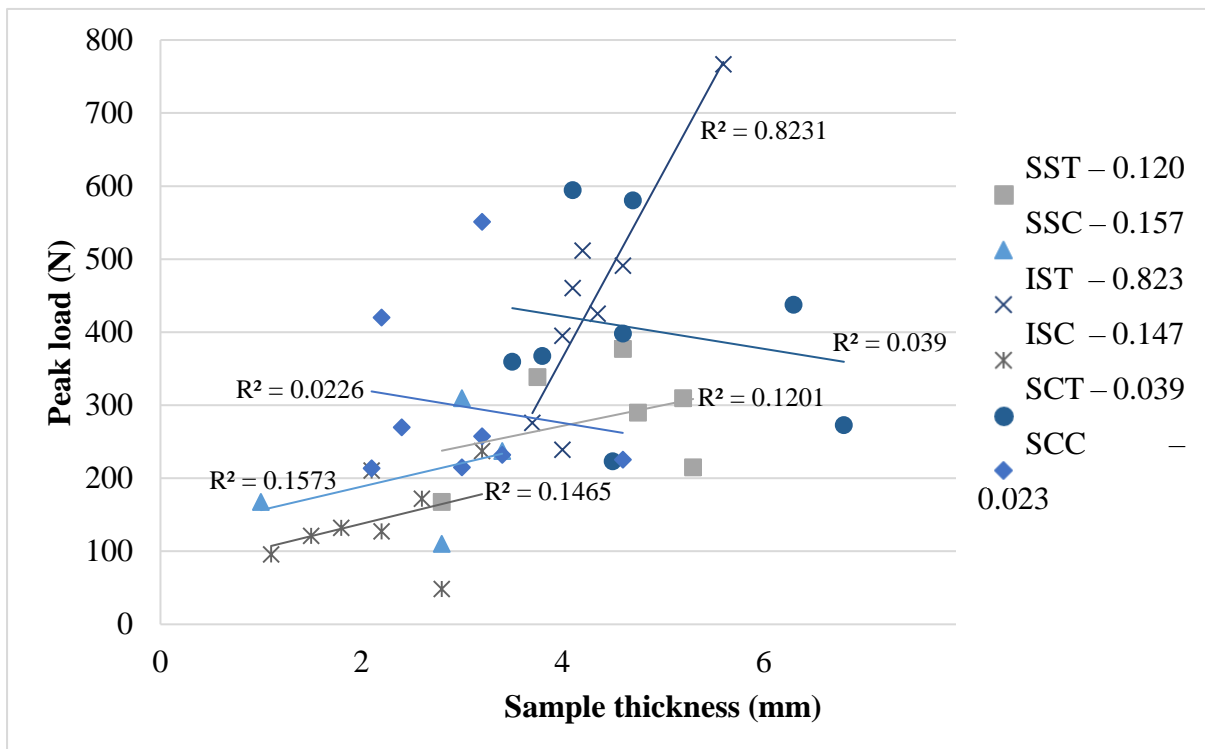


Figure 4.2.3. Linear regression of peak load and sample thickness for tendinous (T) and capsular (C) layers of SS, IS, and SC, displayed as R² values.

Linear regression values were obtained for both the layers of each RC unit (Figure 4.2.3). Linear regression graphs were generated with sample thickness on the x axis as the independent variable, and peak load values on the y-axis as the dependent variable. The equation used to calculate linear regression is as follows:

$$y = b_0 + b_1 \cdot x$$

In the equation, y represents the dependent variable (peak load), b_0 represents the intercept, b_1 represents the slope, and x is the independent variable (sample thickness). According to the graphs, linear regression values were obtained ranging from 0.023 (for SCC) to 0.823 (for IST).

Table 4.2.3. T-test for significance of mean values between RC components and between all capsular and tendinous layers respectively	
T-Tests per RC component	P-Value
SSC = SST	0.169
ISC = IST	0.003
SCC = SCT	0.019
T-Tests among capsular layers	
SSC = ISC	0.049
SSC = SCC	0.068
ISC = SCC	0.010
T-Tests among tendinous layers	
SST = IST	0.039
SST = SCT	0.018
IST = SCT	0.613

Table 4.2.3 depicts the t-test results for mean peak load comparisons of the SS, IS, and SC capsular and tendinous layers. The following hypotheses were formulated prior to testing:

H_0 : No significant differences exist between sample means

(SSC=SST; ISC=IST; SCC=SCT; SSC=ISC=SCC; SST=IST=SCT)

H_a : Significant differences exist between sample means

(SSC≠SST; ISC≠IST; SCC≠SCT; SSC≠ISC≠SCC; SST≠IST≠SCT)

Significant differences are seen as p-values less than or equal to 0.05. Once the mean had been recorded for all analysed capsular and tendinous layers, these were compared with t-testing, in order to note whether any significant difference existed between their tension threshold. After t-testing, p-values were obtained, which are reported in Table 4.2.3. Three of the nine comparisons done yielded results which conformed to the null hypothesis, H_0 , which were SSC=SST; SSC=SCC; IST=SCT. It is important to note that though significant differences were not obtained, this does not signify that the means are equal. The remainder of the tests yielded significant differences of p-values less than 0.05.

The following graphs are the product of all peak load values obtained from the Bluehill software linked to the Instron 1342 upon conclusion of testing.

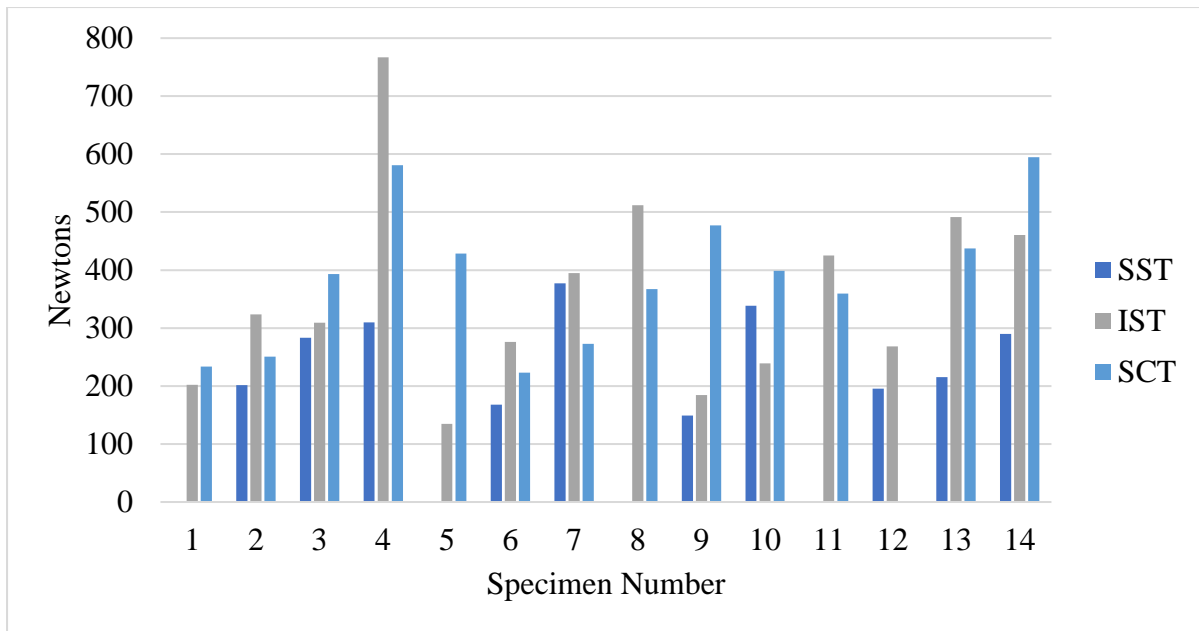


Figure 4.2.4. Comparison of the tendinous layer peak load yields for SS, IS, and SC for all samples.

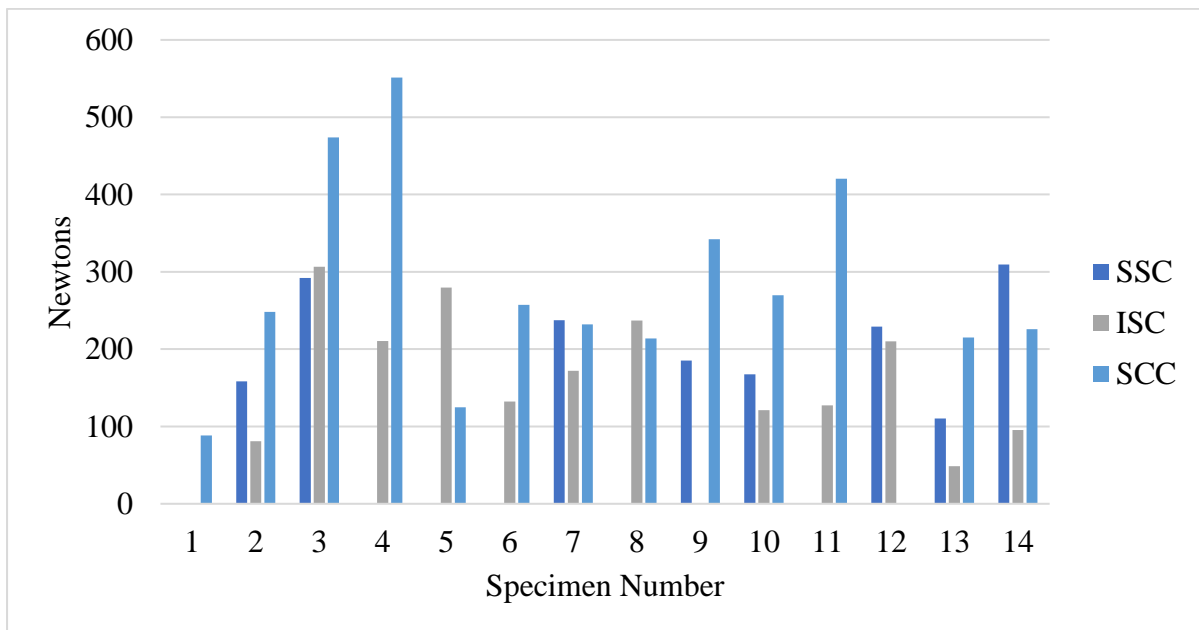


Figure 4.2.5. Comparison of the capsular layer peak load yields for SS, IS, and SC for all samples.

Figures 4.2.4-4.2.5 respectively demonstrate the peak load variation for the tendinous and the capsular layers of the three RC units for all analysed samples. As was noted in the SD for peak load of the samples, we can also visualise in Figure 4.2.4 that more variation existed in the tendinous layers of SS and IS compared to their capsular counterparts, seen in Figure 4.2.5. SC follows a different trend and was observed to have greater peak load variation, and a larger

SD for the capsular layer, compared to the tendinous layer. The tendinous layers of SC and IS consistently reach higher peak load values than SS. SC yielded the greatest peak load values of the capsular layers, followed by SS and lastly IS.

Additional information on tear formation was gathered upon conclusion of peak load analyses. Notes were made regarding the distance of the tear from the tendinous or capsular insertion onto the proximal humerus, and whether the tear was full-thickness, on the deep surface (inside), or on the superficial (outside) surface of the segment.

RC Segment	SSC	SST	ISC	IST	SCC	SCT
Range	1-15	5-20	1-10	5-15	1-10	3-20
Sample (n)	8	10	12	14	13	13

Table 4.2.4 provides a range of where the tear was located from its insertion site, for all of the samples within a layer of a RC unit. Where the tear was not complete (not full-thickness) partial tearing after loss of structural integrity was mainly noted on the deep surface (inside) of the segment. Artificial tearing that occurred at the clamp was noted in 3 of the 70 tests recorded.

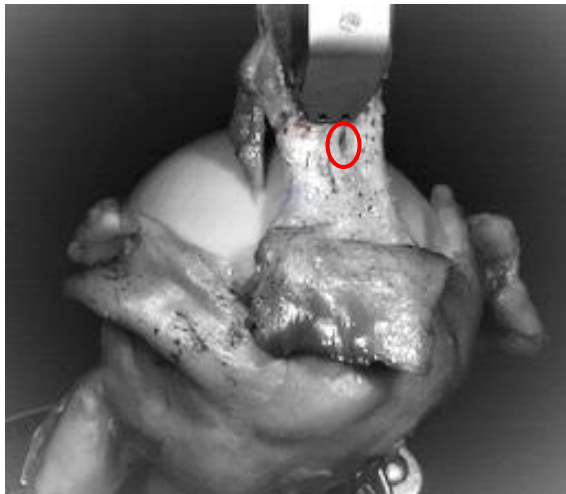


Figure 4.2.6. Red oval indicates a full-thickness tear of SSC for sample 002, of a right arm.

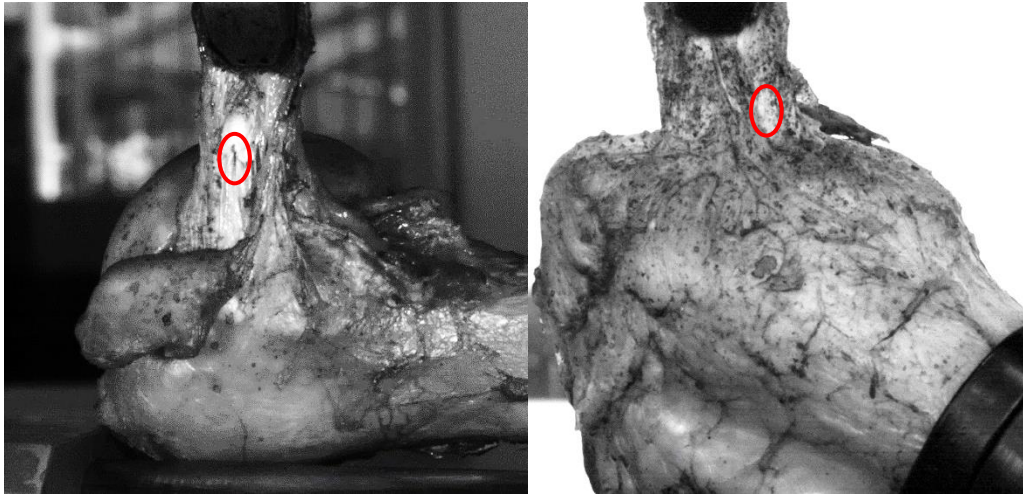


Figure 4.2.7. On the left the red oval highlights a full-thickness tear of ISC for sample 005, from a left arm; on the right the red oval highlights a partial-thickness tear of IST for sample 013, from a left arm.

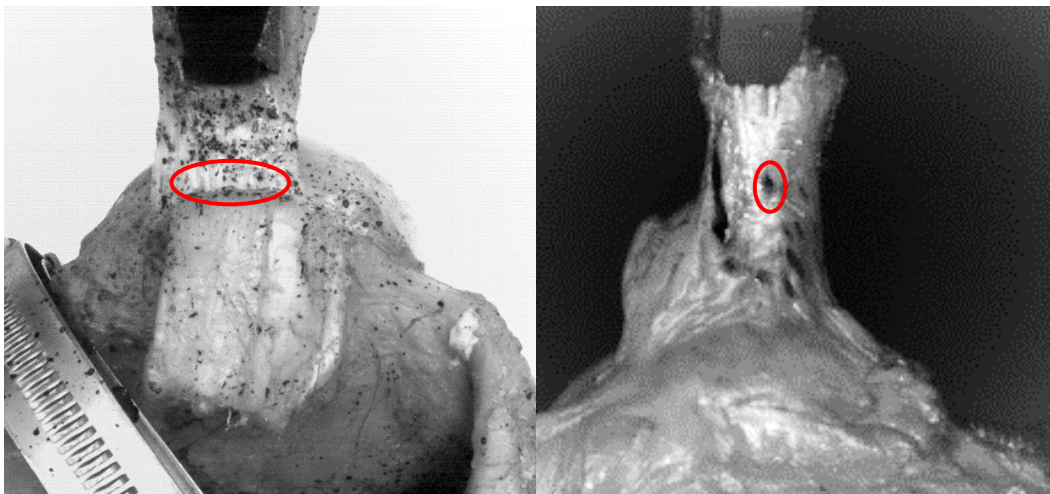


Figure 4.2.8. On the left the red oval highlights full-thickness tearing of SCC near insertion for sample 004, from a left arm; on the right the red oval highlights a full-thickness tear of SCT for sample 002, from a right arm.

Figures 4.2.6-4.2.8 depict photos taken with an IDT NX8-S2 camera positioned to the right and front of the testing area to demonstrate tears in the analysed sections. Since the images were taken from the front, capsular-sided tears of the tendinous portions, and bone-sided tears of capsular portions aren't available for viewing. Figure 4.2.6 demonstrates a full-thickness tear captured during DIC photography of the capsular layer of SS; the tendinous layers for SS failed mainly on the capsular side of the section and are not available for viewing. Figure 4.2.7 shows a full-thickness tear of IS capsular layer, and partial thickness tear of IS tendinous layer

which was also partially torn on the capsular-side (not captured on camera). Figure 4.2.8 demonstrates full-thickness tears of both the capsular and tendinous layers of SC.

4.2.5. Discussion

The current manuscript aimed to provide biomechanical peak load data for the tendinous and capsular layers of SS, IS, and SC. Table 4.2.1 records peak loads obtained for all sections of both layers. When a strip was noted with a higher peak load an increase in extension, compared to strips with lower peak loads, was noted. The strips that yielded the highest peak load values required the most energy to tear. In 1993 Keating and co-authors found in a cadaveric study on the RC that overall strength of the cuff was distributed as 53% by SC, 22% by IS, and 14% by SS. However, their study failed to note the individual strengths of the tendinous and capsular layers for each of these muscles. The present study found for the tendinous layers, SC obtained the highest average peak load throughout testing, followed by IS, followed closely by SS. For the capsular layer, however, it was noted that SC again obtained the highest average peak load, but was followed by SS and then IS. Overall the strongest of the three segments, taken as a whole to include both layers, was the SC, followed by IS, followed by SS.

This peak load pattern correlates closely with the average thickness of the sections that could be recorded, seen in Table 4.2.2. The tendinous layers of SC were the thickest, followed by almost equal SS and IS thicknesses. The capsular layers then ranged from SC being the thickest to IS being the thinnest. Strips that obtained smaller peak load values were also generally thinner than strips that reached higher peak load values. To examine whether a statistical correlation existed between sample thickness and its associated peak load, Pearson's correlation coefficient and linear regression values were obtained. The present study yielded a Pearson's correlation coefficient of 0.551, which dictates a moderate positive relationship exists between sample thickness and peak load. Linear regression values obtained indicate that 2-82% (specimen dependent) of the dependent variable, peak load, could be predicted by the independent variable, sample thickness. These results indicate that, in the small sample used to obtain the current correlation data, segment thickness is not a predicting variable of ultimate peak load obtainable by the sample.

Provided that the two layers of the RC complex respond differently under tensile loading, it is reasonable to think of these layers as biomechanically different structures. To prove this biomechanical theory, t-testing for significant biomechanical difference was done. The mean

values were compared between the two layers of a section, as well as between the sections of each layer. All comparisons revealed that no two RC sections are the same (SSC≠SST, ISC≠IST, SCC≠SCT, SSC≠ISC≠SCC, SST≠IST≠SCT) and significance at a p-value of less than 0.05 was found in 6 of the 9 comparisons (Table 4.2.3). These findings reinforce the fact that the different muscles and different layers making up the RC complex should be treated individually as they have individual load bearing potentials.

In reference to Figures 4.2.4-4.2.5 displaying the peak load differences between all tendinous and all capsular segments, individual variation can be noted. Viewing these graphs alongside the SD values obtained in Table 4.2.1 most clearly represents the distribution within the RC components' tension threshold. The tendinous portions mainly yielded greater peak loads than their capsular counterpart when placed under tensile loading. An increase in peak load was noted with increased extension values, thus we know that the tendinous layer is stronger, more elastic, and can endure greater stresses than the capsular layer of the RC complex.

The failure areas noted in Table 4.2.4 are comparable to previous studies and highlight the existence of the critical area of SS (Itoi *et al.*, 1995; Pandey and Willems, 2015; Naidoo *et al.*, 2016). Literature on the critical zone mainly discuss the involvement of the SS as it is the most frequent of the RC muscles to tear. IS critical areas overlapped somewhat with SS and, although the range for tearing was smaller, IS still tore within the originally described critical zone. Failure of the SC was noted in much smaller ranges than for either the SS or IS. SC capsular and tendinous tear locations additionally showed no overlap, which could mean even if a tear is observed in the tendinous portion, the capsular tear may be hidden during exploratory examination used in arthroscopic techniques. For all comparisons of SS, IS, and SC, tears could be observed to form closer to the insertion point for the capsular layers than the tendinous layers. Franchi *et al.* (2007) found that collagen fibres are arranged in less parallel directions as the tendon nears its insertion onto bone. This more mesh-like, crimped organisation of the tendinous layer could aid in its resistance to tensile loading and strengthen its insertion. However, the capsular layer is arranged in a more parallel fashion and thus the pull-out strength from the insertion is less than for tendon, and thus tears would more easily form near the bone (Nordin *et al.*, 2001). These findings are reported with the acknowledgement that tears resulted under testing conditions in fresh tissue samples and don't necessarily correspond to in-situ RC tearing, but are still of note.

4.2.6. Conclusion

Keeping in mind specimen placement in exact anatomical position was limited by testing equipment and tears artificially formed during tensile loading, vital new biomechanical information was gathered. Till recently many studies investigating the RC complex have ignored the capsular layer, instead analysing the muscular complex as though each of its components consisted of single tendons. However, during dissection it was found that the SS, IS, and SC interdigitate with one another as they near their insertion, and all three muscles consist of two layers. This study further found that biomechanical differences existed throughout the RC complex. Peak load differences were found between the tendinous and capsular layers, as well as between the different components of these layers. As statistically significant differences exist between the individual components that form the interdigitated RC complex, it is reasonable that surgeons should operate on these segments independently. Should surgeons neglect the biomechanically weaker capsular layer in their reconstruction on patients with RC pathology, they may instead further damage the load bearing capacity of the unit. Since the capsular layer is biomechanically weaker it would not be able to withstand some forces that the tendinous component can. Repairing these two layers as one would lead to more strain being exerted on the capsular component than it may be able to withstand and may lead to patients needing to return for a similar surgery due to an inappropriate original operation. Although the study is small the methods applied yielded firm results and paves the way for future research to bulk-up the sample size and validate the present findings.

4.2.7. References

Abraham, A.C., Shah, S.A., Thomopoulos, S., 2017. Targeting inflammation in rotator cuff tendon degeneration and repair. *Techniques in Shoulder and Elbow Surgery*. 18: 84–90.

Bryant, L., Shnier, R., Bryant, C., Murrell, G.A.C., 2002. A comparison of clinical estimation, ultrasonography, magnetic resonance imaging, and arthroscopy in determining the size of rotator cuff tears. *Journal of Shoulder and Elbow Surgery*. 11: 219–224.

Chow, J.C.Y., Gu, Y., 2004. Case report: Material reaction to suture anchor. *Arthroscopy: The Journal of Arthroscopic and Related Surgery*. 20: 314–316.

Codman, E.A., 1934. The shoulder: Rupture of the supraspinatus tendon and other lesions in or about the subacromial bursa, *The shoulder*. R.E. Kreiger.

Codman, E.A., Akerson, I.B., 1931. The pathology associated with rupture of the supraspinatus tendon. *Annals of Surgery*. 93: 348–359.

Dubin, A.E., Patapoutian, A., 2010. Nociceptors: The sensors of the pain pathway. *The Journal of Clinical Investigation*. 120: 3760–3772.

Franchi, M., Trirè, A., Quaranta, M., Orsini, E., Ottani, V., 2007. Collagen structure of tendon relates to function. *The Scientific World Journal*. 7: 404–420.

Halder, A., Zobitz, M.E., Schultz, F., An, K.N., 2000. Mechanical properties of the posterior rotator cuff. *Clinical Biomechanics*. 15: 456–462.

Halder, A.M., Zobitz, M.E., Schultz, F., An, K.N., 2000. Structural properties of the subscapularis tendon. *Journal of Orthopaedic Research*. 18: 829–834.

Hyatt, A.E., Lavery, K., Mino, C., Dhawan, A., 2016. Suture anchor biomechanics after rotator cuff footprint decortication. *Arthroscopy: The Journal of Arthroscopic and Related Surgery*. 32: 544–550.

Itoi, E., Berglund, L.J., Grabowski, J.J., Schultz, F.M., Growney, E.S., Money, B.F., An, K.-N., 1995. Tensile properties of the supraspinatus tendon. *Journal of Orthopaedic Research*. 13: 578–584.

Keating, J.F., Waterworth, P., Shaw-Dunn, J., Crossan, J., 1993. The relative strengths of the rotator cuff muscles: A cadaver study. *The Journal of Bone and Joint Surgery*. 75: 137–140.

Lee, S.B., Nakajima, T., Luo, Z.P., Zobitz, M.E., Chang, Y.W., An, K.N., 2000. The bursal and articular sides of the supraspinatus tendon have a different compressive stiffness. *Clinical Biomechanics*. 15: 241–247.

Levy, O., Relwani, J., Zaman, T., Even, T., Venkateswaran, B., Copeland, S., 2008. Measurement of blood flow in the rotator cuff using laser Doppler flowmetry. *The Journal of Bone and Joint Surgery. British Volume*. 90-B: 893–898.

Lin, T.W., Cardenas, L., Soslowky, L.J., 2004. Biomechanics of tendon injury and repair. *Journal of Biomechanics*. 37: 865–877.

Luo, Z.P., Hsu, H.C., Grabowski, J.J., Morrey, B.F., An, K.N., 1998. Mechanical environment associated with rotator cuff tears. *Journal of Shoulder and Elbow Surgery*. 7: 616–620.

Mall, N.A., Kim, H.M., Keener, J.D., Steger-May, K., Teefey, S.A., Middleton, W.D., Stobbs, G., Yamaguchi, K., 2010. Symptomatic progression of asymptomatic rotator cuff tears: A prospective study of clinical and sonographic variables. *Journal of Bone and Joint Surgery - American Volume*. 92: 2623–2633.

McMaster, W., Troup, T., 1993. A survey of interfering shoulder pain in United States competitive swimmers. *American Journal of Sports Medicine*. 21: 67–70.

McMonagle, J.S., Vinson, E.N., 2011. MRI of the shoulder: Rotator cuff. *Applied Radiology*. 41: 20–28.

Moosmayer, S., Tariq, R., Stiris, M., Smith, H.-J., 2013. The natural history of asymptomatic rotator cuff tears: A three-year follow-up of fifty cases. *Journal of Bone and Joint Surgery - American Volume*. 95: 1249–1255.

Naidoo, N., Lazarus, L., Satyapal, K.S., 2016. The histological analysis of the glenohumeral “critical zone.” *International Journal of Morphology*. 34: 1051–1057.

Nakajima, T., Rokuuma, N., Hamada, K., Tomatsu, T., Fukuda, H., 1994. Histologic and biomechanical characteristics of the supraspinatus tendon: Reference to rotator cuff tearing. *Journal of Shoulder and Elbow Surgery*. 3: 79–87.

Neer, C.S., 1972. Anterior acromioplasty for the chronic impingement syndrome in the shoulder. *The Journal of Bone and Joint Surgery*. 54: 41–50.

Nordin, M., Lorenz, T., Campello, M., 2001. Biomechanics of tendons and ligaments, in: Nordin, M., Frankel, V.H. (Eds.), *Basic Biomechanics of the Musculoskeletal System*. Lippincott Williams and Wilkins, pp. 102–125.

Pandey, V., Willems, W.J., 2015. Rotator cuff tear: A detailed update. *Asia-Pacific Journal of Sports Medicine, Arthroscopy, Rehabilitation and Technology*. 2: 1–14.

Sano, H., Hatta, T., Yamamoto, N., Itoi, E., 2013. Stress distribution within rotator cuff tendons with a crescent-shaped and an L-shaped tear. *The American Journal of Sports Medicine*. 41: 2262–2269.

Standring, S., 2016. Pectoral girdle and upper limb, in: Birch, R. (Ed.), *Gray's Anatomy: The Anatomical Basis of Clinical Practice*. Elsevier, pp. 822–824.

Tawfik, A.M., El-Morsy, A., Badran, M.A., 2014. Rotator cuff disorders: How to write a surgically relevant magnetic resonance imaging report? *World Journal of Radiology*. 6: 274–283.

Via, A.G., de Cupis, M., Spoliti, M., Oliva, F., 2013. Clinical and biological aspects of rotator cuff tears. *Muscles, Ligaments and Tendons Journal*. 3: 70–79.

Chapter 5: Synopsis

5.1. Findings for Chapter 2

The objectives of the current study were to provide information on the composition and biomechanical differences of the rotator cuff (RC) complex. Using a fresh tissue sample from a South African population randomly obtained from the National Tissue Bank, the elastic moduli (MPa) and peak loads (N) for supraspinatus (SS), infraspinatus (IS), and subscapularis (SC) tendinous (T) and capsular (C) layers were tested.

Macroscopic inspection of the SS, IS, and SC revealed these muscles originate separately on the scapula, but then taper towards a common insertional cuff. The SS blends with both the IS (posteriorly) and the SC (anteriorly) via deep oblique fibres. When the sections forming the RC complex are reverse dissected to their insertion and trimmed to 2cm long strips, two layers can be observed: the more superficial tendinous and deeper capsular layer. By following the course from their scapular origins the three RC muscles were separated into +/-2cm wide sections. Each section was divided into its tendinous and capsular layer for biomechanical testing. Testing equipment consisted of an Instron (model 1342) standard materials testing system (MTS) machine coupled to a software program, Bluehill 2, which recorded the peak load for the individual sections. Cameras were also set up facing the testing area of the Instron which allowed for digital image correlation (DIC) that is currently the best method of obtaining elastic modulus data.

Results of these tests have been thoroughly documented in Chapter 4 and in summary each layer and each section of the RC complex has unique biomechanical characteristics. Findings showed that the tendinous layer was more elastic and more resistant to tensile loading than the capsular layer per section (i.e. SST vs. SSC etc.). Outliers to these findings, where capsular layers yielded better results than tendinous layers, were found to have consistency between the elastic modulus and peak load values. This is to say, when the capsular layer of one segment yielded a greater elastic modulus than the tendinous layer, the peak load value for the capsular layer was also found to be higher than the tendinous layer for that specimen.

Additionally, interindividual elastic modulus variation could be observed for the same RC segment (e.g. IST) of different samples. Where segments were compared for peak load variation, significant differences were found for 6 of the 9 comparisons. No two sections

compared were found to have the same mean peak load p-value, further emphasising biomechanical differences within the RC complex. Although sample thickness could not be directly correlated with peak load or elastic modulus readings, positive correlations did exist, and generally where segments were thicker, higher MPa and N readings were obtained. Critical areas where the various sections tore by tensile loading were additionally recorded. SS's critical zone expanded over the widest range and SC over the shortest range.

5.2. Limitations

The following limitations were encountered in this study: Sample size, time and financial constraints, previous use, and soft tissue properties. The small sample size, due to the expense of obtaining fresh tissue and time constraints of testing each specimen, can only constitute an observational study. However, the observations made are of significant importance as these findings have highlighted the almost independent portion of the capsular layer as well as the biomechanical differences between the two layers of the RC. Although the sample size of the present study meant shoulder side (left vs. right), hand dominance, sex, and population weren't considered, future studies of larger sample sizes should consider these factors as differences can be expected.

SC was found to be the strongest of the tendinous samples analysed, followed by IS, and lastly SS. This data may be skewed due to the fact that most of the tests that could not be done involved SS tendinous and capsular layers. The lack of an SS sample population that is comparable with SC and IS samples may be attributed to the sample composition of mainly older individuals. Older individuals have been found with the highest percentage of RC degeneration and tears, especially affecting the SS. Another factor would be that the SS samples had been used in another tensile loading study, and these previous tests may have affected the results of the current study.

The final limitations of this study were the inherent properties of soft tissue. As the tissue was still fresh, it was rather moist and proved difficult to clamp for tensile loading. Where strip slipping and humeral pull-out involving the clamps occurred, second tests needed to be done. When a segment is mechanically loaded it becomes stiff and there may be micro-failure, therefore the second test performed may have yielded sub-optimal peak load data. Viscoelastic and non-homogeneity of soft tissue meant that formulae for elastic modulus had to be adapted as this property is normally measured for hard materials.

5.3. Future direction

Incorporating a larger sample of shoulders in future would serve to validate the current findings. If it would be possible to select shoulders from individuals younger than 40 years, it is likely that more SS samples would be available for testing. The clamp used to hold the strips should be modified to be as broad or broader than the strip breadth, to lessen artificial defects in tear formation and elastic modulus tracking. To maximise the time spent loading samples onto the Instron, it would be advisable to construct a humeral clamp with an inner circumference of 15cm. Constructing a rigid camera stand with simple docking for lights and cameras may save on set-up time during testing for DIC analysis. Optimally a set-up of two line-lasers measuring three-dimensional cross-sectional area of segments, accompanied by a single camera, would be recommended.

5.4. Clinical relevance

Arthroscopy is becoming the main technique for repairing RC lesions. Studies have found that arthroscopy often overlooks deeper capsular tears, and repairs are made by binding the tendinous and capsular layer to the bone together, instead of considering individual layer biomechanics. With the knowledge provided on the tensile strength and elastic modulus differences between individual muscles and individual layers of the RC, orthopaedic surgeons should treat these layers separately. Should surgeons continue to repair RC tears as though the tendinous and capsular layers were one in the same, they would knowingly be altering the inherent biomechanics of each layer, leading to motion deficits in treated patients. The weaker and less elastic capsular layer would especially be at risk of damage as it would be expected to withstand tensile forces that only the tendinous layer is able to withstand.

5.5. Conclusion

The main objective of this study was to provide evidence for the need to repair the capsular and tendinous layers of the RC separately. The findings of interdigitated capsular and tendinous layers that yielded different elastic modulus and peak load results for SS, IS, and SC express the biomechanical intricacies within the RC complex. Not only were the findings statistically significant, but they were surgically relevant. Surgeons who operate on lesions in the RC, treating the capsular and tendinous layers separately, have noted better post-operative return to pre-tear function, avoidance of related ailments such as osteonecrosis, and reduced pain.

The generally stronger and more elastic tendinous layer should be treated separate to the capsular layer in surgery so as to avoid compromising the inherent biomechanical characteristics. The capsular layer being weaker and less elastic would be placed under more strain than it could bear if a tear were repaired as though these layers were a single structure. Whereas the tendinous layer contributes mainly to strength, the capsular layer having stiffer properties adds to stability of the GHJ. Together these layers add individual qualities of stability and mobility to the shoulder that aid individuals in completing everyday tasks such as lifting the arm to reach high places, carrying objects, and even throwing a ball. The shoulder is one of the most significant and vital complexes in the human body when it is functioning optimally and is not a source of pain and dysfunction.

Shoulder complications have been noted since the beginning of medical history, but surgery was avoided in past times due to associated risks. Current technology allows for optimal surgical approach and repair, and with the data gathered in the present study, surgeons are equipped with the knowledge of how to adjust their technique to their patients' optimal gain.

Chapter 6: References for Chapters 1 and 3

- Abraham, A.C., Shah, S.A., Thomopoulos, S., 2017. Targeting inflammation in rotator cuff tendon degeneration and repair. *Techniques in Shoulder and Elbow Surgery*. 18: 84–90.
- Akhtar, R., Sherratt, M.J., Cruickshank, J.K., Derby, B., 2011. Characterizing the elastic properties of tissues. *Materials Today*. 14: 96–105.
- Aydin, N., Karaismailoglu, B., 2017. High-grade bursal-side partial rotator cuff tears: Comparison of mid- and long-term results following arthroscopic repair after conversion to a full-thickness tear. *Journal of Orthopaedic Surgery and Research*. 12: 1–6.
- Bankart, A.S.B., 1923. Recurrent or habitual dislocation of the shoulder-joint. *The British Medical Journal*. 2: 1132–1133.
- Bedi, A., Maak, T., Walsh, C., Rodeo, S.A., Grande, D., Dines, D.M., Dines, J.S., 2012. Cytokines in rotator cuff degeneration and repair. *Journal of Shoulder and Elbow Surgery*. 21: 218–227.
- Benjamin, M., Evans, E.J., Copp, L., 1986. The histology of tendon attachments to bone in man. *American Journal of Sports Medicine*. 14: 89–100.
- Benson, R.T., McDonnell, S.M., Knowles, H.J., Rees, J.L., Carr, A.J., Hulley, P.A., 2010. Tendinopathy and tears of the rotator cuff are associated with hypoxia and apoptosis. *The Journal of bone and joint surgery: British Volume*. 92-B: 448–453.
- Bigliani, L.U., Ticker, J.B., Flatow, E.L., Soslowsky, L.J., Mow, V.C., 1991. The relationship of acromial architecture to rotator cuff disease. *Clinics in Sports Medicine*. 10: 823–838.
- Buck, F.M., Grehn, H., Hilbe, M., Pfirrmann, C.W.A., Manzanell, S., Hodler, J., 2010. Magnetic resonance histologic correlation in rotator cuff tendons. *Journal of Magnetic Resonance Imaging*. 32: 165–172.
- Chaudhury, S., Holland, C., Thompson, M.S., Vollrath, F., Carr, A.J., 2012. Tensile and shear mechanical properties of rotator cuff repair patches. *Journal of Shoulder and Elbow Surgery*. 21: 1168–1176.
- Chillemi, C., Petrozza, V., Franceschini, V., Garro, L., Pacchiarotti, A., Porta, N., Cirenza, M., Santone, F.S., Castagna, A., 2016. The role of tendon and subacromial bursa in rotator

- cuff tear pain: A clinical and histopathological study. *Knee Surgery, Sports Traumatology, Arthroscopy*. 24: 3779–3786.
- Clark, J., Harryman, D., 1992. Tendons, ligaments, and capsule of the rotator cuff: Gross and microscopic anatomy. *The Journal of Bone and Joint Surgery: American Volume*. 74: 713–725.
- Codman, E.A., 1934. The shoulder: Rupture of the supraspinatus tendon and other lesions in or about the subacromial bursa, *The shoulder*. R.E. Kreiger.
- Codman, E.A., Akerson, I.B., 1931. The pathology associated with rupture of the supraspinatus tendon. *Annals of Surgery*. 93: 348–359.
- Cowan, P.T., Varacallo, M., 2018. Anatomy, back, scapula. NCBI: Anatomy and Basic Science. NBK531475.
- Davidson, J., Burkhart, S.S., 2010. The Geometric Classification of rotator cuff tears: A system linking tear pattern to treatment and prognosis. *Arthroscopy: The Journal of Arthroscopic and Related Surgery*. 26: 417–424.
- Dean, B.J.F., Franklin, S.L., Carr, A.J., 2012. A systematic review of the histological and molecular changes in rotator cuff disease. *Bone and Joint Research*. 1: 158–66.
- DeOrio, J.K., Cofield, R.H., 1984. Results of a second attempt at surgical repair of a failed initial rotator-cuff repair. *The Journal of Bone and Joint Surgery*. 66: 563–567.
- Drake, R., Mitchell, A.W.M., Vogl, A.W., 2014. Upper limb, in: *Gray's Anatomy for Students*. Elsevier, pp. 710–717.
- Edwards, P., Ebert, J., Joss, B., Bhabra, G., Ackland, T., 2016. Clinical commentary exercise rehabilitation in the non-operative management of rotator cuff tears: A review of the literature 11: 279–301.
- Elkhatatny, S., Mahmoud, M., Mohamed, I., Abdulraheem, A., 2017. Development of a new correlation to determine the static Young's modulus. *Journal of Petroleum Exploration and Production Technology*. 8: 17–30.
- Ellman, H., 1990. Diagnosis and treatment of incomplete rotator cuff tears. *Clinical Orthopaedics and Related Research*. 254: 64–74.

- Factor, D., Dale, B., 2014. Current concepts of rotator cuff tendinopathy. *The International Journal of Sports Physical Therapy*. 9: 274–288.
- Fealy, S., Adler, R.S., Drakos, M.C., Kelly, A.M., Allen, A.A., Cordasco, F.A., Warren, R.F., O'Brien, S.J., 2006. Patterns of vascular and anatomical response after rotator cuff repair. *American Journal of Sports Medicine*. 34: 120–127.
- Fukuda, H., Mikasa, M., Yamanaka, K., 1987. Incomplete thickness rotator cuff tears diagnosed by subacromial bursography. *Clinical Orthopaedics and Related Research*. 223: 51–58.
- Gamradt, S.C., Gallo, R.A., Adler, R.S., Maderazo, A., Altchek, D.W., Warren, R.F., Fealy, S., 2010. Vascularity of the supraspinatus tendon three months after repair: Characterization using contrast-enhanced ultrasound. *Journal of Shoulder and Elbow Surgery*. 19: 73–80.
- Gartsman, G.M., 2001. Arthroscopic rotator cuff repair. *Clinical Orthopaedics and Related Research*. 390: 95–106.
- Gerster, E., 1884. Subcoracoid dislocation (recurrent) of the humerus; paralysis of the serratus magnus; arthrotomy. *Medical News Philadelphia*. 44: 423.
- Goutallier, D., Postel, J.M., Bernageau, J., Lavau, L., Voisin, M.C., 1994. Fatty muscle degeneration in cuff ruptures: Pre- and postoperative evaluation by CT scan. *Clinical Orthopaedics and Related Research*. 304: 78–83.
- Gouw, G.J., Wevers, H.W., 1982. Behaviour of an Instron 1122 under cyclic testing over a small displacement range. *Journal of Biomedical Engineering*. 4: 72–74.
- Gray, H., 1858. *Anatomy: Descriptive and surgical*, 1st ed. London: J.W.Parker.
- Gumina, S., Borroni, M., 2016. Classifications of the rotator cuff tears, in: Gumina, S. (Ed.), *Rotator Cuff Tear: Pathogenesis, Evaluation and Treatment*. Springer, Cham, pp. 123–131.
- Halder, A., Zobitz, M.E., Schultz, F., An, K.N., 2000. Mechanical properties of the posterior rotator cuff. *Clinical Biomechanics*. 15: 456–462.
- Halder, A.M., Itoi, E., An, K.N., 2000a. *Anatomy and biomechanics of the shoulder*.

Orthopedic Clinics of North America. 31: 159–176.

Halder, A.M., Zobitz, M.E., Schultz, F., An, K.N., 2000b. Structural properties of the subscapularis tendon. *Journal of Orthopaedic Research*. 18: 829–834.

Hashimoto, T., Nobuhara, K., Hamada, T., 2003. Pathologic evidence of degeneration as a primary cause of rotator cuff tear. *Clinical Orthopaedics and Related Research*. 415: 111–120.

Heary, R.F., Parvathreddy, N., Sampath, S., Agarwal, N., 2017. Elastic modulus in the selection of interbody implants. *Journal of Spine Surgery*. 3: 163–167.

Hirji, Z., Hunjun, J.S., Choudur, H.N., 2011. Imaging of the bursae. *Journal of Clinical Imaging Science*. 1: 22.

Illinois Tool Works Incorporated. Bluehill 2 software: Simplicity and power for material testing applications, 2008. Report.

Ishii, H., Brunet, J.A., Welsh, R.P., Uthoff, H.K., 1997. “Bursal reactions” in rotator cuff tearing, the impingement syndrome, and calcifying tendinitis. *Journal of Shoulder and Elbow Surgery*. 6: 131-136.

Itoi, E., Berglund, L.J., Grabowski, J.J., Schultz, F.M., Growney, E.S., Morrey, B.F., An, K.N., 1995. Tensile properties of the supraspinatus tendon. *Journal of Orthopaedic Research: Official Publication of the Orthopaedic Research Society*. 13: 578–584.

Karas, V., Wang, V.M., Dhawan, A., Cole, B.J., 2011. Biomechanical factors in rotator cuff pathology. *Sports Medicine and Arthroscopy Review*. 19: 202–206.

Kim, H.J., Kim, J.Y., Kee, Y.M., Rhee, Y.G., 2018. Bursal-sided rotator cuff tears: Simple versus everted type. *The American Journal of Sports Medicine*. 46: 441–448.

Lee, S.B., Nakajima, T., Luo, Z.P., Zobitz, M.E., Chang, Y.W., An, K.N., 2000. The bursal and articular sides of the supraspinatus tendon have a different compressive stiffness. *Clinical Biomechanics*. 15: 241–247.

Levy, O., Relwani, J., Zaman, T., Even, T., Venkateswaran, B., Copeland, S., 2008. Measurement of blood flow in the rotator cuff using laser Doppler flowmetry. *The Journal of Bone and Joint Surgery. British Volume*. 90-B: 893–898.

- Lewis, J.S., 2010. Rotator cuff tendinopathy: A model for the continuum of pathology and related management. *British Journal of Sports Medicine*. 44: 918–923.
- Li, D., Li, C.C., Li, X., 2011. Influence of sample height-to-width ratios on failure mode for rectangular prism samples of hard rock loaded in uniaxial compression. *Rock Mechanics and Rock Engineering*. 44: 253–267.
- Lin, T.W., Cardenas, L., Soslowsky, L.J., 2004. Biomechanics of tendon injury and repair. *Journal of Biomechanics*. 37: 865–877.
- Lippitt, S.B., Vanderhooft, J.E., Harris, S.L., Sidles, J.A., Harryman, D.T., Matsen, F.A., 1993. Glenohumeral stability from concavity-compression: A quantitative analysis. *Journal of Shoulder and Elbow Surgery*. 2: 27–35.
- Longo, U.G., Berton, A., Khan, W.S., Maffulli, N., Denaro, V., 2011. Histopathology of rotator cuff tears. *Sports Medicine and Arthroscopy Review*. 19: 227–236.
- Luo, Z.P., Hsu, H.C., Grabowski, J.J., Morrey, B.F., An, K.N., 1998. Mechanical environment associated with rotator cuff tears. *Journal of Shoulder and Elbow Surgery*. 7: 616–620.
- Maffulli, N., Furia, J.P., 2012. *Rotator cuff disorders: Basic science and clinical medicine*. JP Medical Ltd.
- Mallett, K.F., Arruda, E.M., 2017. Digital image correlation-aided mechanical characterization of the anteromedial and posterolateral bundles of the anterior cruciate ligament. *Acta Biomaterialia*. 56: 44–57.
- Mazzocca, A.D., Bollier, M.J., Obopilwe, E., DeAngelis, J.P., Burkhart, S.S., Warren, R.F., Arciero, R.A., 2010. Biomechanical Evaluation of Arthroscopic Rotator Cuff Repairs Over Time. *Arthroscopy: The Journal of Arthroscopic and Related Surgery*. 26: 592–599.
- McCormick, N., Lord, J., 2010. Digital image correlation. *Materials Today*. 13: 52–54.
- McLaughlin, H.L., 1944. Lesions of the musculotendinous cuff of the shoulder: The exposure and treatment of tears with retraction. *The Journal of Bone and Joint Surgery*. 26: 31–51.
- McMaster, W., Troup, T., 1993. A survey of interfering shoulder pain in United States competitive swimmers. *American Journal of Sports Medicine*. 21: 67–70.
- McMonagle, J.S., Vinson, E.N., 2011. MRI of the shoulder: Rotator cuff. *Applied Radiology*.

41: 20–28.

- Melis, B., Nemoz, C., Walch, G., 2009. Muscle fatty infiltration in rotator cuff tears: Descriptive analysis of 1688 cases. *Orthopaedics and Traumatology: Surgery and Research*. 95: 319–324.
- Mochizuki, T., Nimura, A., Miyamoto, T., Koga, H., Akita, K., Muneta, T., 2016. Repair of rotator cuff tear with delamination: Independent repairs of the infraspinatus and articular capsule. *Arthroscopy Techniques*. 5: e1129–e1134.
- Monro, A., 1788. *A description of all the bursae mucosae of the human body*. Elliot and Kay.
- Moore, K.L., Dalley, A.F., Agur, A.M.R., 2014. Upper limb, in: *Clinically Oriented Anatomy*. Wolters Kluwer Health/Lippincott Williams and Wilkins, pp. 703–707.
- Naidoo, N., Lazarus, L., De Gama, B.Z., Ajayi, N.O., Satyapal, K.S., 2014. Arterial supply to the rotator cuff muscles. *International Journal of Morphology*. 32: 136–140.
- Naidoo, N., Lazarus, L., Satyapal, K.S., 2016. The histological analysis of the glenohumeral “critical zone.” *International Journal of Morphology*. 34: 1051–1057.
- Nakajima, T., Rokuuma, N., Hamada, K., Tomatsu, T., Fukuda, H., 1994. Histologic and biomechanical characteristics of the supraspinatus tendon: Reference to rotator cuff tearing. *Journal of Shoulder and Elbow Surgery*. 3: 79–87.
- Neer, C.S., 1983. Impingement lesions. *Clinical Orthopaedics and Related Research*. 173: 70–77.
- Neer, C.S., 1972. Anterior acromioplasty for the chronic impingement syndrome in the shoulder. *The Journal of Bone and Joint Surgery*. 54: 41–50.
- Netter, F.H., 2014. Upper limb, in: Hansen, J.T. (Ed.), *Netter’s Atlas of Human Anatomy*. Elsevier Inc., Philadelphia, pp. 405–413.
- Nimura, A., Kato, A., Yamaguchi, K., Mochizuki, T., Okawa, A., Sugaya, H., Akita, K., 2012. The superior capsule of the shoulder joint complements the insertion of the rotator cuff. *Journal of Shoulder and Elbow Surgery*. 21: 867–872.
- Nyffeler, R.W., Meyer, D.C., 2017. Acromion and glenoid shape: Why are they important predictive factors for the future of our shoulders? *EFORT Open Reviews*. 2: 141–150.

- Ohzono, H., Gotoh, M., Nakamura, H., Honda, H., Mitsui, Y., Kakuma, T., Okawa, T., Shiba, N., 2017. Effect of preoperative fatty degeneration of the rotator cuff muscles on the clinical outcome of patients with intact tendons after arthroscopic rotator cuff repair of large/massive cuff tears. *The American Journal of Sports Medicine*. 45: 2975–2981.
- Osti, L., Buda, M., Del Buono, A., 2013. Fatty infiltration of the shoulder: Diagnosis and reversibility. *Muscles, Ligaments and Tendons Journal*. 3: 351–354.
- Pandey, V., Willems, W.J., 2015. Rotator cuff tear: A detailed update. *Asia-Pacific Journal of Sports Medicine, Arthroscopy, Rehabilitation and Technology*. 2: 1–14.
- Park, M.C., ElAttrache, N.S., Tibone, J.E., Ahmad, C.S., Jun, B.J., Lee, T.Q., 2007. Part I: Footprint contact characteristics for a transosseous-equivalent rotator cuff repair technique compared with a double-row repair technique. *Journal of Shoulder and Elbow Surgery*. 16: 461–468.
- Paufenberger, L., Heuberger, P.R., Dyrna, F., Obopilwe, E., Kriegleder, B., Anderl, W., Mazzocca, A.D., 2018. Double-layer rotator cuff repair: Anatomic reconstruction of the superior capsule and rotator cuff improves biomechanical properties in repairs of delaminated rotator cuff tears. *The American Journal of Sports Medicine*. 46: 3165–3173.
- Riley, G.P., Curry, V., DeGroot, J., van El, B., Versijl, N., Hazleman, B.L., Bank, R.A., 2002. Matrix metalloproteinase activities and their relationship with collagen remodelling in tendon pathology. *Matrix Biology*. 21: 185–195.
- Sambandam, S.N., Khanna, V., Gul, A., Mounasamy, V., 2015. Rotator cuff tears: An evidence based approach. *World Journal of Orthopedics*. 6: 902–918.
- Sano, H., Hatta, T., Yamamoto, N., Itoi, E., 2013. Stress distribution within rotator cuff tendons with a crescent-shaped and an L-shaped tear. *The American Journal of Sports Medicine*. 41: 2262–2269.
- Saremi, H., 2016. Interstitial tear of the subscapularis tendon, arthroscopic findings and technique of repair. *The Archives of Bone and Joint Surgery*. 4: 177–180.
- Seitz, A.L., McClure, P.W., Finucane, S., Boardman, N.D., Michener, L.A., 2011. Mechanisms of rotator cuff tendinopathy: Intrinsic, extrinsic, or both? *Clinical Biomechanics*. 26: 1–12.

- Sejersen, M.H.J., Frost, P., Hansen, T.B., Deutch, S.R., Svendsen, S.W., 2015. Proteomics perspectives in rotator cuff research: A systematic review of gene expression and protein composition in human tendinopathy. *PLoS ONE*. 10: e0119974.
- Smith, J., 1834. Pathologic appearance of seven cases of injury of the shoulder joint: With remarks. *London Medical Gazette*. 14: 280–285.
- Standring, S., 2016. Pectoral girdle and upper limb, in: Birch, R. (Ed.), *Gray's Anatomy: The Anatomical Basis of Clinical Practice*. Elsevier, pp. 822–824.
- Tank, P.W., 2013. The upper limb, in: *Grant's Dissector2*. Wolters Kluwer Health/Lippincott Williams and Wilkins, pp. 24–26.
- Tawfik, A.M., El-Morsy, A., Badran, M.A., 2014. Rotator cuff disorders: How to write a surgically relevant magnetic resonance imaging report? *World Journal of Radiology*. 6: 274–283.
- Uthoff, H.K., Sarkar, K., 1991. Surgical repair of rotator cuff ruptures: The importance of the subacromial bursa. *The Journal of Bone and Joint Surgery: British Volume*. 73: 399–401.
- Vaidya, A., Pathak, K., 2018. Mechanical stability of dental materials, in: Asiri, A.M., Inamuddin, A.M. (Eds.), *Applications of Nanocomposite Materials in Dentistry*. Elsevier Imprint: Woodhead Publishing, pp. 285–305.
- Via, A.G., de Cupis, M., Spoliti, M., Oliva, F., 2013. Clinical and biological aspects of rotator cuff tears. *Muscles, Ligaments and Tendons Journal*. 3: 70–79.
- Vosloo, M., Keough, N., de Beer, M.A., 2017. The clinical anatomy of the insertion of the rotator cuff tendons. *European Journal of Orthopaedic Surgery and Traumatology*. 27: 359–366.
- Watson, S., Allen, B., Robbins, C., Bedi, A., Gagnier, J.J., Miller, B., 2018. Does the rotator cuff tear pattern influence clinical outcomes after surgical repair? *The Orthopaedic Journal of Sports Medicine*. 6: 2325967118763107.
- Weiss, L.J., Wang, D., Hendel, M., Buzzerio, P., Rodeo, S.A., 2018. Management of rotator cuff injuries in the elite athlete. *Current Reviews in Musculoskeletal Medicine*. 11: 102–112.

- Yadav, H., Nho, S., Romeo, A., MacGillivray, J.D., 2009. Rotator cuff tears: Pathology and repair. *Knee Surgery, Sports Traumatology, Arthroscopy*. 17: 409–421.
- Yamaguchi, K., Ditsios, K., Middleton, W.D., Hildebolt, C.F., Galatz, L.M., Teefey, A., 2006. The demographic and morphological features of rotator cuff disease. *The Journal of Bone and Joint Surgery*. 88-A: 1699–1704.
- Yamamoto, N., Itoi, E., 2015. A review of biomechanics of the shoulder and biomechanical concepts of rotator cuff repair. *Asia-Pacific Journal of Sports Medicine, Arthroscopy, Rehabilitation and Technology*. 2: 27–30.
- Yeh, W.C., Li, P.C., Jeng, Y.M., Hsu, H.C., Kuo, P.L., Li, M.L., Yang, P.M., Lee, P.H., 2002. Elastic modulus measurements of human liver and correlation with pathology. *Ultrasound in Medicine and Biology*. 28: 467–474.
- Yuan, J., Murrell, G.A.C., Wei, A.Q., Wang, M.X., 2002. Apoptosis in rotator cuff tendonopathy. *Journal of Orthopaedic Research*. 20: 1372–1379.
- Zhou, B., Ravindran, S., Ferdous, J., Kidane, A., Sutton, M.A., Shazly, T., 2016. Using digital image correlation to characterize local strains on vascular tissue specimens. *Journal of Visualized Experiments*. 107: e53625.

Chapter 7: Annexures

7.1. Annexure 1: Ethics approval letter



Faculty of Health Sciences

The Research Ethics Committee, Faculty Health Sciences, University of Pretoria complies with ICH-GCP guidelines and has US Federal wide Assurance.

- FWA 00002567, Approved dd 22 May 2002 and Expires 03/20/2022.
- IRB 0000 2235 IORG0001762 Approved dd 22/04/2014 and Expires 03/14/2020.

15 August 2019

Ms JY Cronje
Department of Anatomy
Faculty of Health Science
University of Pretoria

Dear Ms JY Cronje

RE: Reports on Medication Trials for Protocol Number 384/2018

Number	384/2018
New Title	A novel approach for investigating the tendinous and capsular layers of the rotator cuff complex: A biomechanical study
Investigator	Ms JY Cronjé
Supervisor	Dr N Keough
Sponsor	

The above mentioned document has been tabled and considered at the meeting of 14 August 2019.

Yours sincerely

Dr R Sommers

MChB MMed (Int) MPharmMed PhD

Deputy Chairperson of the Faculty of Health Sciences Research Ethics Committee, University of Pretoria

The Faculty of Health Sciences Research Ethics Committee complies with the SA National Act 61 of 2003 as it pertains to health research and the United States Code of Federal Regulations Title 45 and 46. This committee abides by the ethical norms and principles for research, established by the Declaration of Helsinki, the South African Medical Research Council Guidelines as well as the Guidelines for Ethical Research: Principles Structures and Processes, Second Edition 2015 (Department of Health)

Research Ethics Committee
Room 4-60, Level 4, Tswelopele Building
University of Pretoria, Private Bag X323
Arcadia 0007, South Africa
Tel +27 (0)12 356 3084
Email deepeka.behari@up.ac.za
www.up.ac.za

Fakulteit Gesondheidswetenskappe
Lefapha la Disaense tša Maphelo

7.2. Annexure 2: Letter of permission from the National Tissue Bank



UNIVERSITEIT VAN PRETORIA
UNIVERSITY OF PRETORIA
YUNIBESITHI YA PRETORIA

Faculty of Health Sciences
Department of Anatomy

To: Acting Head of National Tissue Bank
University of Pretoria
Ms A Morkel

From: The Investigators
UP Department of Anatomy
Dr N Keough

RE: Permission to do the following research at the National Tissue Bank

Dear Ms Morkel, I, Ms JY Cronjé (Department of Anatomy, University of Pretoria), Dr MA de Beer a private orthopaedic surgeon from Little Company of Mary and Doctor N Keough (senior lecturer at UP) are requesting permission to conduct our study at the National Tissue bank, which will involve access to the donors on the premises.

The title of our study is:

1) A new testing method for investigating the tendinous and capsular layers of the rotator cuff complex: A biomechanical study

Research design

This project is a quantitative, inter-departmental and cross-disciplinary research project that focusses on the gross morphological analysis of the rotator cuff muscles (supraspinatus, infraspinatus, subscapularis) and the study of the varying biomechanical properties (peak load to failure and modulus of elasticity) of the tendinous and capsular layers of the rotator cuff unit.

Sample size

A total sample of 15 shoulders (fresh) will be included in this study. Shoulders should fall within the age range of 20 – 70 years and only shoulders free from prior injury or surgery will be considered for the sample.

Objective of the Rotator Cuff study

To determine the biomechanical properties (peak load of failure, modulus of elasticity) of the tendinous and capsular layers of the rotator cuff unit (supraspinatus, infraspinatus, subscapularis) in 15 shoulders using an MTS machine.

Method

The intact rotator cuff muscles (supraspinatus, infraspinatus, subscapularis) of the 15 shoulders will be exposed via careful reverse dissection. The humerus will be mounted and stabilised while the clavicle and scapula are removed. The rotator cuff complex will be separated into tendinous and capsular segments of 15mm x 10mm wide strips. The MTS machine will then apply load to the tendinous and capsular segments of the supraspinatus, infraspinatus, and subscapularis individually and this will be recorded to determine and measure the biomechanical properties (peak load of failure, modulus of elasticity).

The results of this study aim to be published in a professional journal and will be presented at the 2019/2020 ASSA (Anatomical Society of Southern Africa) conference.

In addition, we request in terms of the requirements of the Promotion of Access, Act No. 2 of 2000, that we be granted access to clinical records, files and other databases.

We accept not to proceed with the study until we have received approval from Faculty of Health Sciences Research Ethics Committee, University of Pretoria.

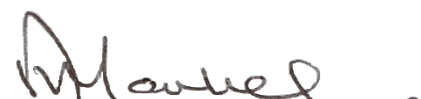
Kind regards


Signature of principal investigator

Permission to do research studies at the hospital and access to information, is hereby approved.

Acting Head of National Tissue Bank
University of Pretoria

Ms A Morkel


Signature of Acting Head of National Tissue Bank

Fakulteit Gesondheidswetenskappe
Departement Anatomie
Lefapha la Disaense tša Maphelo
Kgoro ya Anatomi

7.3. Annexure 3: Ethics renewal for 2019 approval letter



UNIVERSITEIT VAN PRETORIA
UNIVERSITY OF PRETORIA
YUNIBESITHI YA PRETORIA

Faculty of Health Sciences

The Research Ethics Committee, Faculty Health Sciences, University of Pretoria complies with ICH-GCP guidelines and has US Federal wide Assurance.

- FWA 00002567, Approved dd 22 May 2002 and Expires 03/20/2022.
- IRB 0000 2235 IORG0001762 Approved dd 22/04/2014 and Expires 03/14/2020.

9 October 2019

Approval Certificate Annual Renewal

Ethics Reference No.: 384/2018

Title: A novel approach for investigating the tendinous and capsular layers of the rotator cuff complex: A biomechanical study

Dear Ms JY Cronje

The **Annual Renewal** as supported by documents received between 2019-09-20 and 2019-10-09 for your research, was approved by the Faculty of Health Sciences Research Ethics Committee on its quorate meeting of 2019-10-09.

Please note the following about your ethics approval:

- Renewal of ethics approval is valid for 1 year, subsequent annual renewal will become due on 2020-10-09.
- Please remember to use your protocol number (384/2018) on any documents or correspondence with the Research Ethics Committee regarding your research.
- Please note that the Research Ethics Committee may ask further questions, seek additional information, require further modification, monitor the conduct of your research, or suspend or withdraw ethics approval.

Ethics approval is subject to the following:

- The ethics approval is conditional on the research being conducted as stipulated by the details of all documents submitted to the Committee. In the event that a further need arises to change who the investigators are, the methods or any other aspect, such changes must be submitted as an Amendment for approval by the Committee.

We wish you the best with your research.

Yours sincerely

Dr R Sommers

MBCbB MMed (Int) MPharmMed PhD

Deputy Chairperson of the Faculty of Health Sciences Research Ethics Committee, University of Pretoria

The Faculty of Health Sciences Research Ethics Committee complies with the SA National Act 61 of 2003 as it pertains to health research and the United States Code of Federal Regulations Title 45 and 46. This committee abides by the ethical norms and principles for research, established by the Declaration of Helsinki, the South African Medical Research Council Guidelines as well as the Guidelines for Ethical Research: Principles Structures and Processes, Second Edition 2015 (Department of Health)

Research Ethics Committee
Room 4-60, Level 4, Tswelopele Building
University of Pretoria, Private Bag X323
Arcadia 0007, South Africa
Tel +27 (0)12 356 3084
Email deepeka.behari@up.ac.za
www.up.ac.za

Fakulteit Gesondheidswetenskappe
Lefapha la Disaense tša Maphelo

7.4. Annexure 4: Copyright permission letter concerning Figure 3.2 of image contained in article by Clark and Harryman, 1992

9/26/2019 Rightslink® by Copyright Clearance Center

<https://s100.copyright.com/AppDispatchServlet 1/1>

Title: Tendons, ligaments, and capsule of the rotator cuff. Gross and microscopic anatomy.

Author: J M Clark and D T Harryman

Publication: Journal of Bone & Joint Surgery

Publisher: Wolters Kluwer Health, Inc.

Date: Jun 1, 1992

Copyright © 1992, Copyright © 1992 by The Journal of Bone and Joint Surgery, Incorporated

Logged in as: Myleen Oosthuizen

University of Pretoria

Account #: 3001523664

Order Completed

Thank you for your order.

This Agreement between University of Pretoria -- Myleen Oosthuizen ("You") and Wolters Kluwer Health, Inc. ("Wolters Kluwer Health, Inc.") consists of your license details and the terms and conditions provided by Wolters Kluwer Health, Inc. and Copyright Clearance Center. Your confirmation email will contain your order number for future reference.

License Number 4676301000610

License Date Sep 26, 2019

Licensed Content

Publisher Wolters Kluwer Health, Inc.

Licensed Content

Publication Journal of Bone & Joint Surgery

Licensed Content Title Tendons, ligaments, and capsule of the rotator cuff. Gross and microscopic anatomy.

Licensed Content Author J M Clark and D T Harryman

Licensed Content Date Jun 1, 1992

Licensed Content Volume 74

Licensed Content Issue 5

Type of Use Dissertation/Thesis

Requestor type Individual

Portion Figures/table/illustration

Number of figures/tables/illustrations 1

Figures/tables/illustrations used fig 5-A

Author of this Wolters

Kluwer article No

Title of your thesis / dissertation A novel approach for investigating the tendinous and capsular layers of the rotator cuff complex: A biomechanical study

Expected completion date Dec 2019

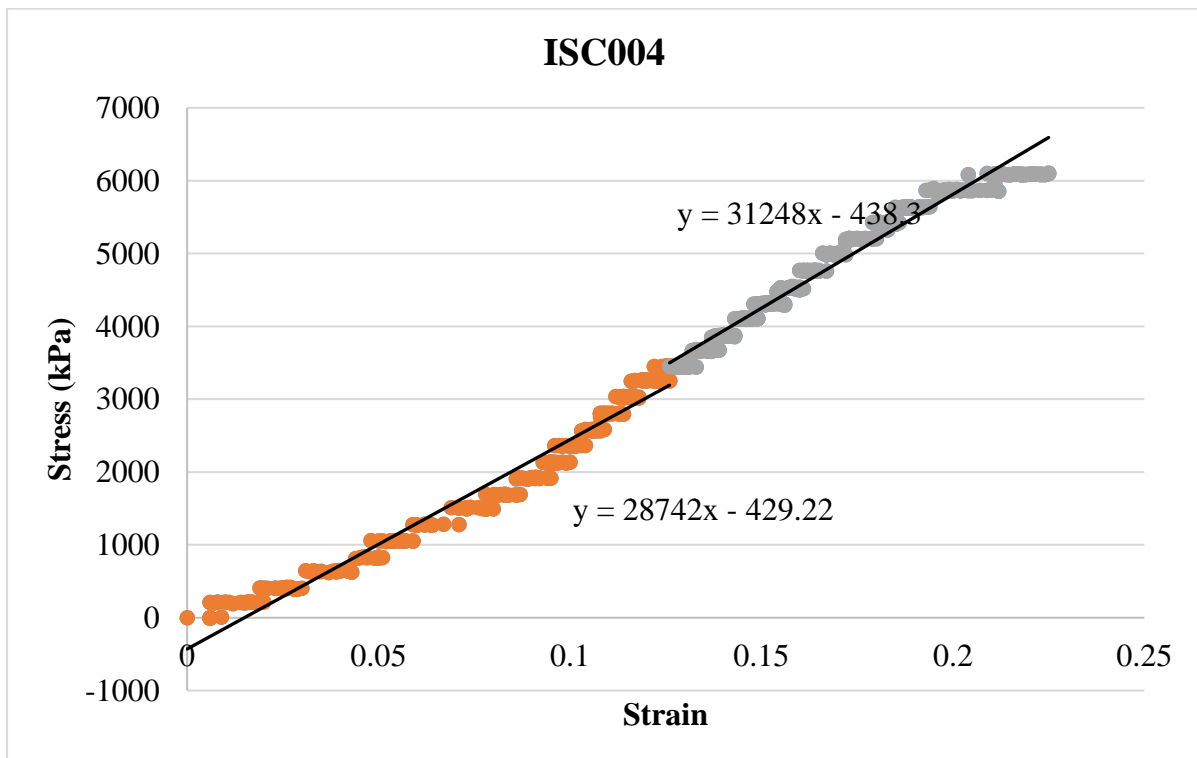
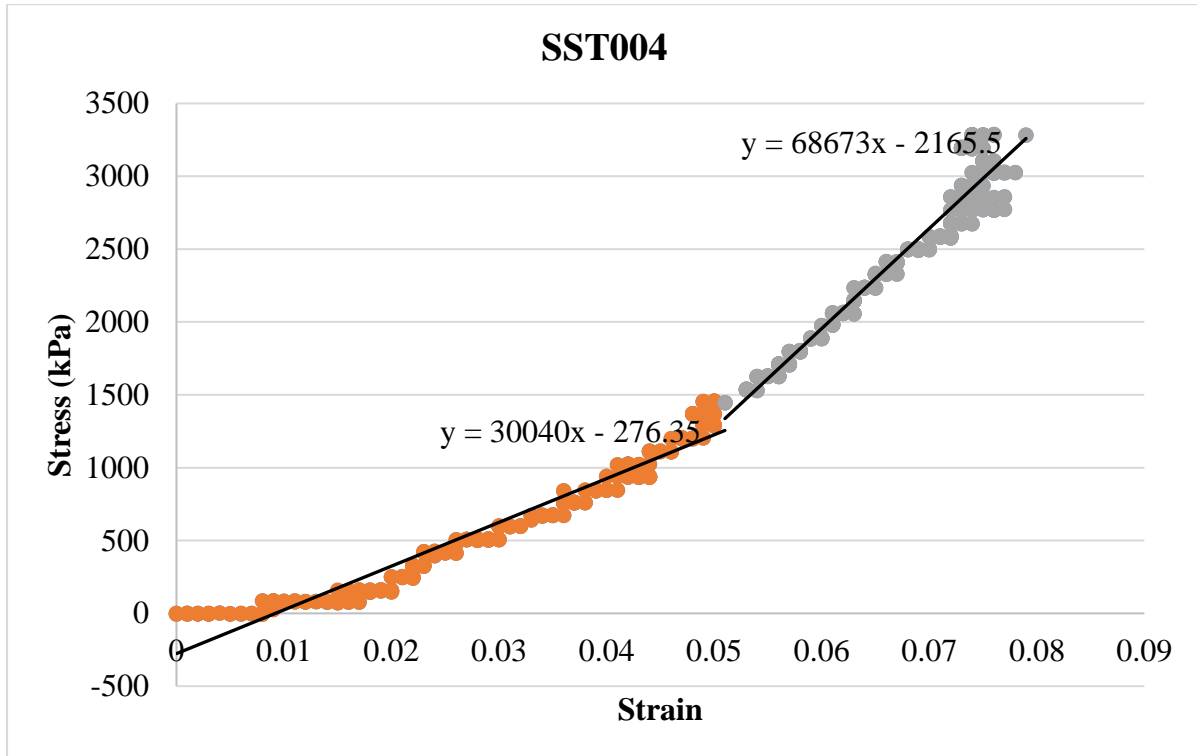
Estimated size(pages) 115

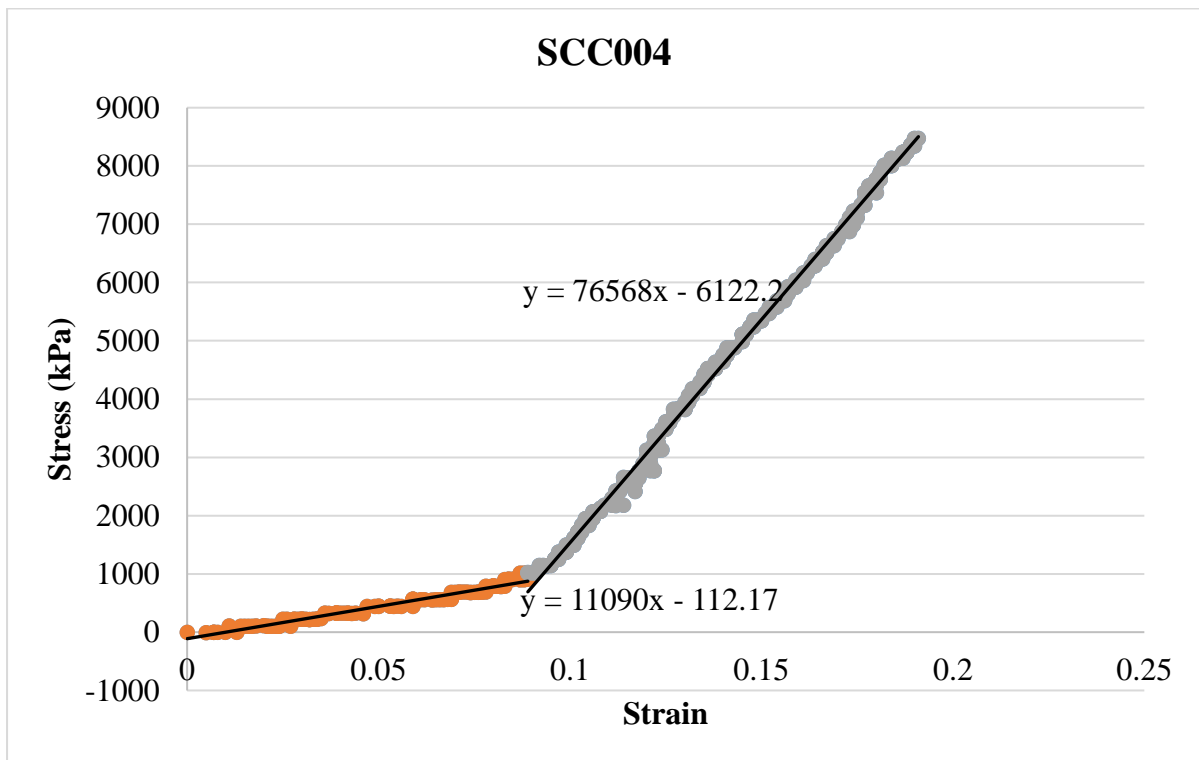
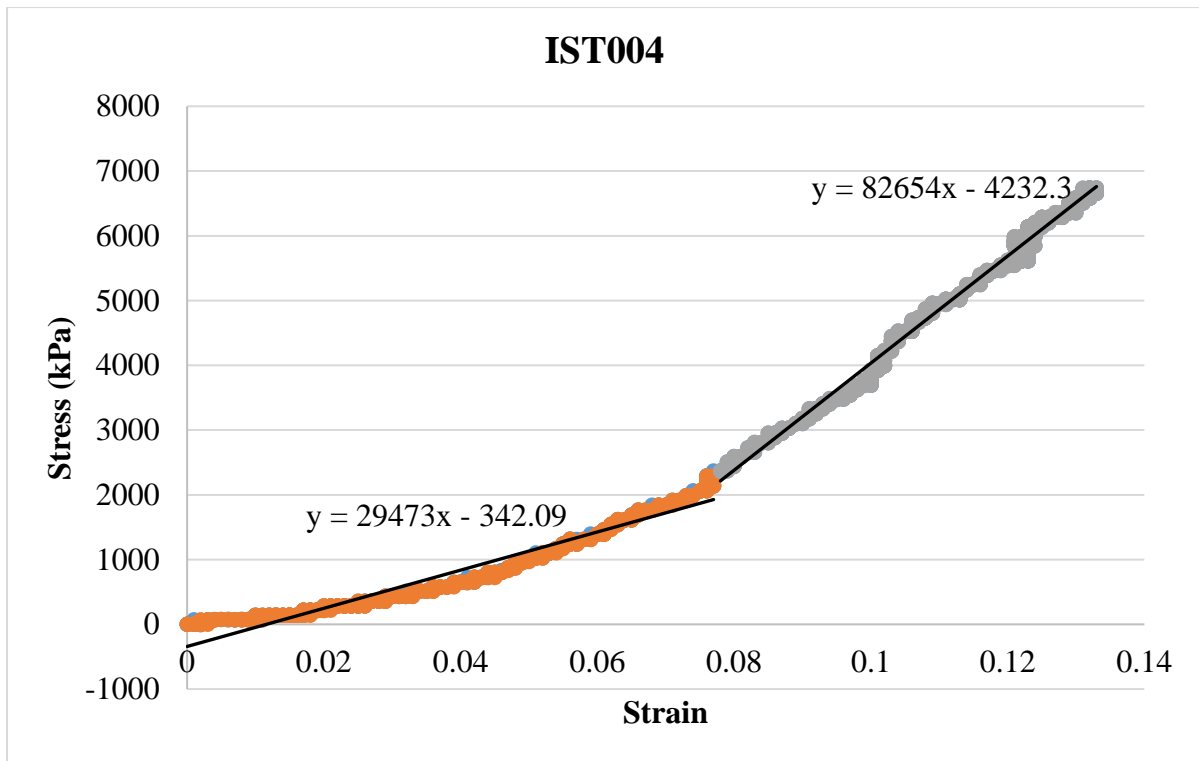
Requestor Location University of Pretoria, Faculty of Health Sciences, BMS Library, Gezina, Pretoria, Gauteng 0001, South Africa, Attn: University of Pretoria

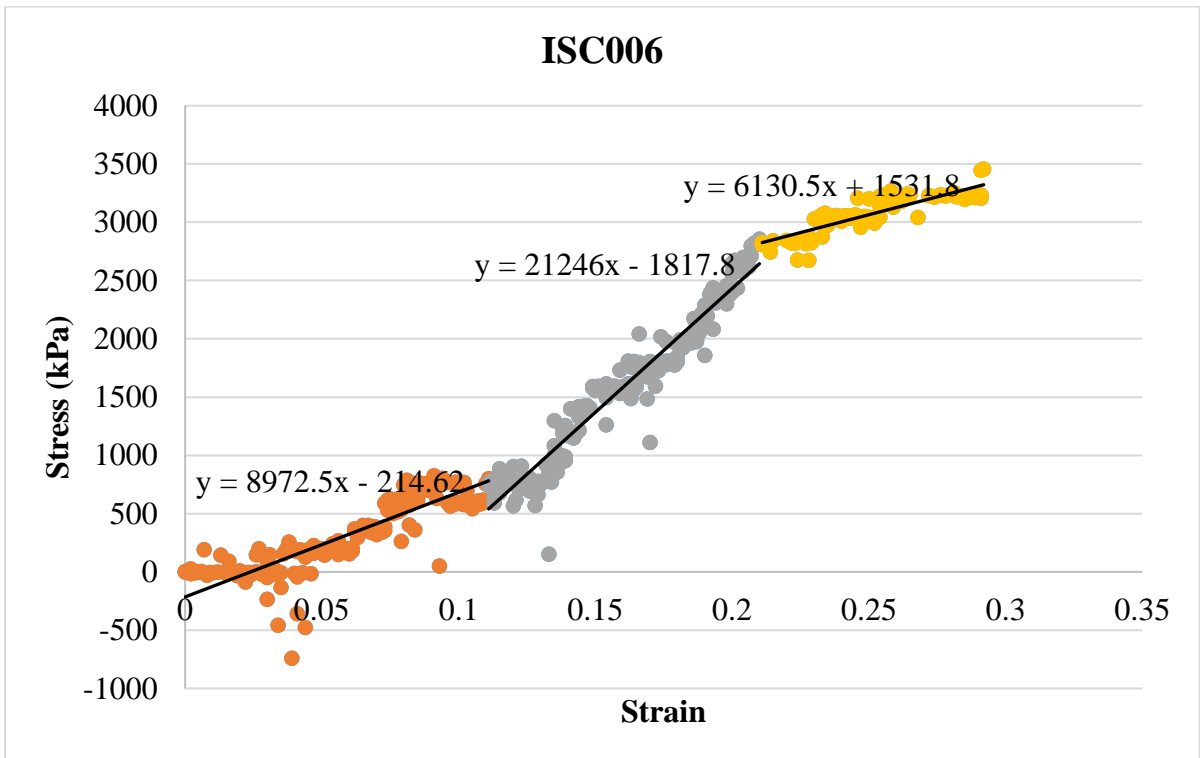
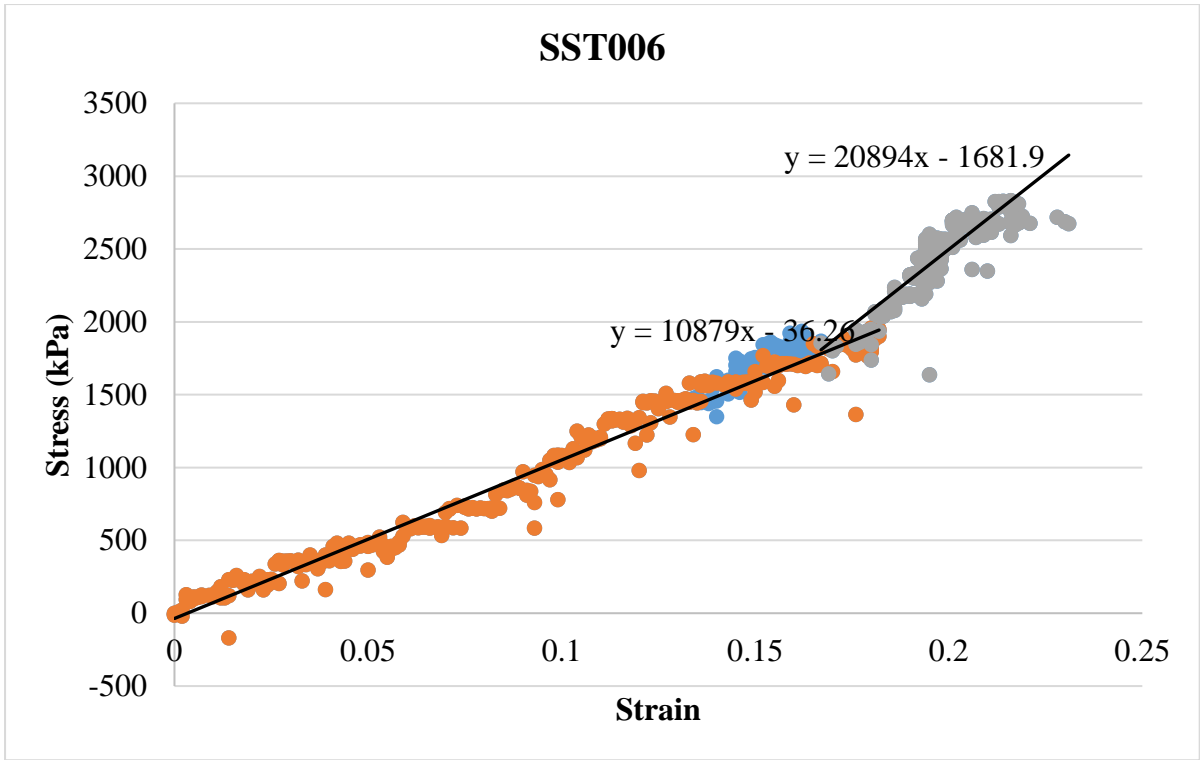
Publisher Tax ID 4070265758

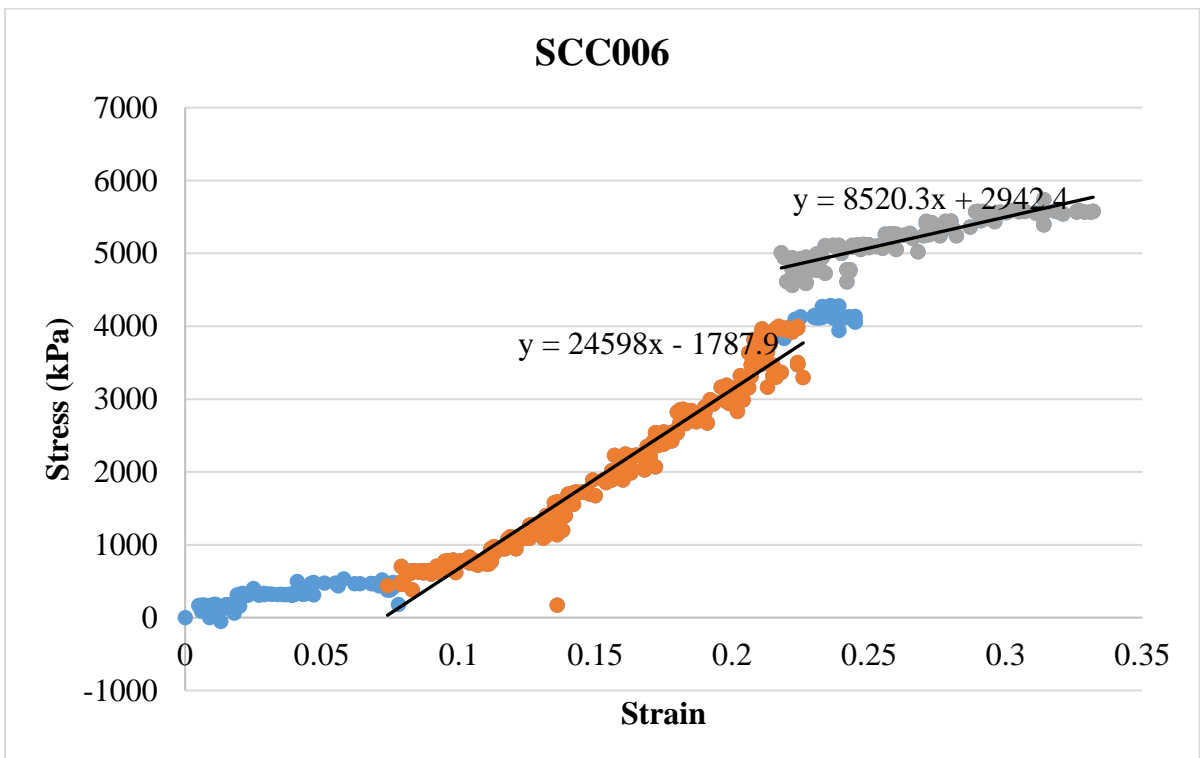
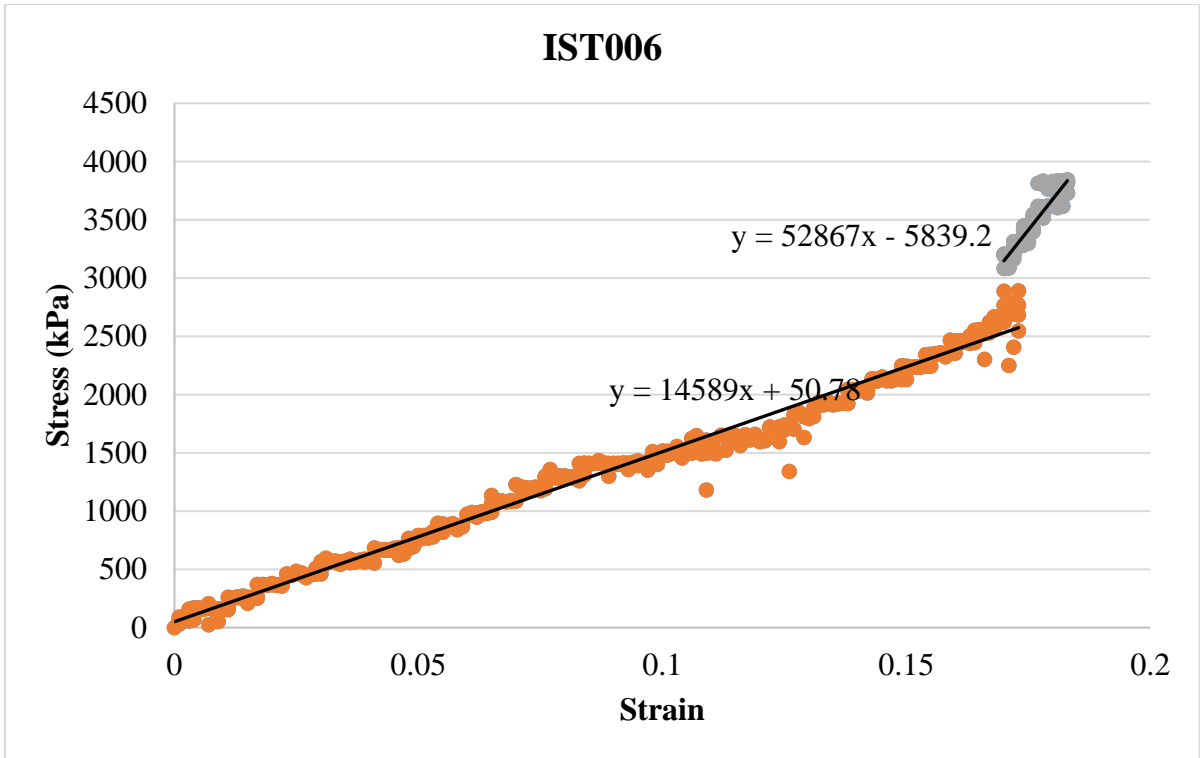
Total 0.00 USD

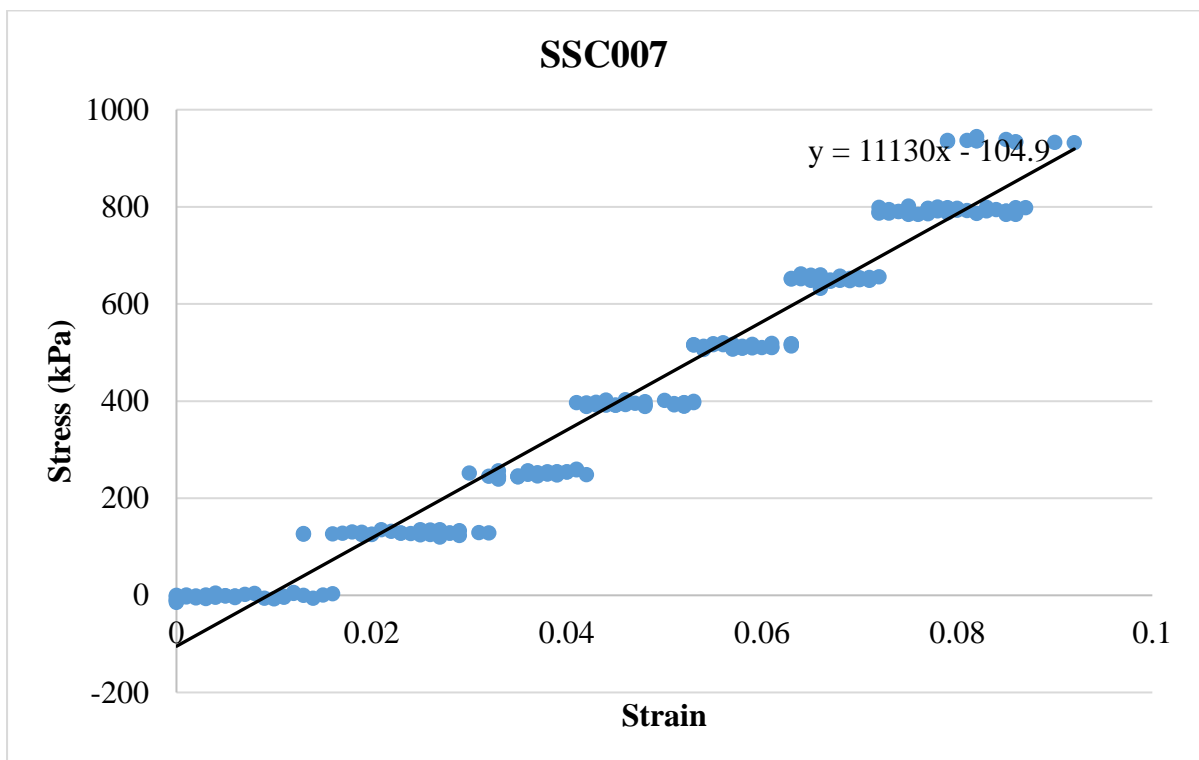
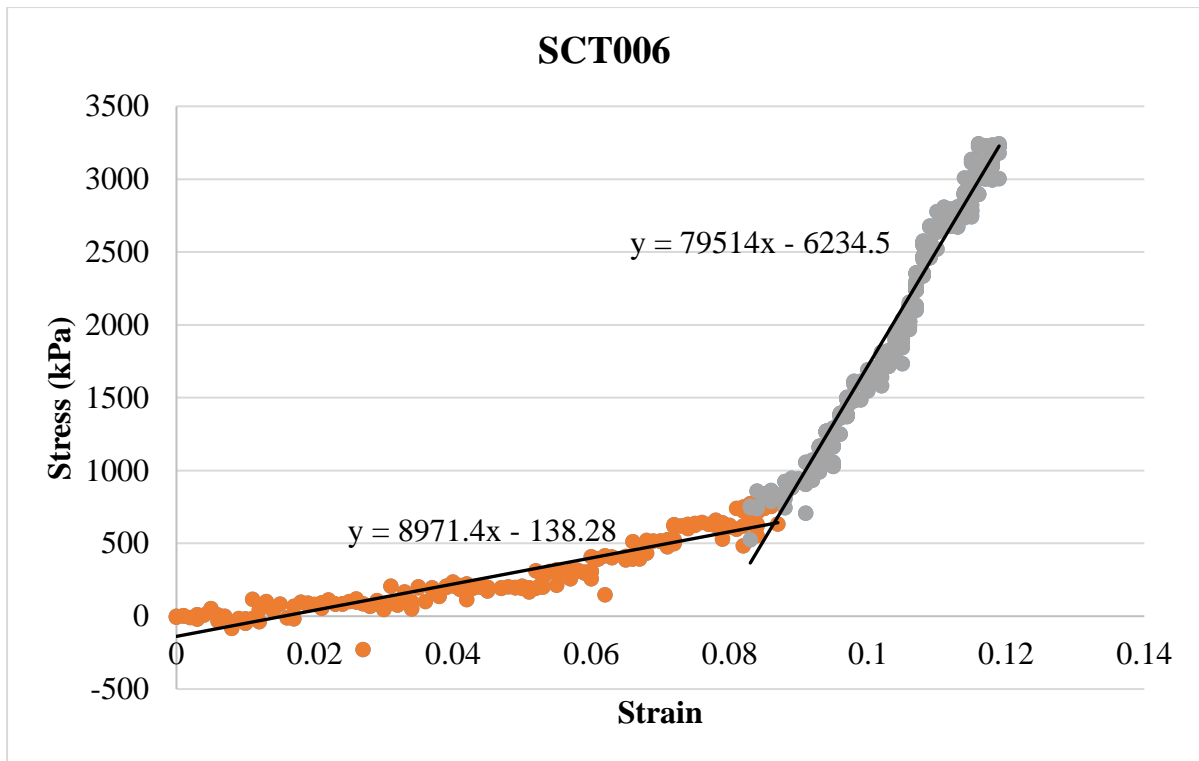
7.5. Annexure 5: Graphic representation for individual elastic modulus findings in Chapter 4, Section 4.1.4.

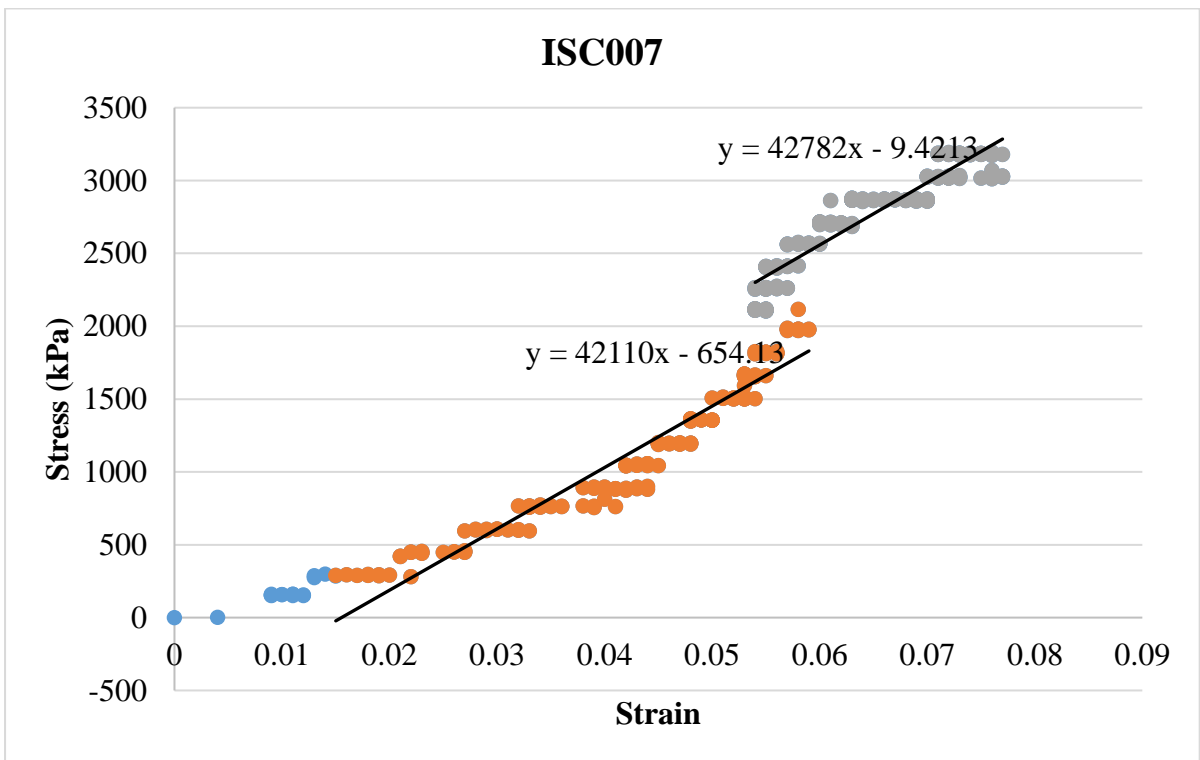
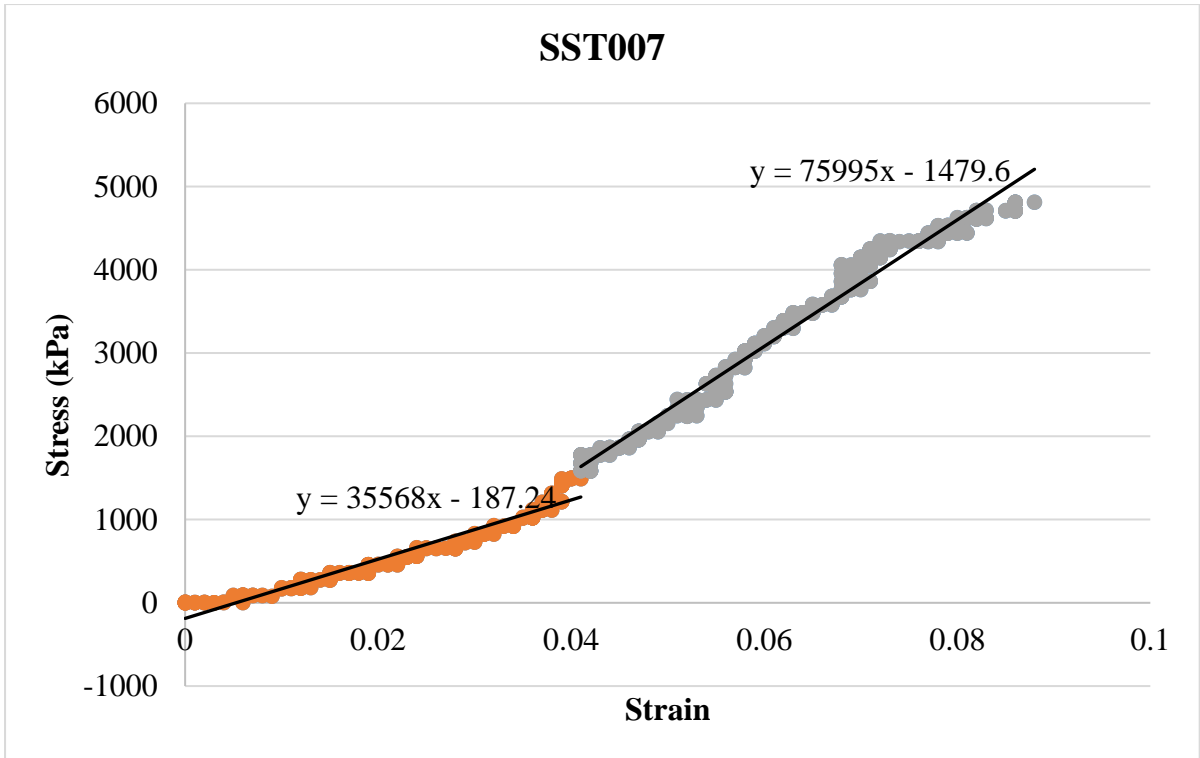


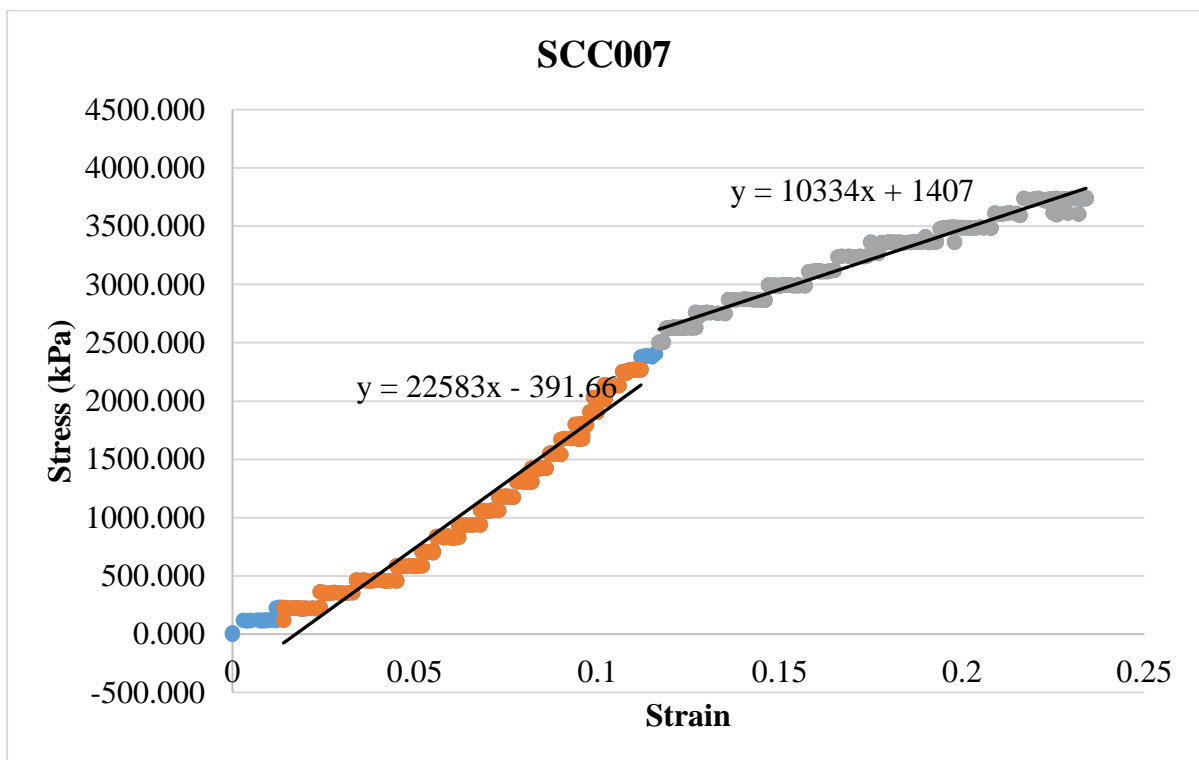
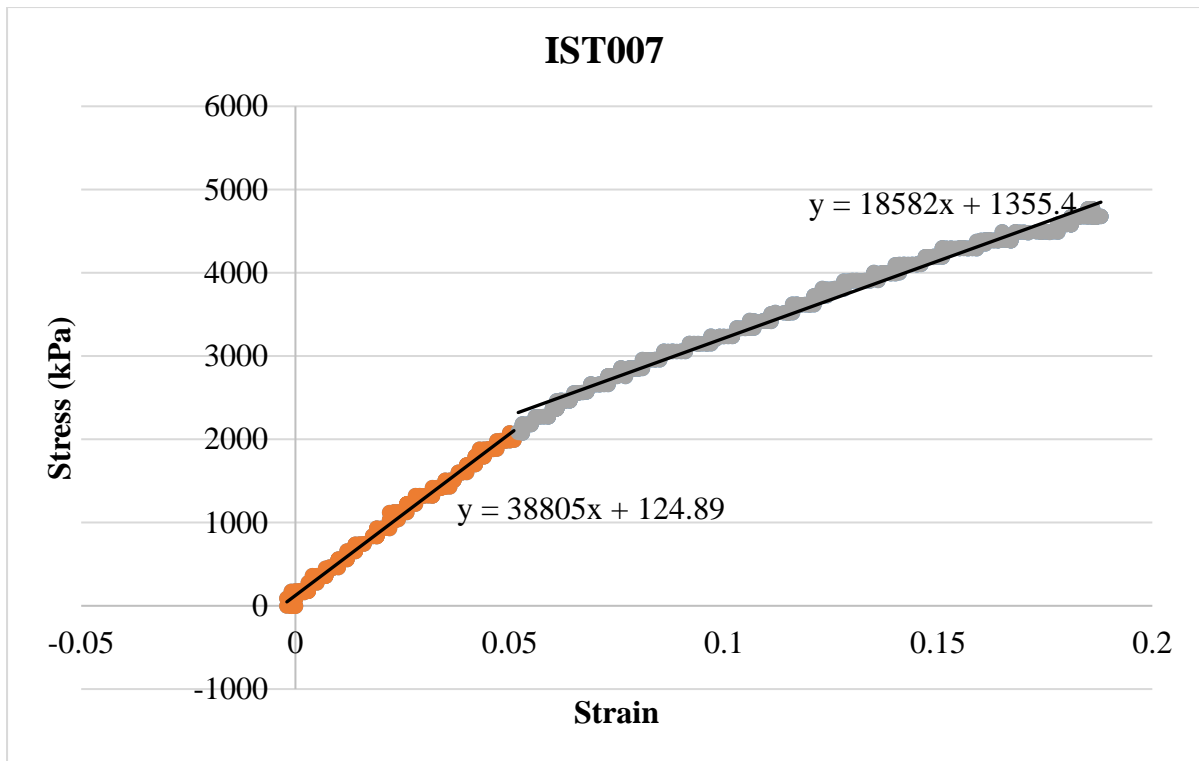


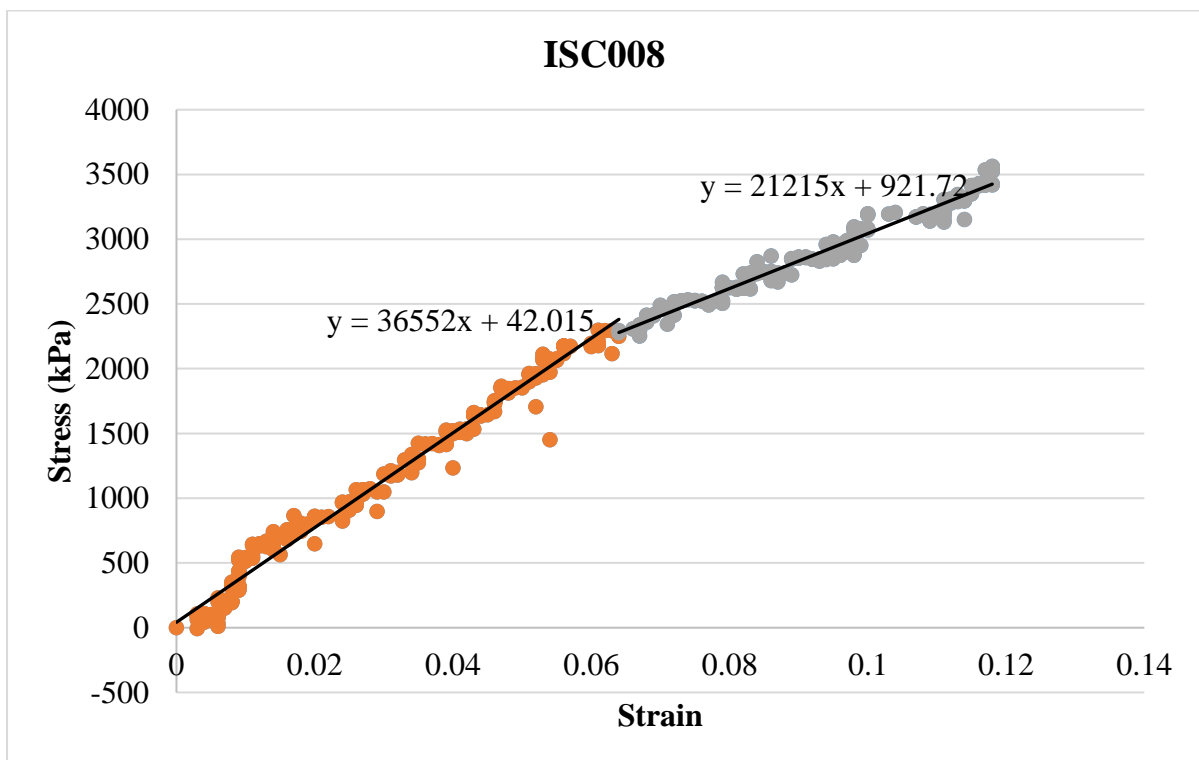
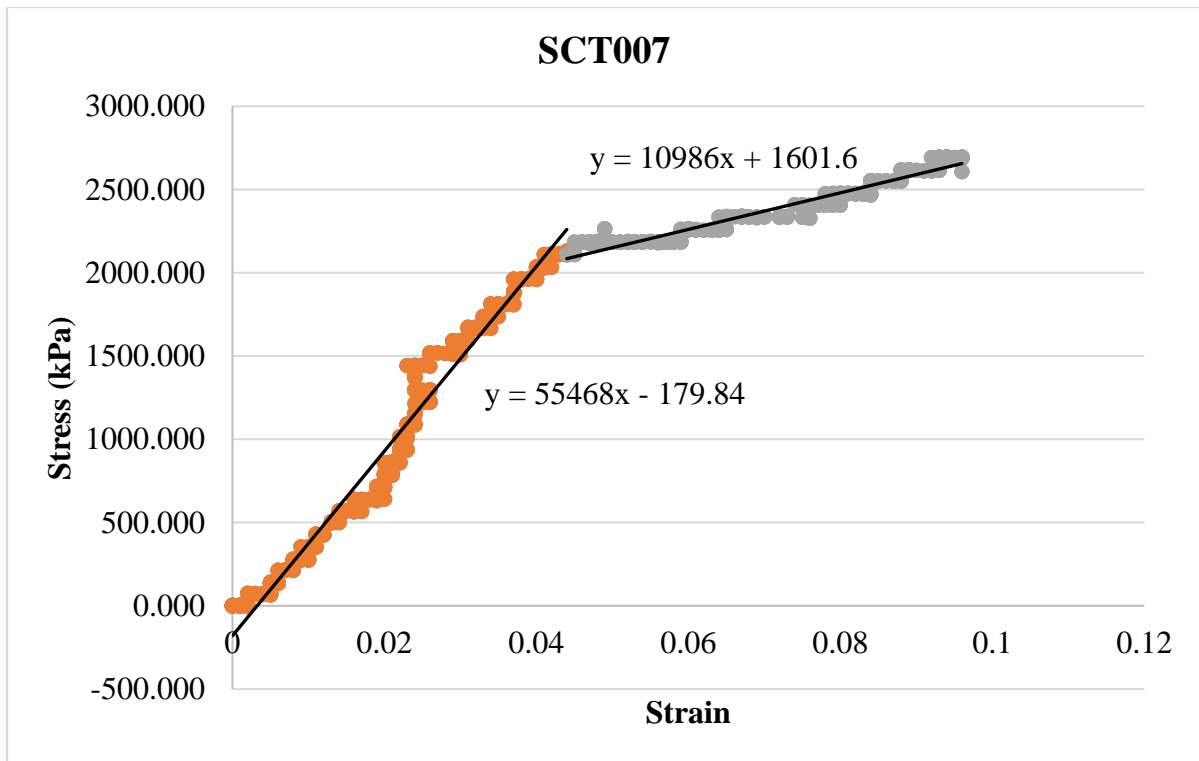


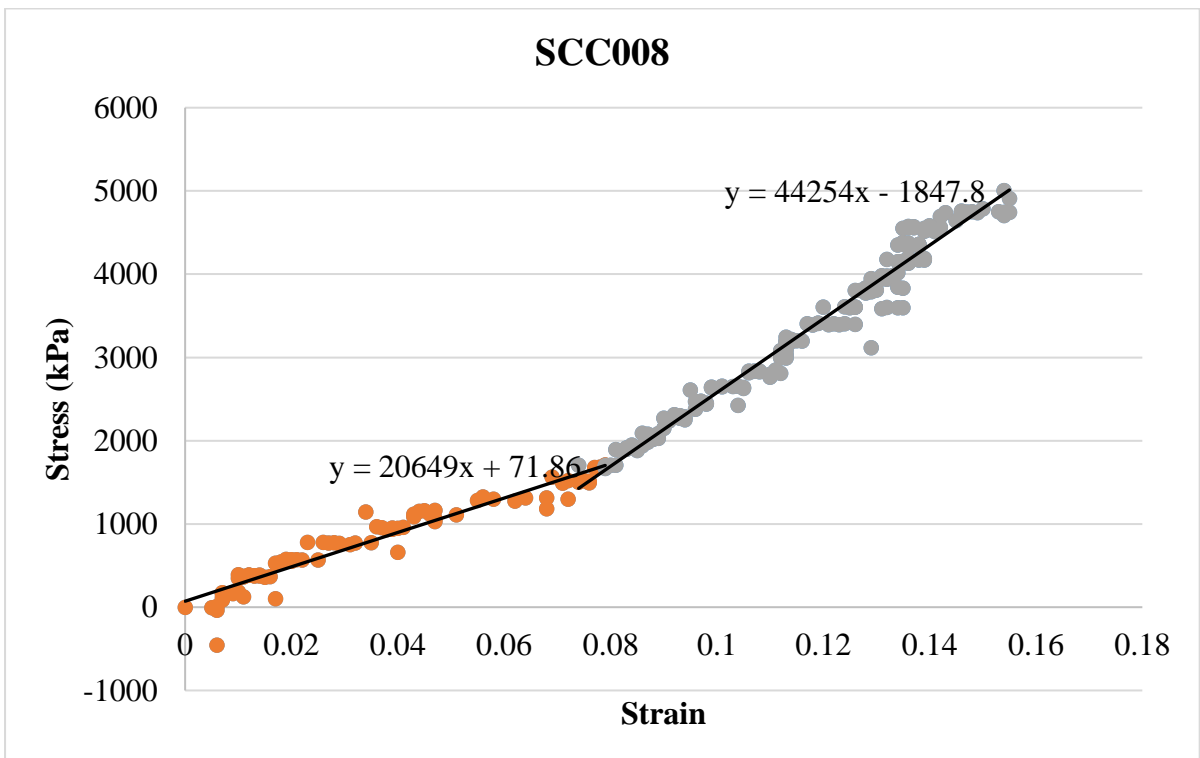
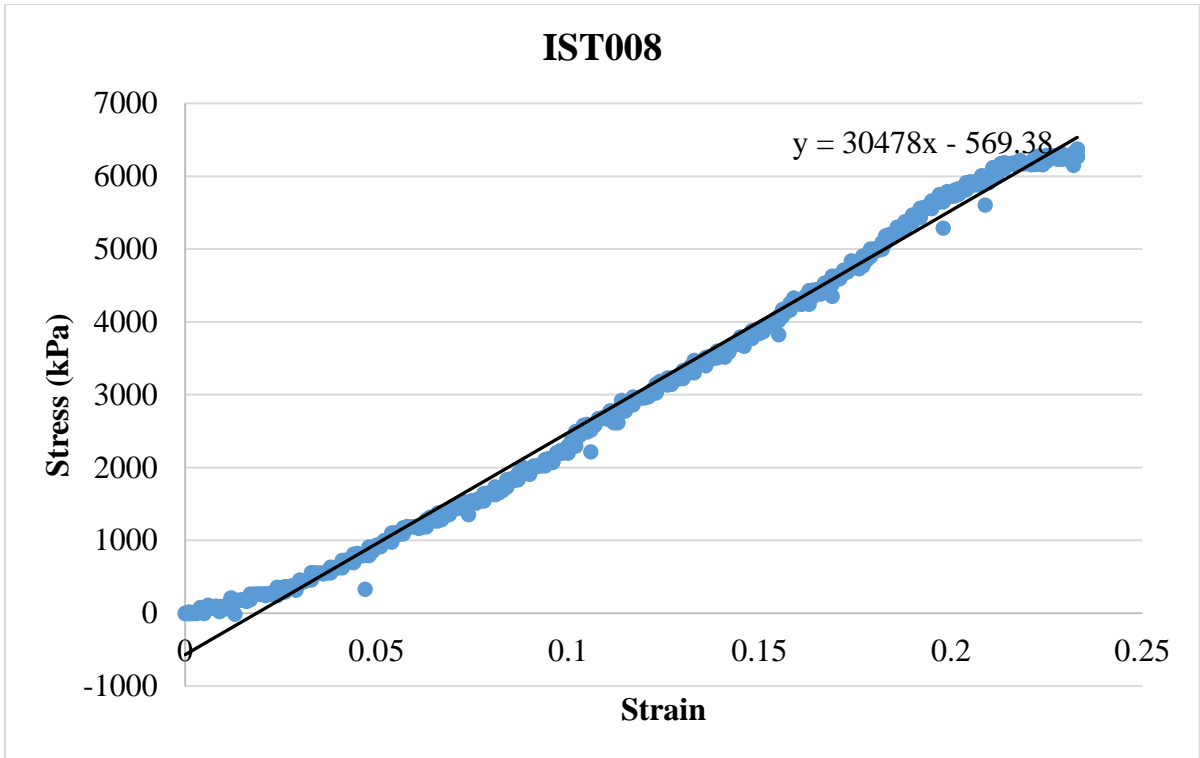


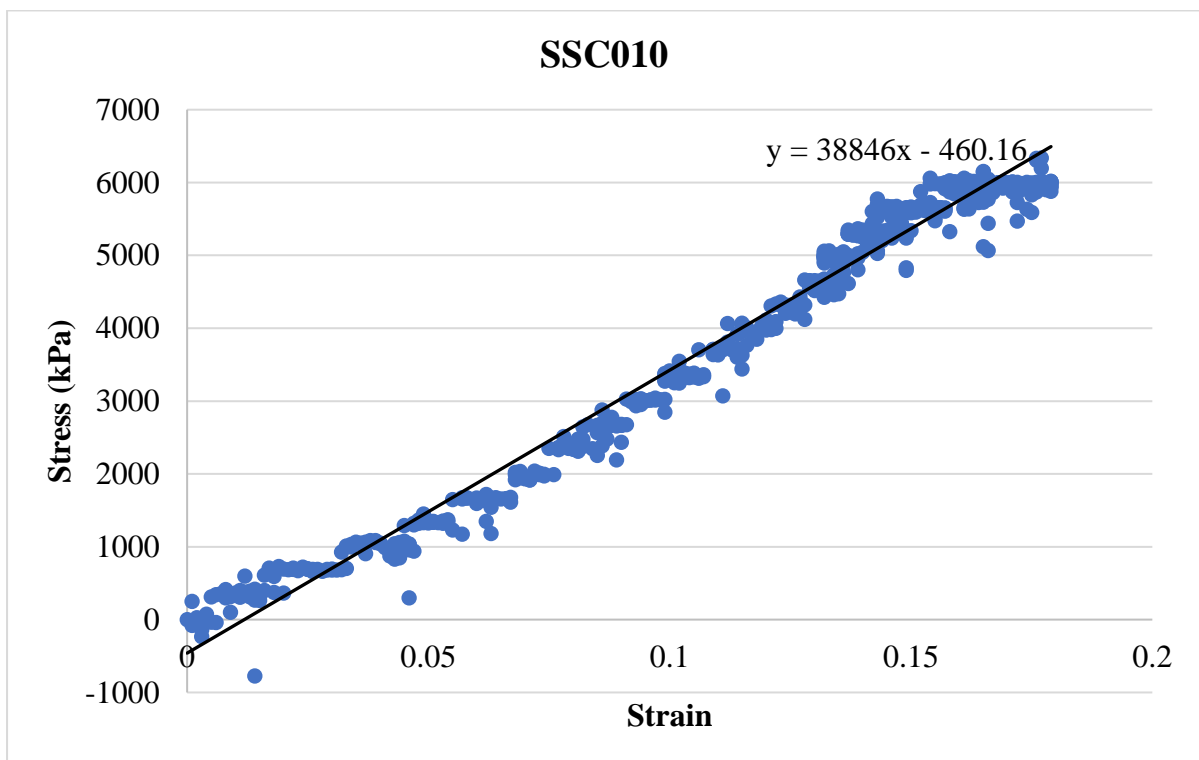
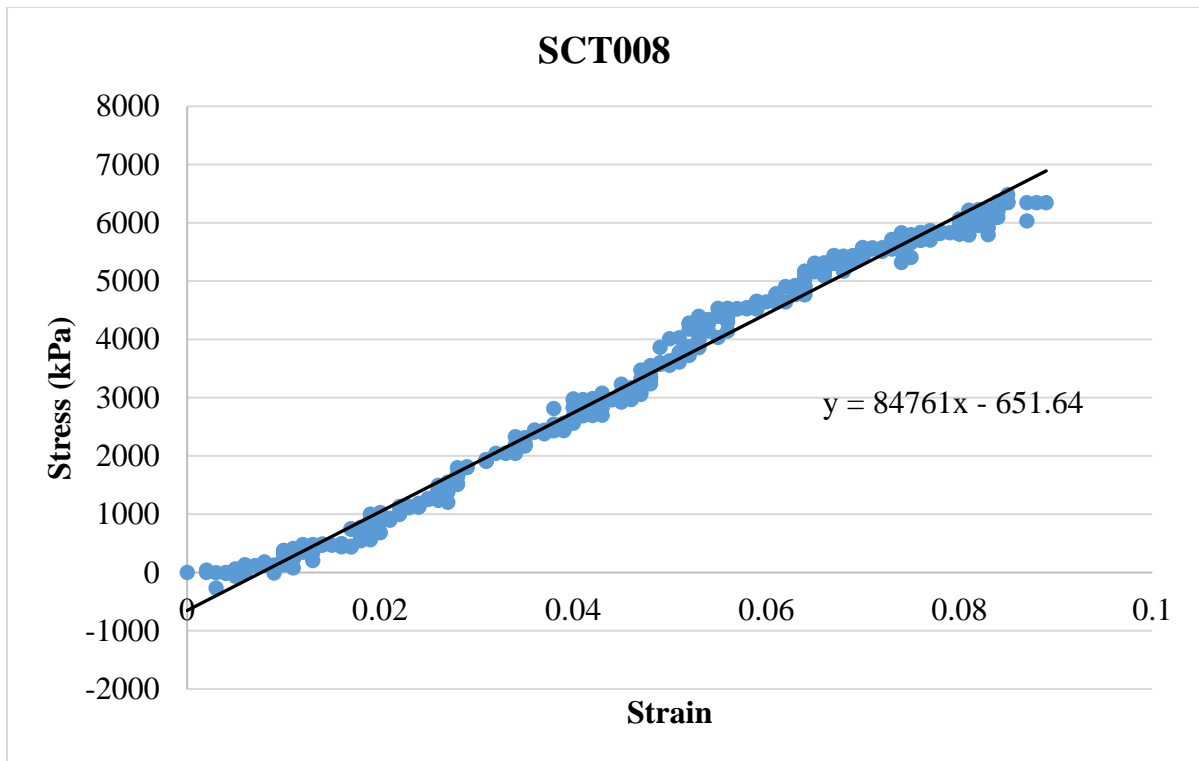


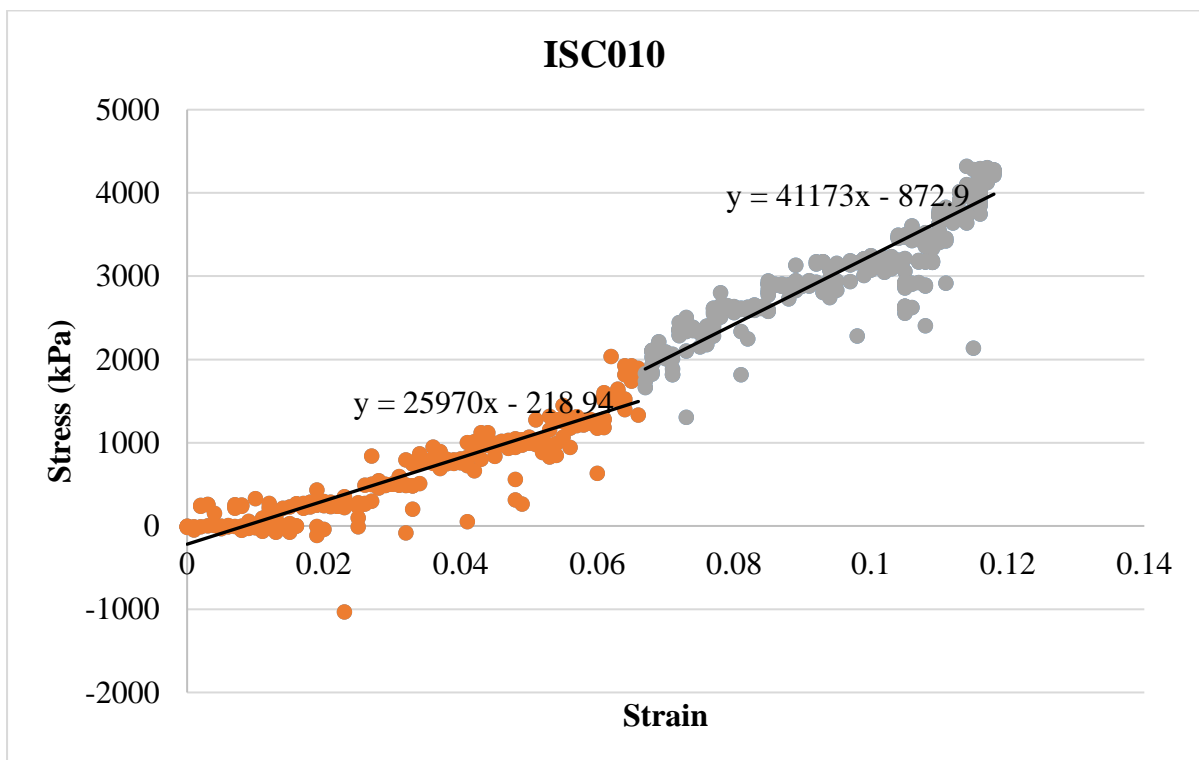
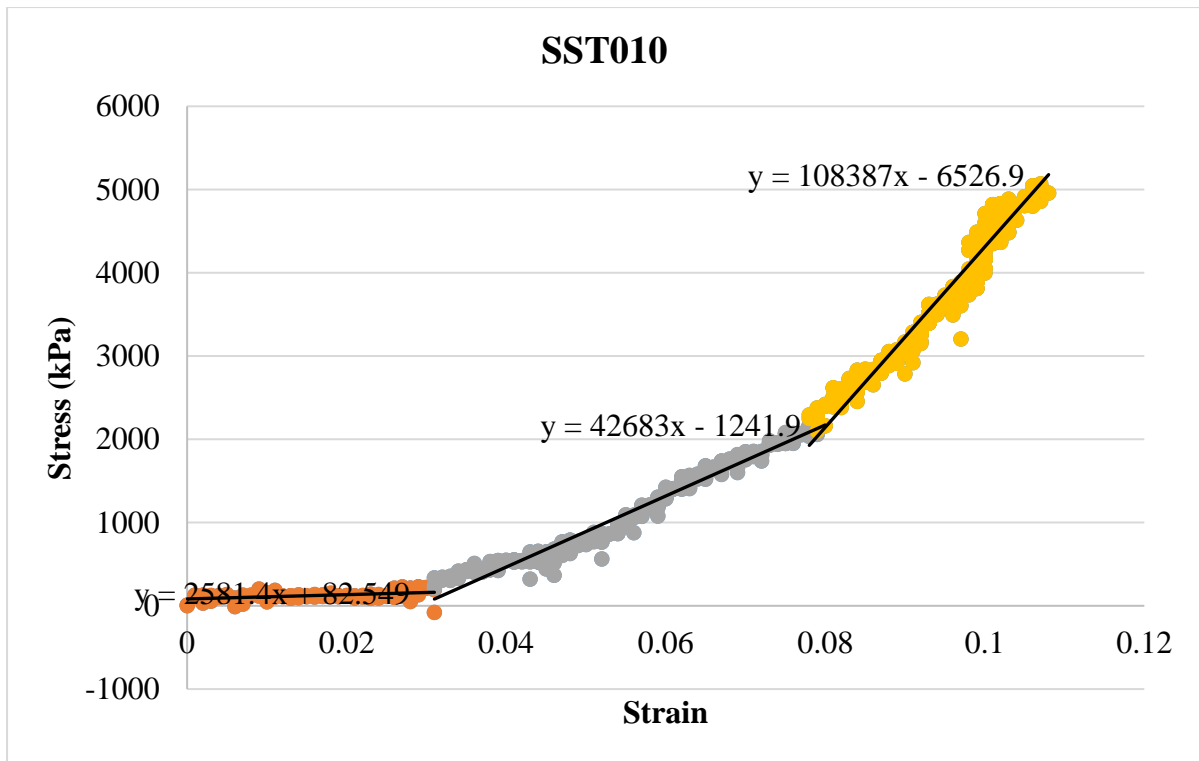


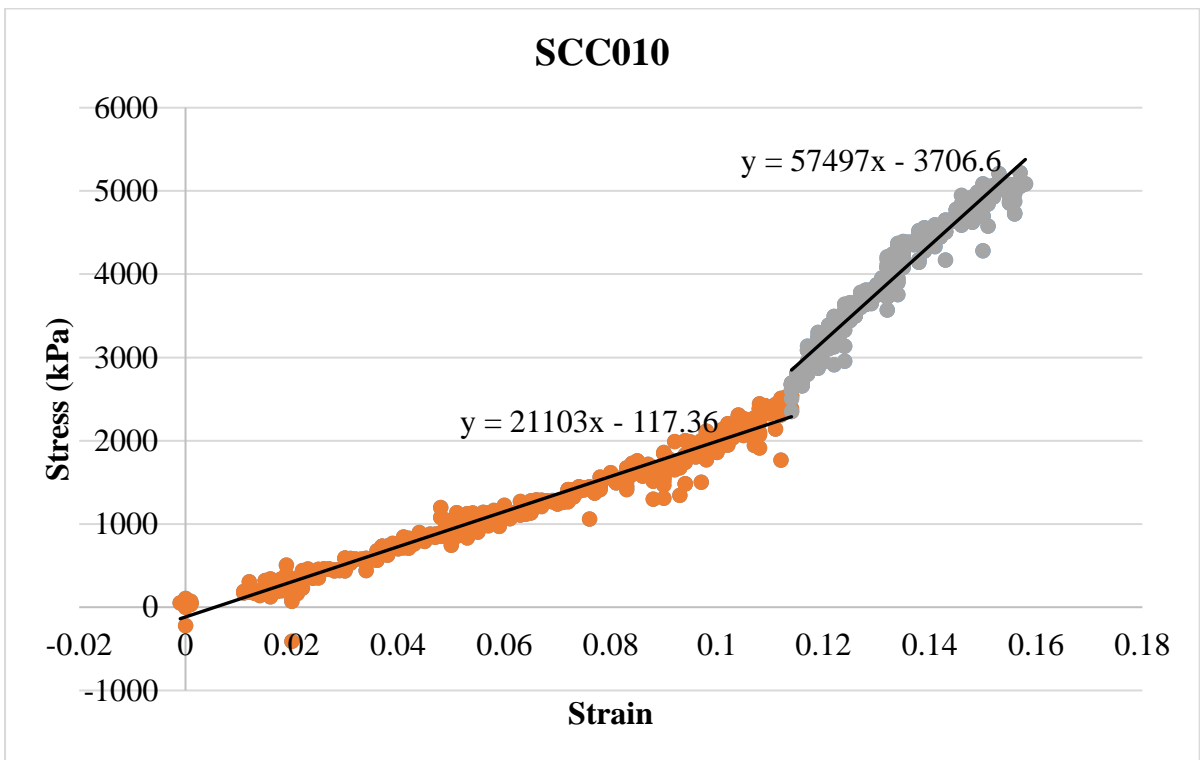
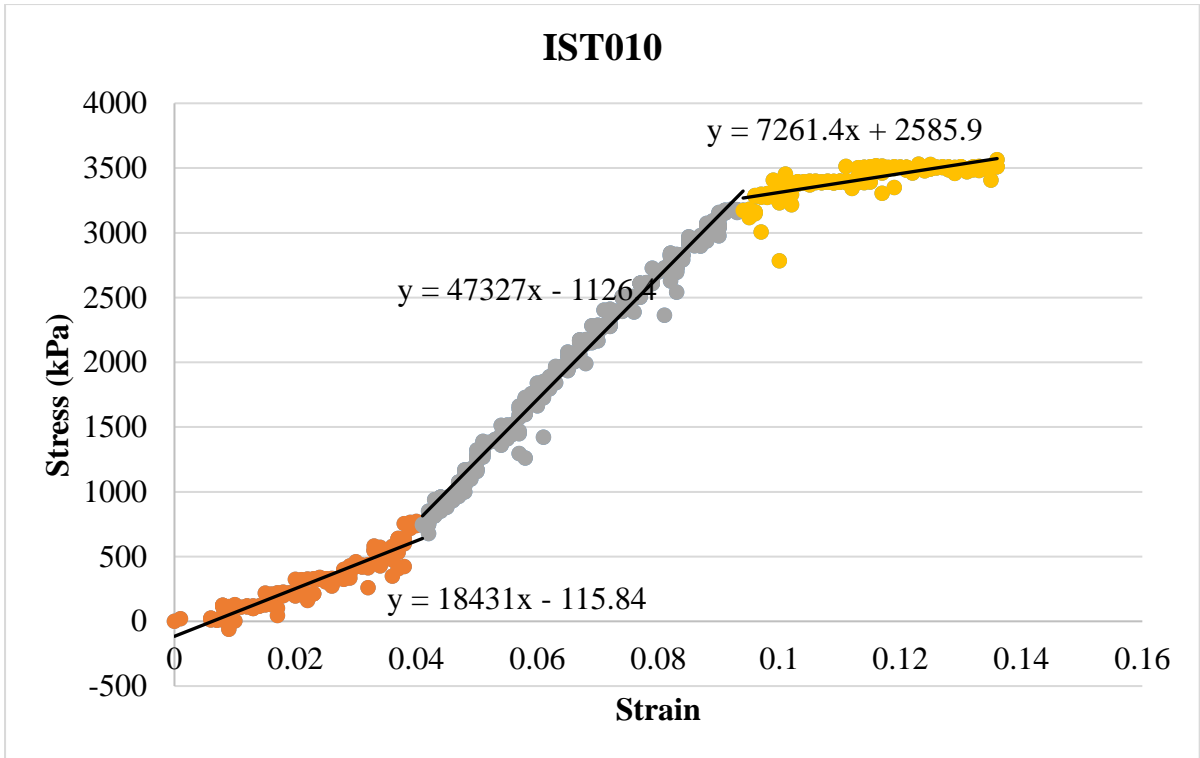


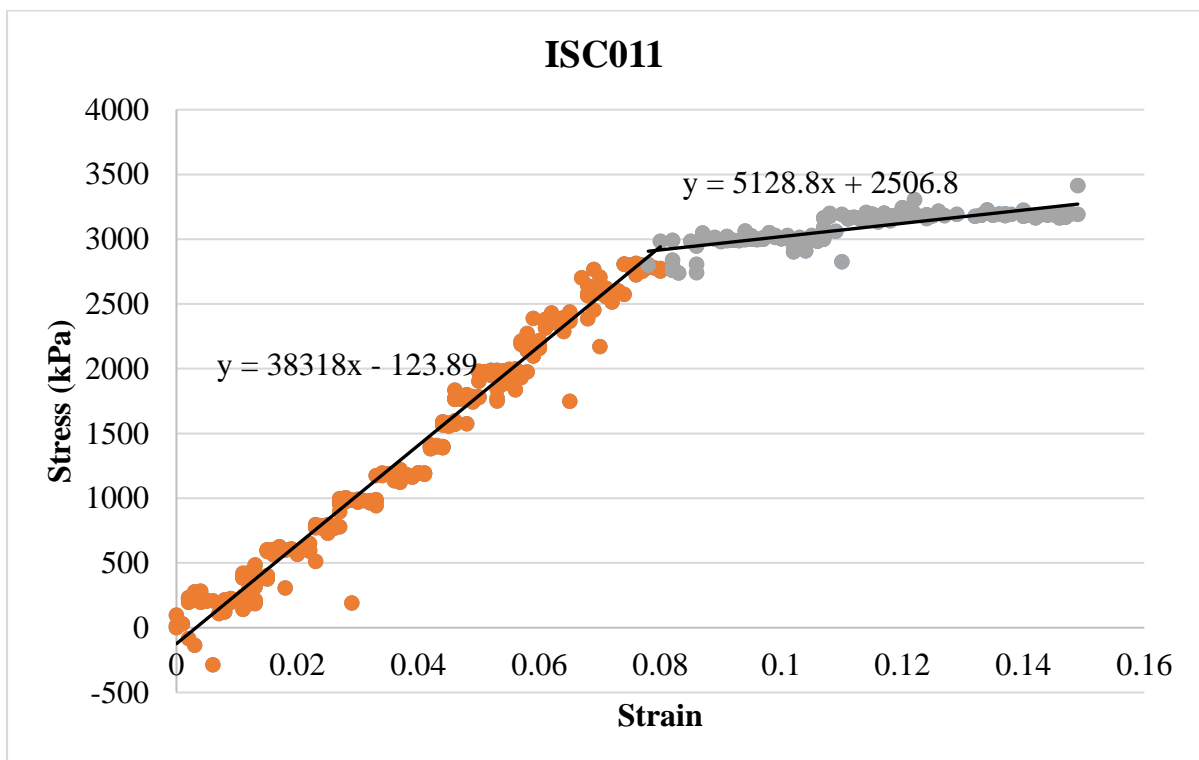
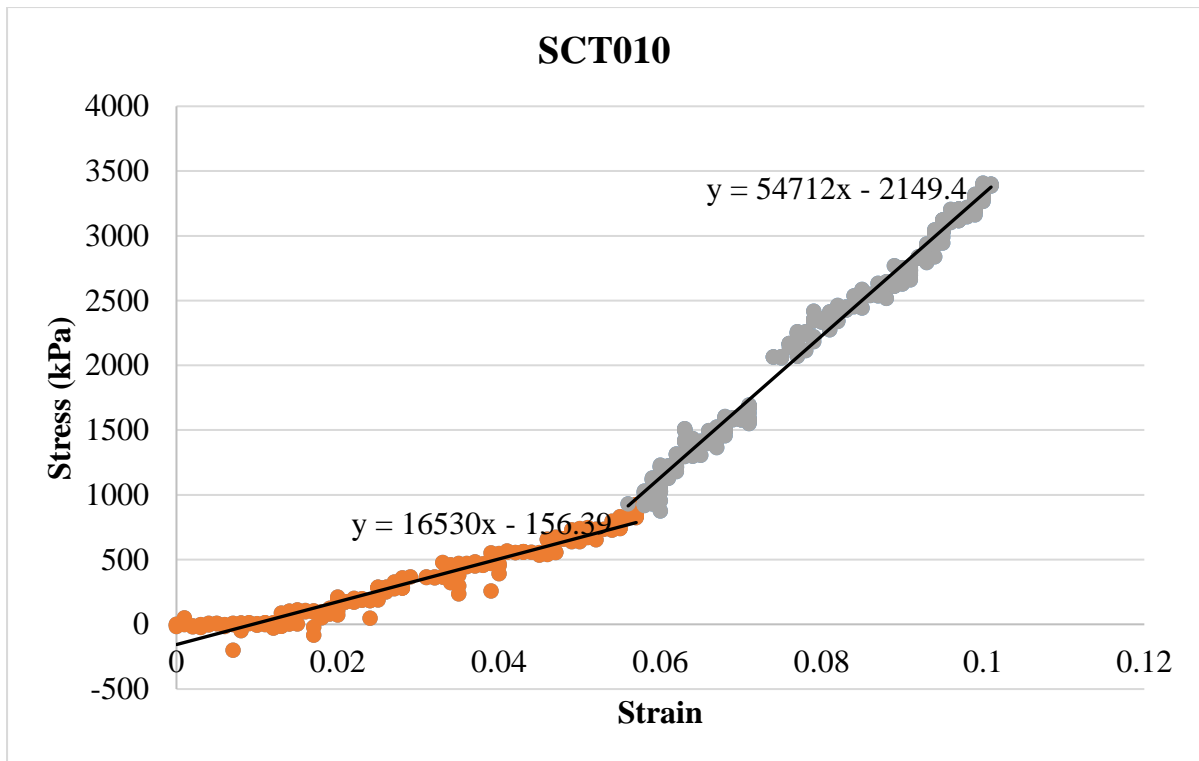


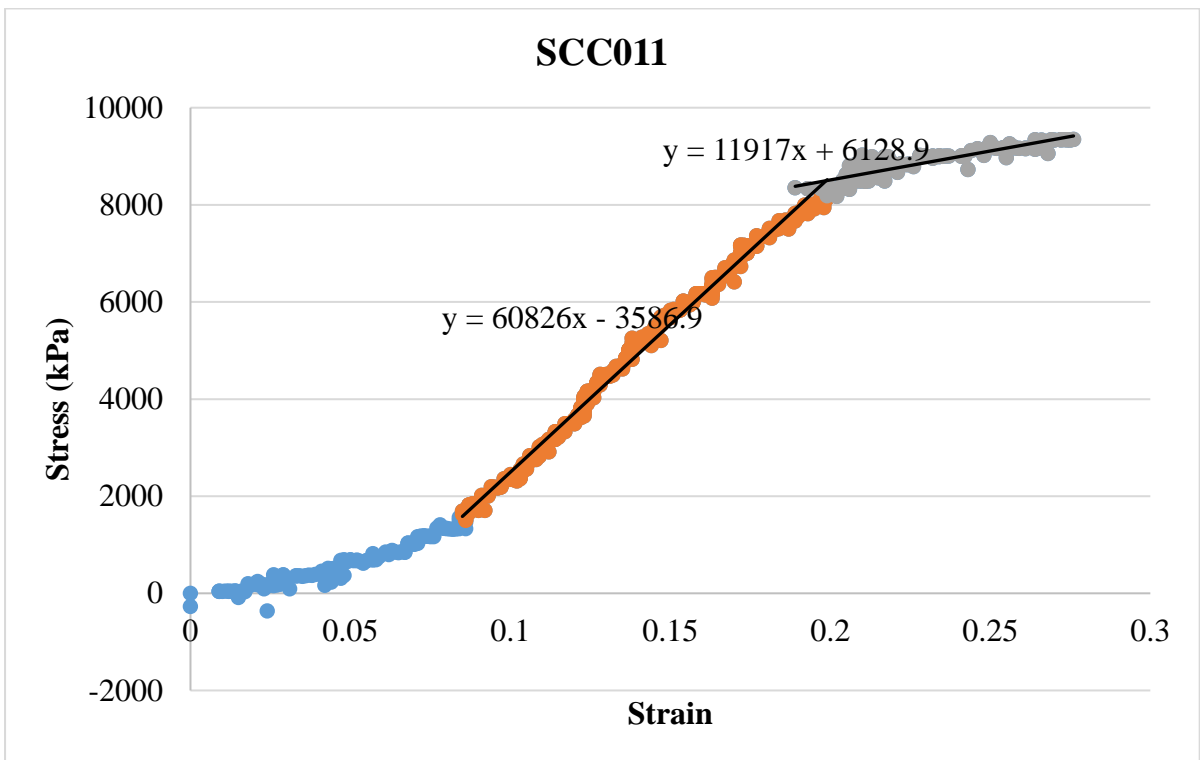
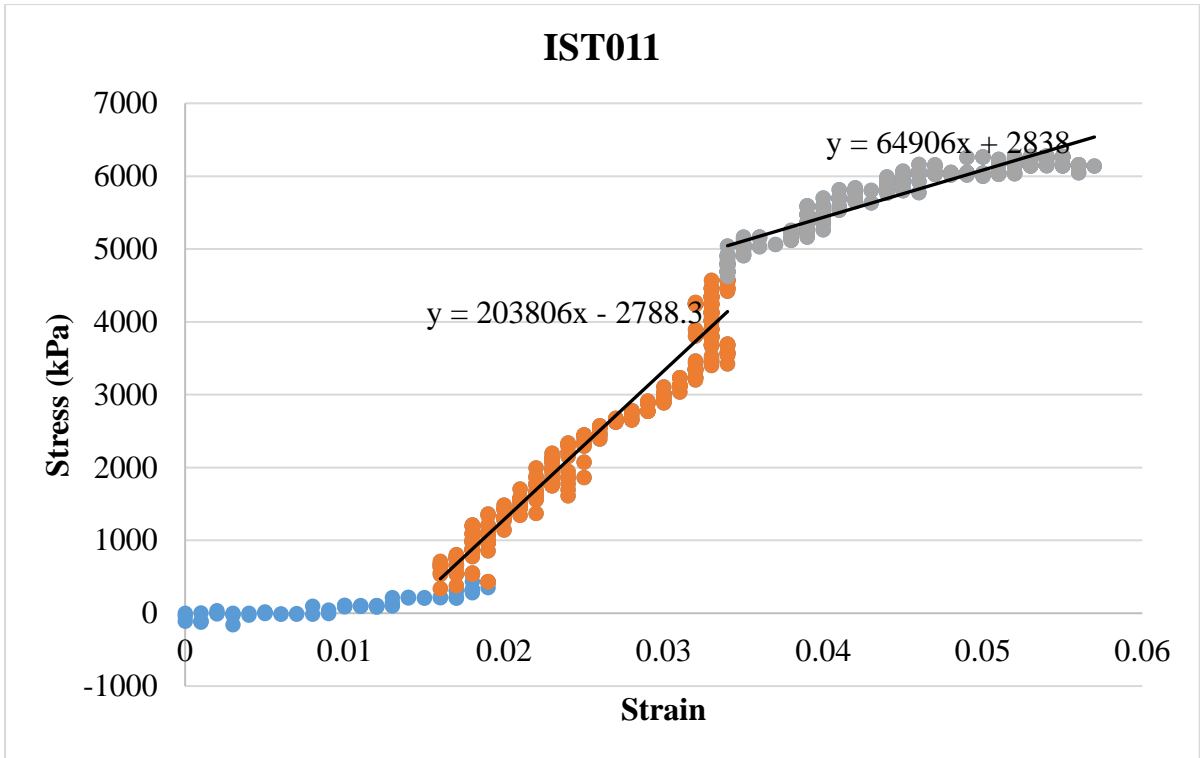


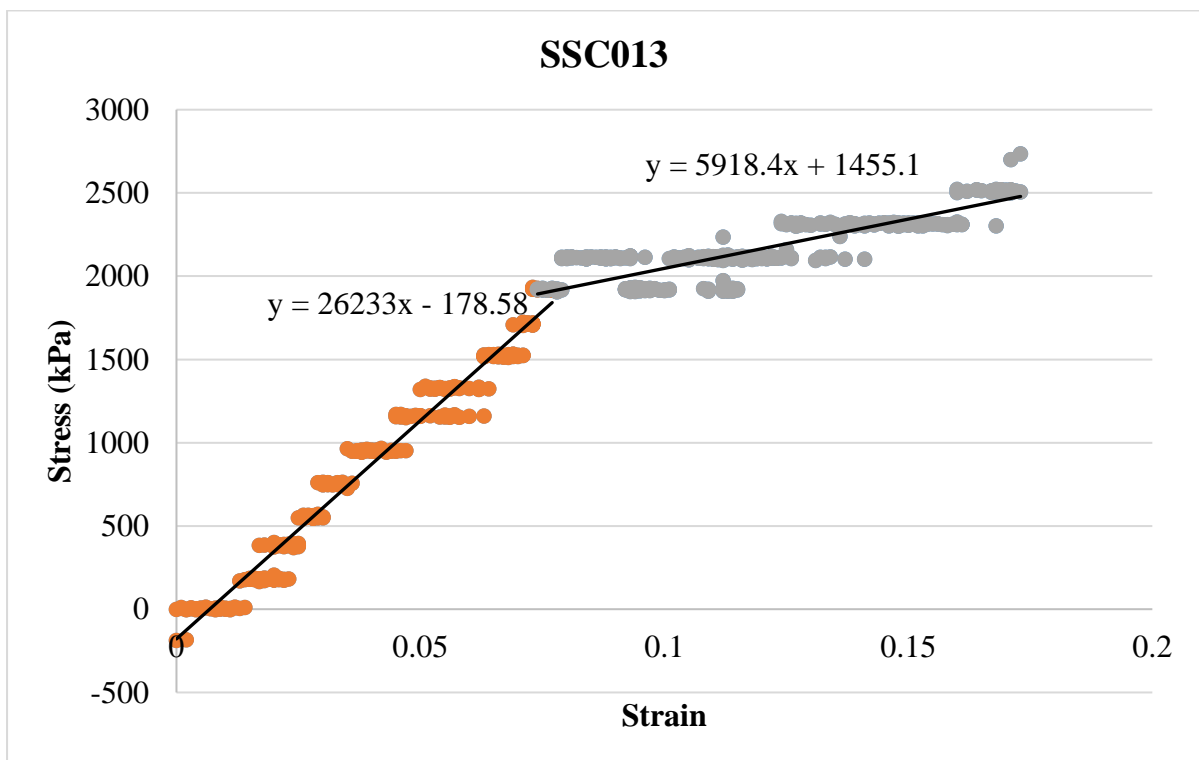
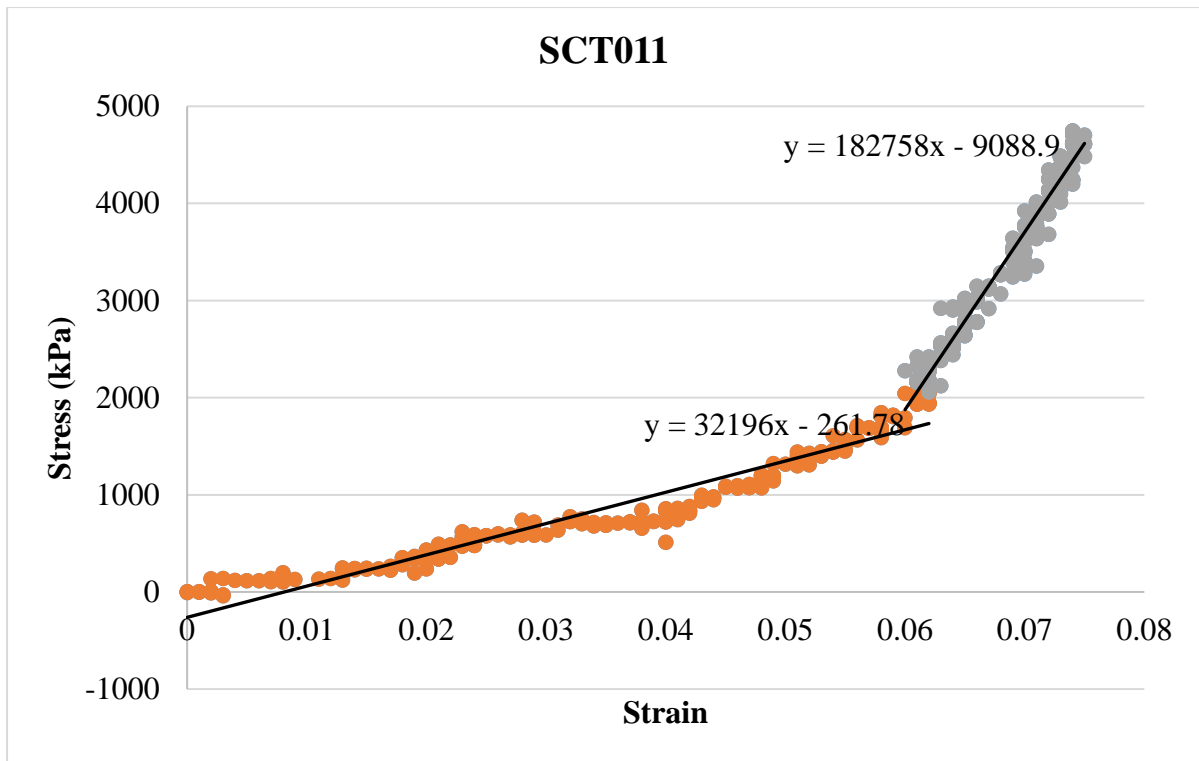


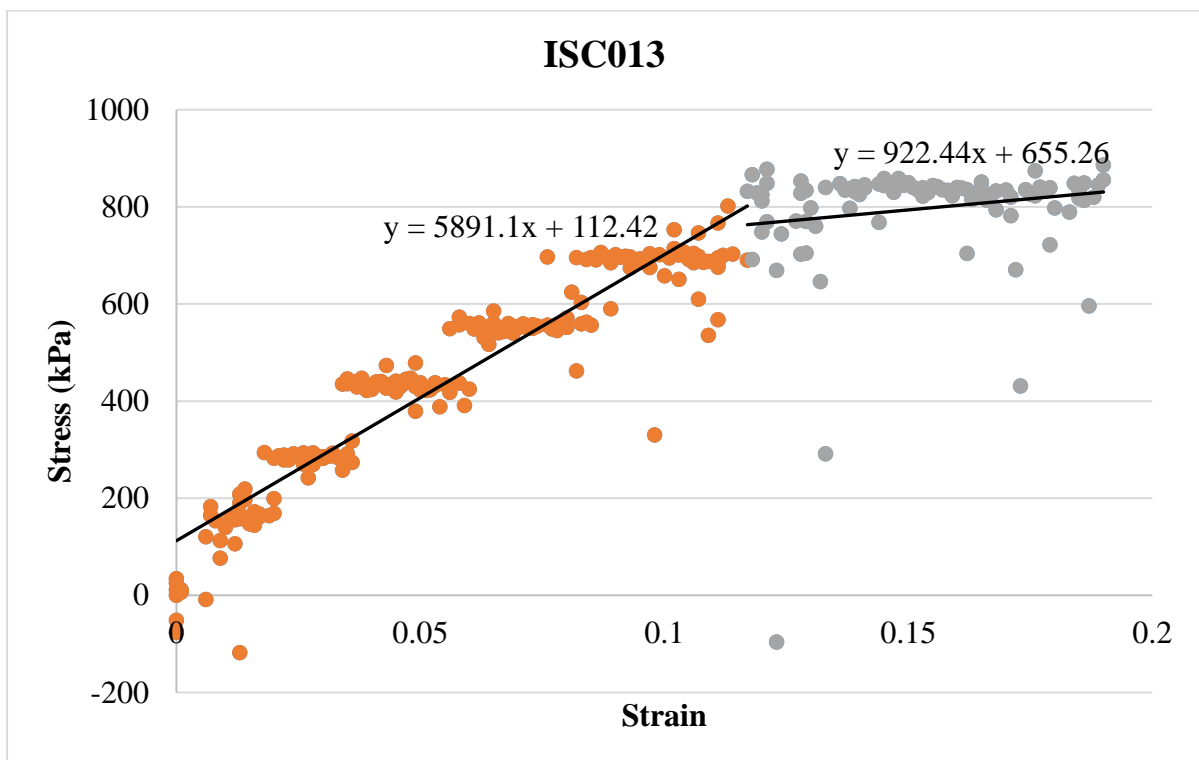
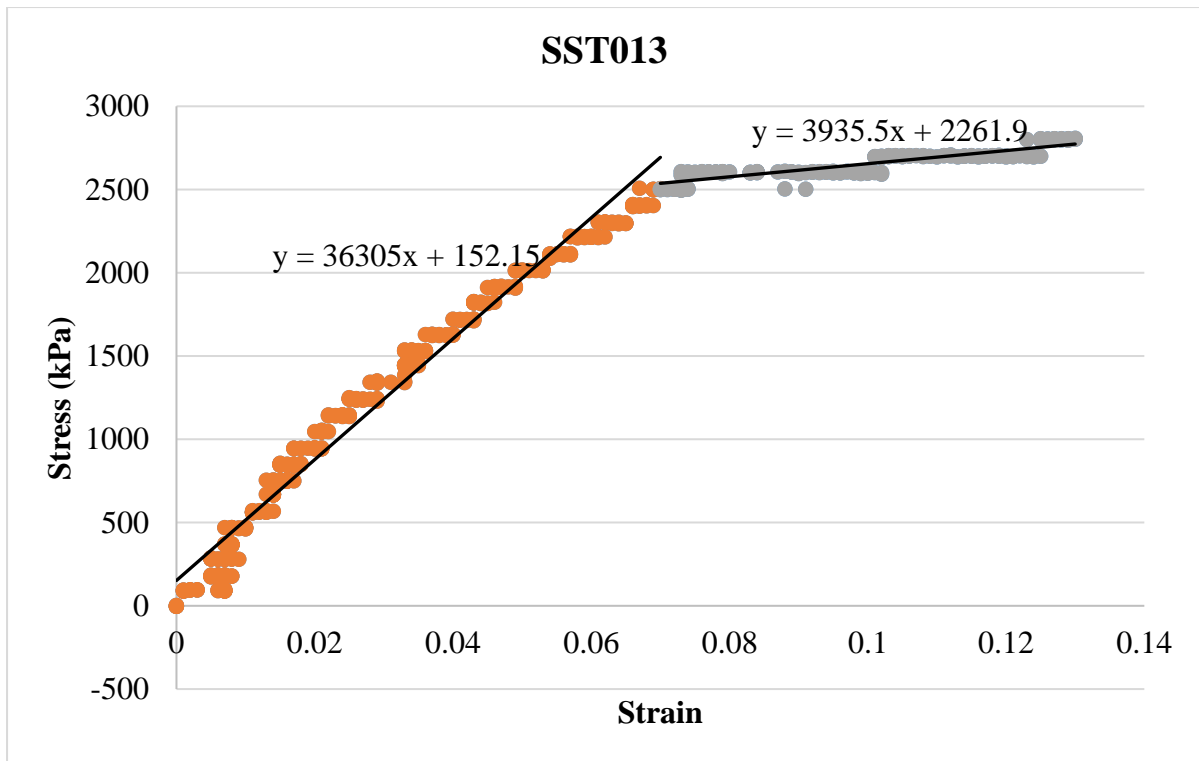


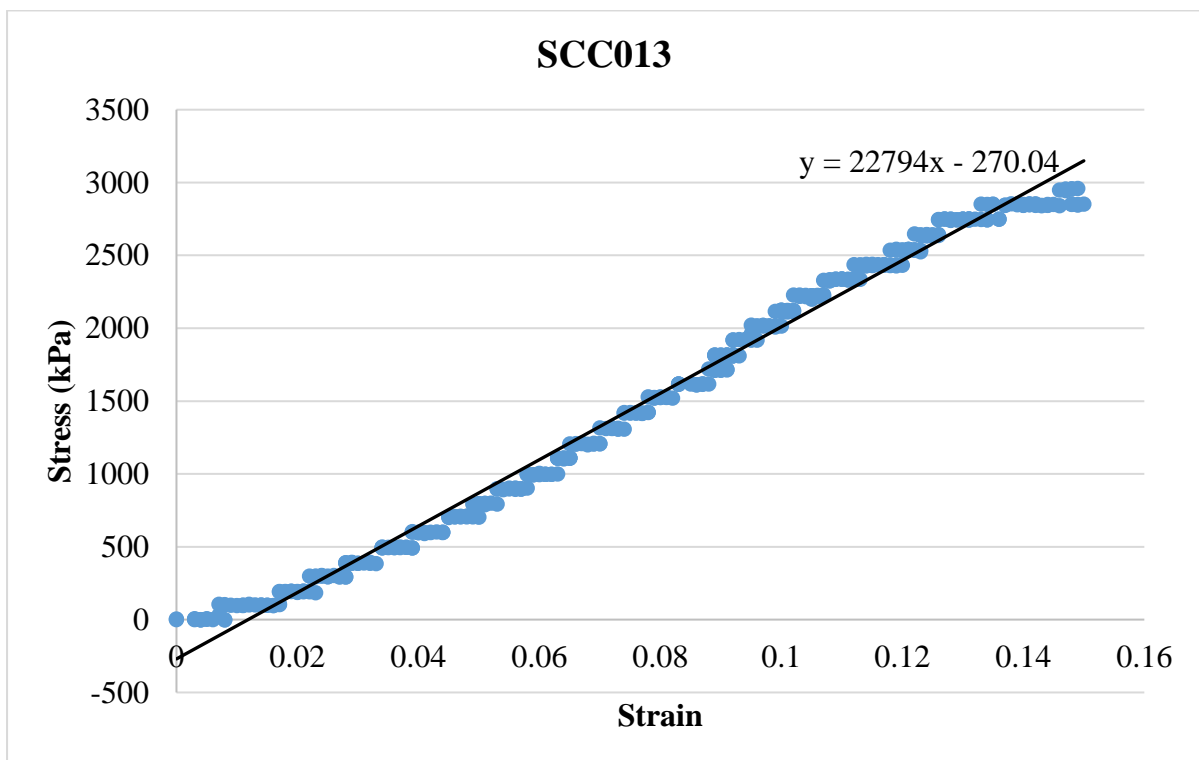
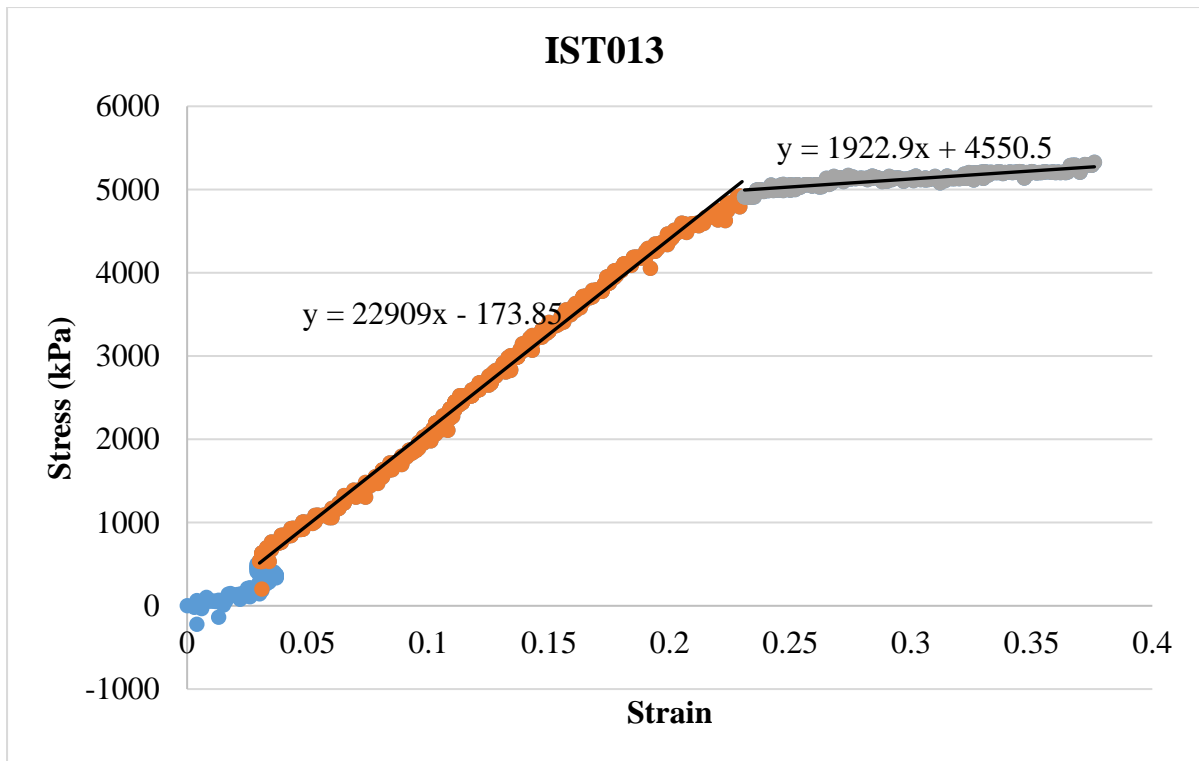


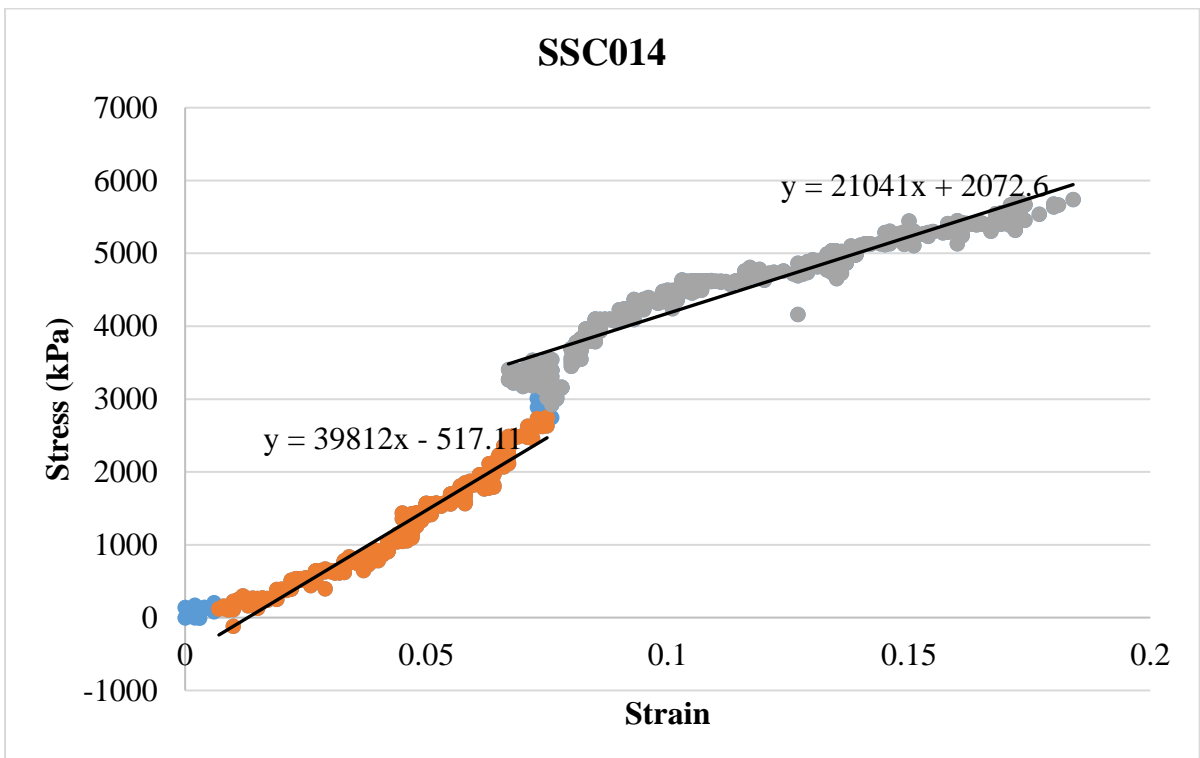
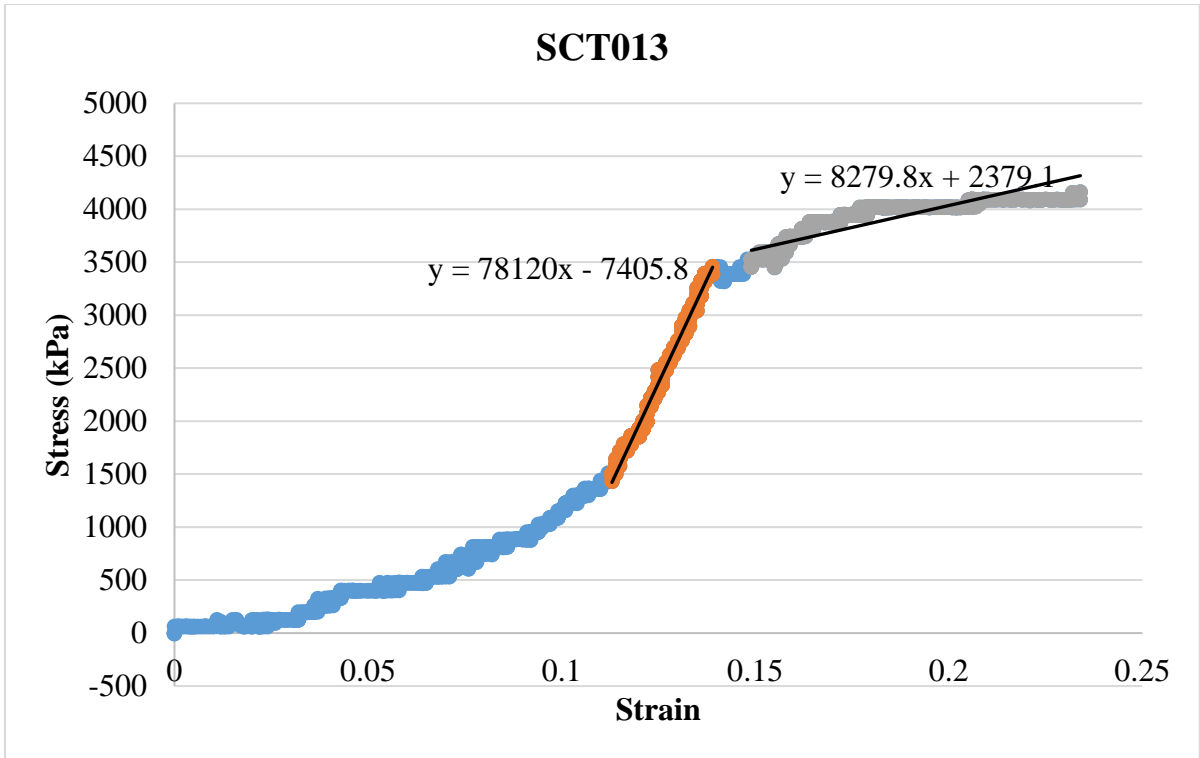


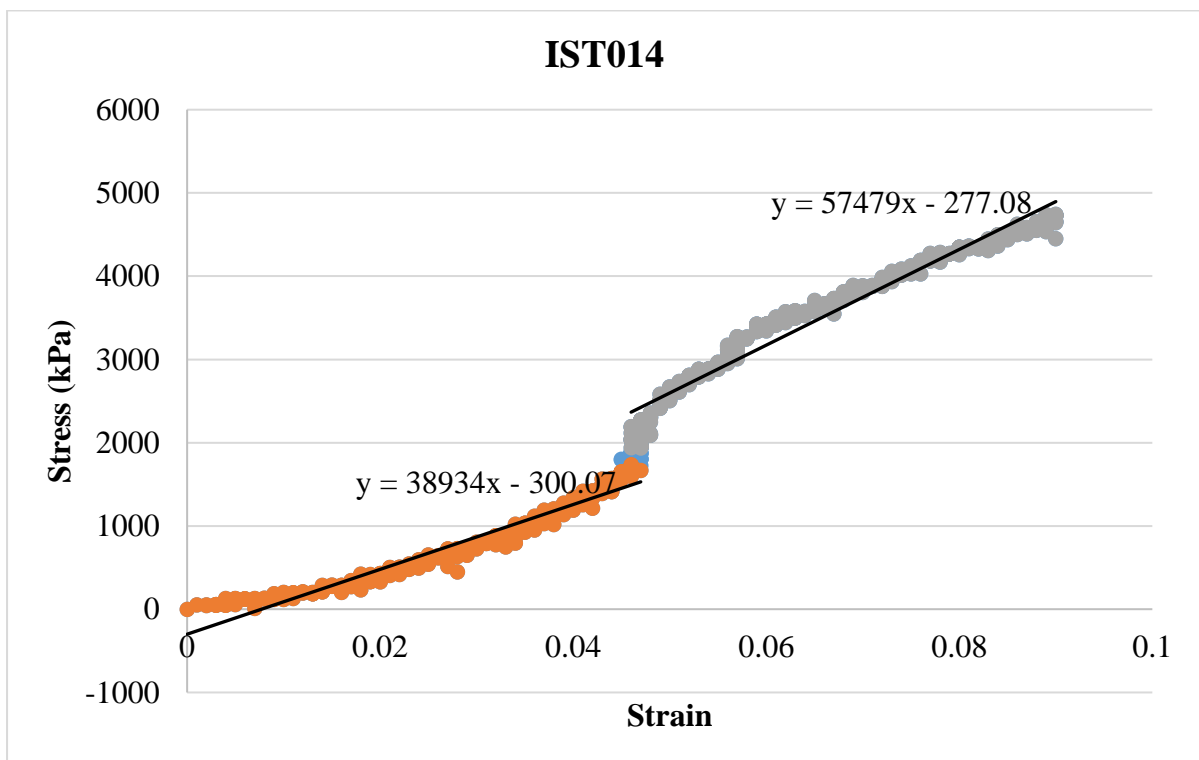
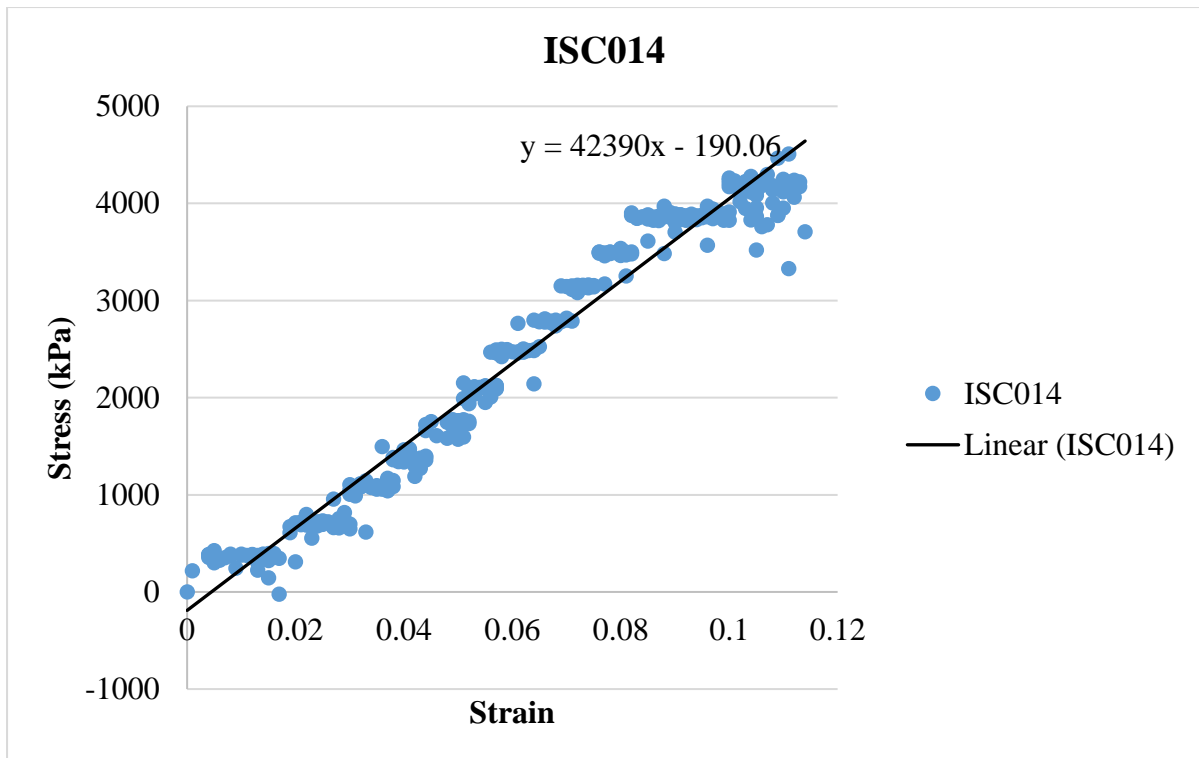


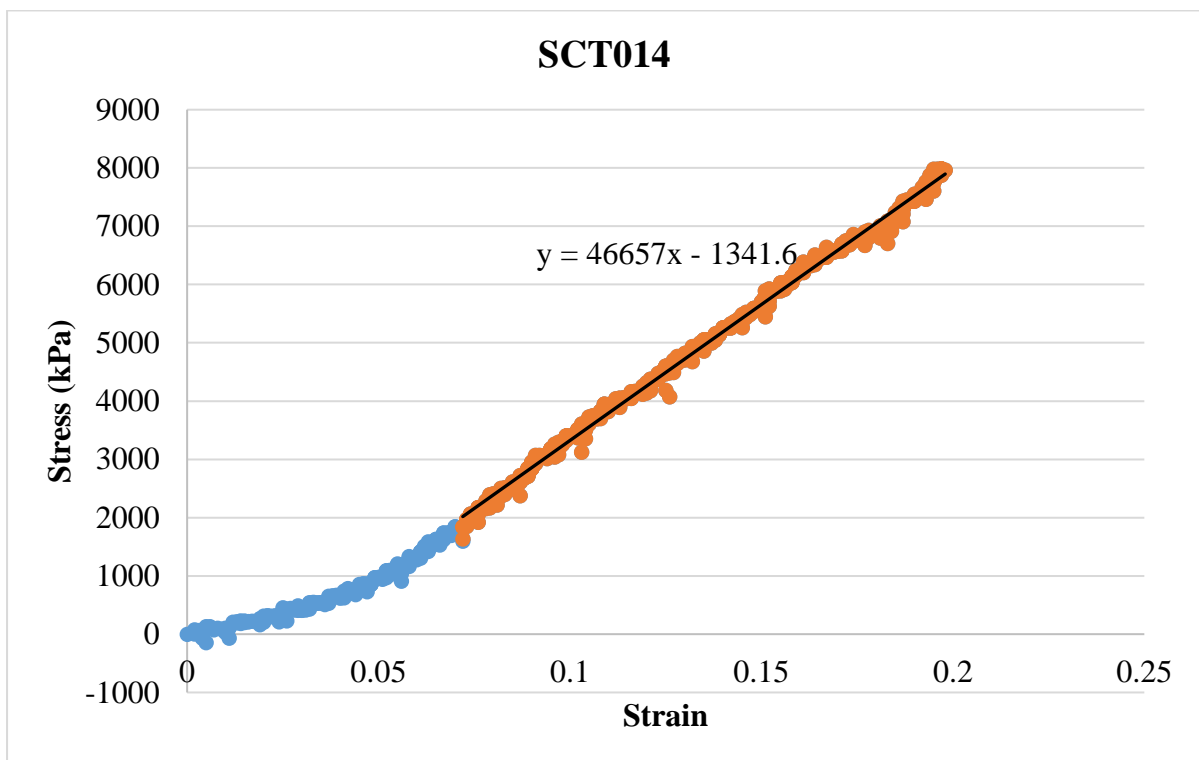
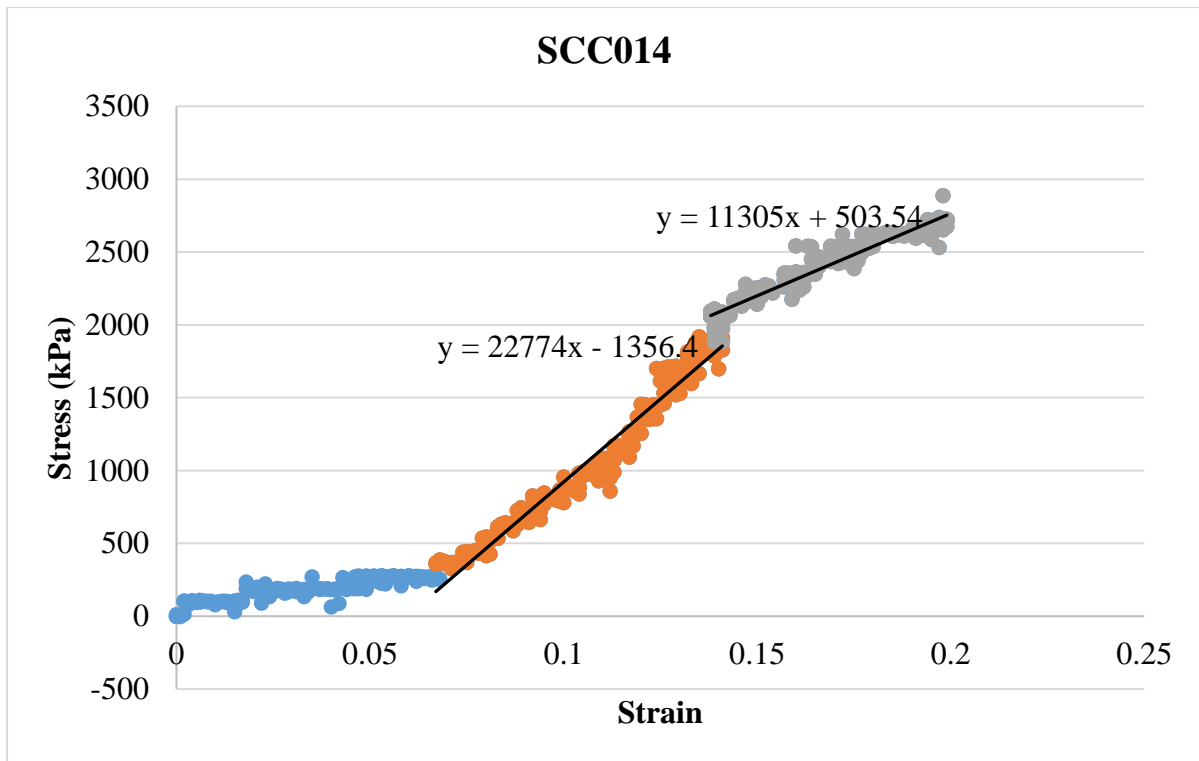




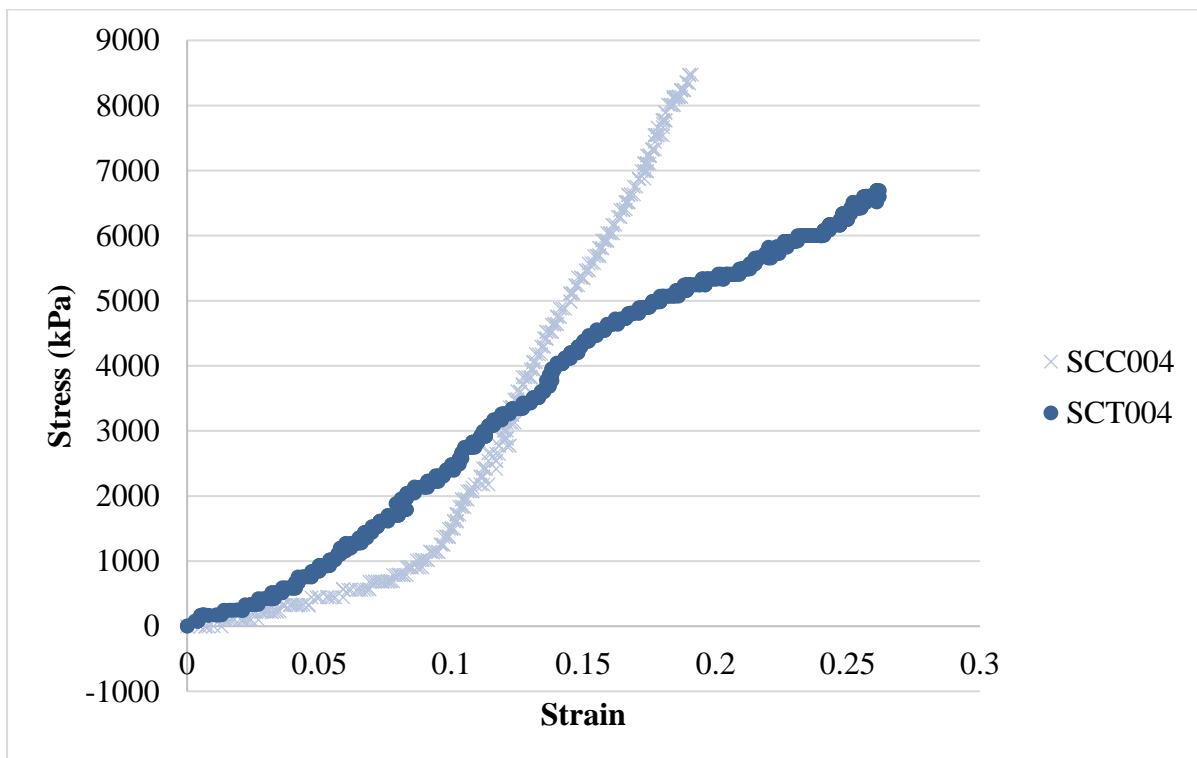
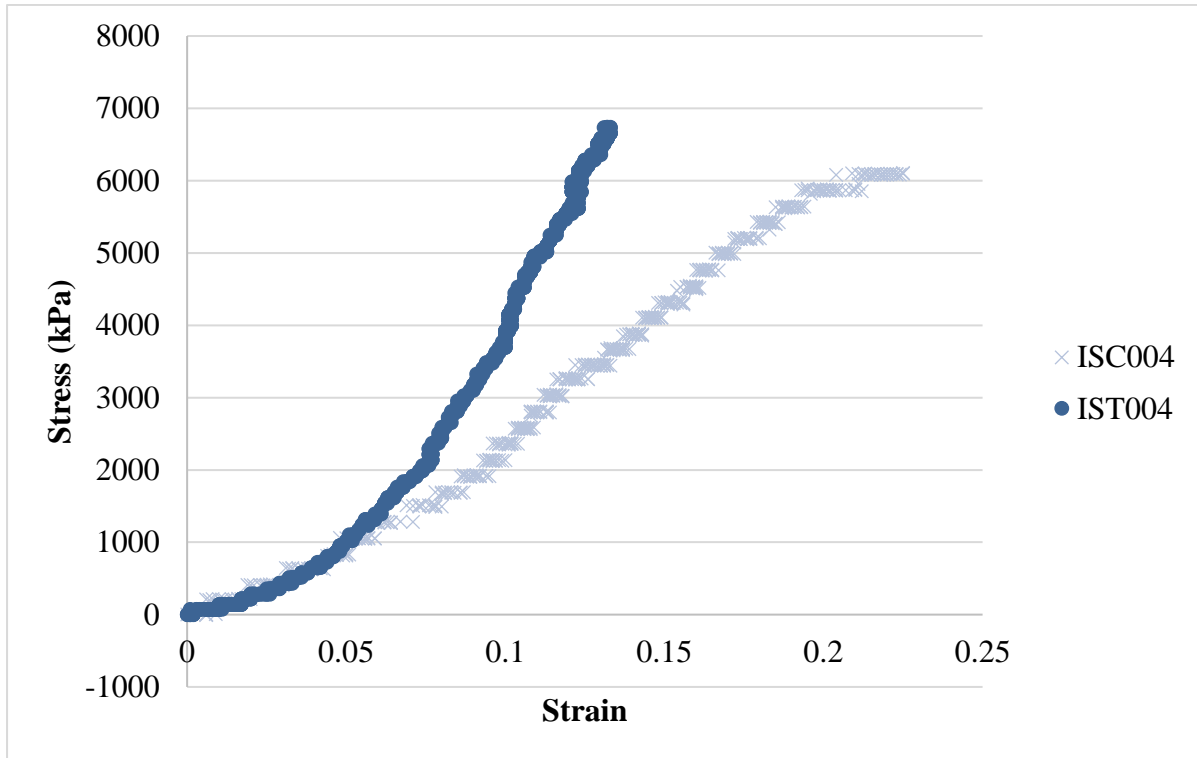


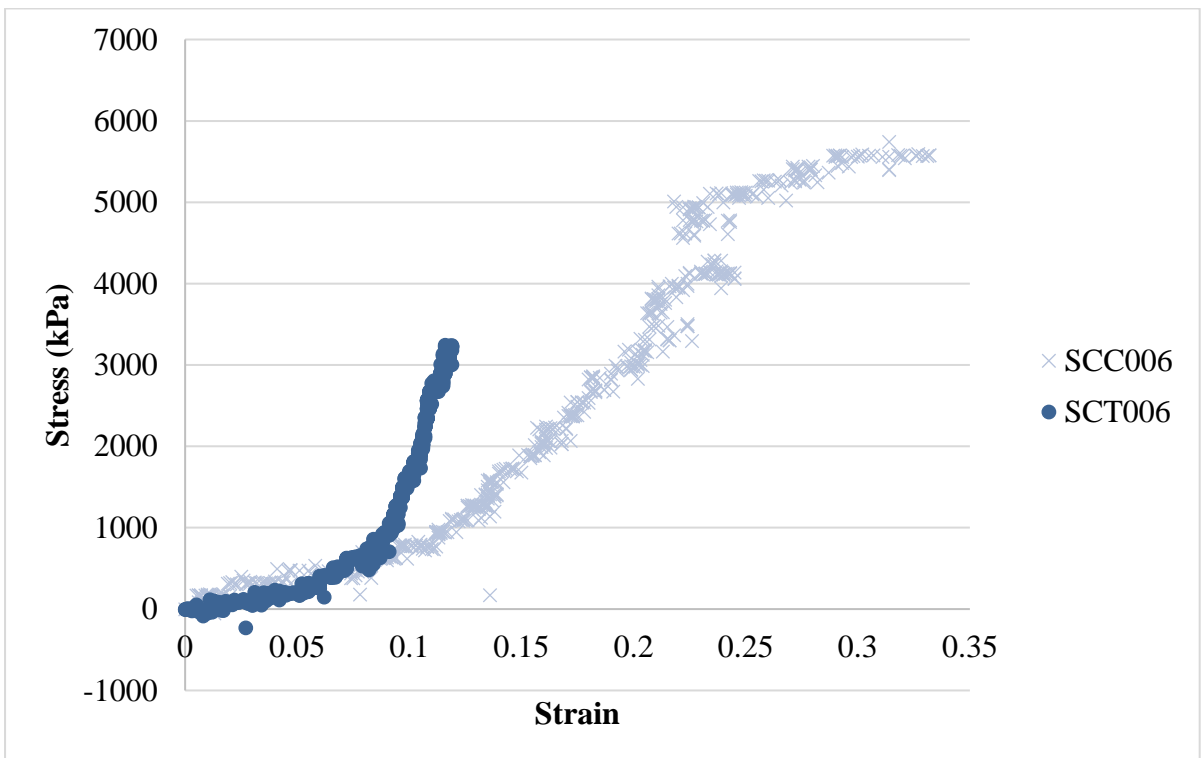
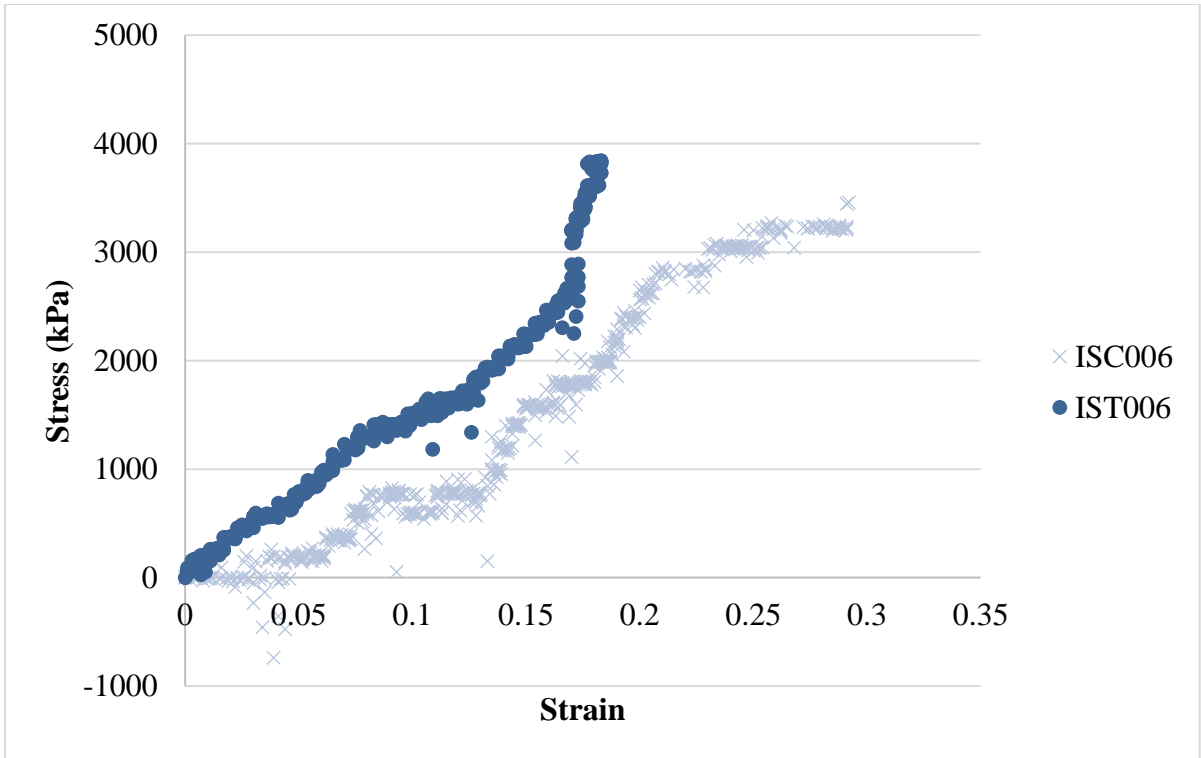


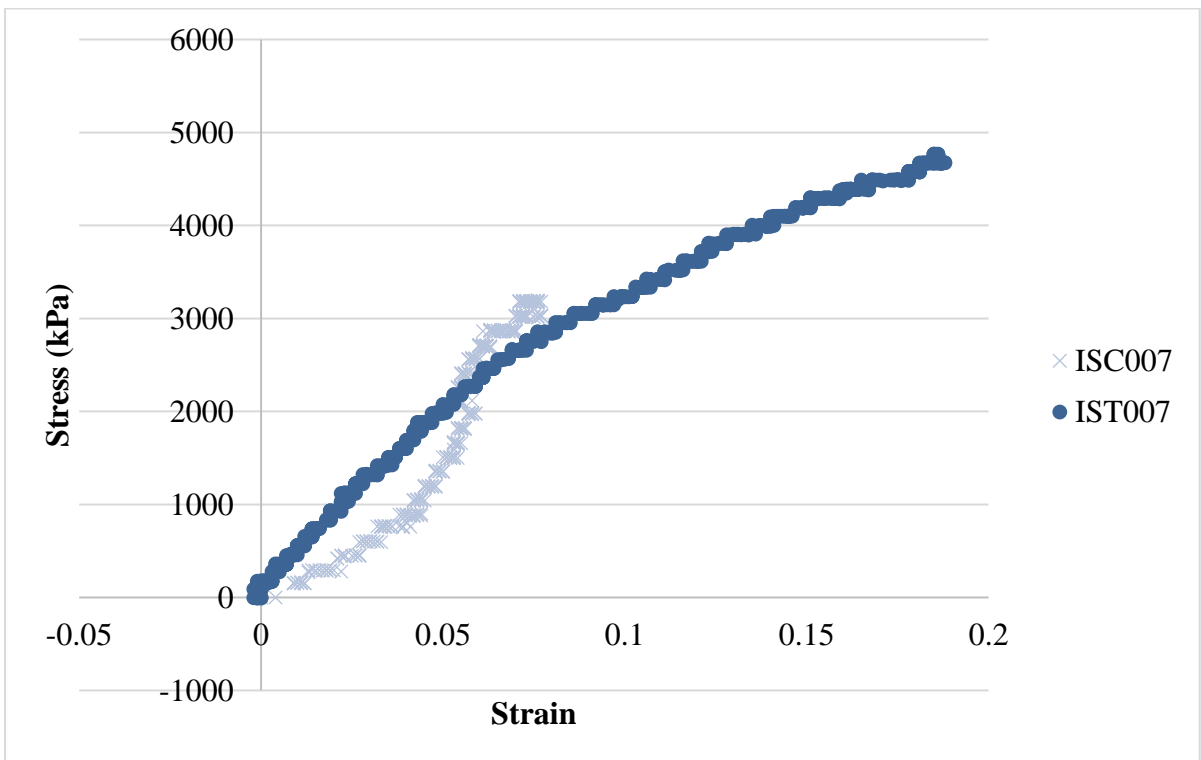
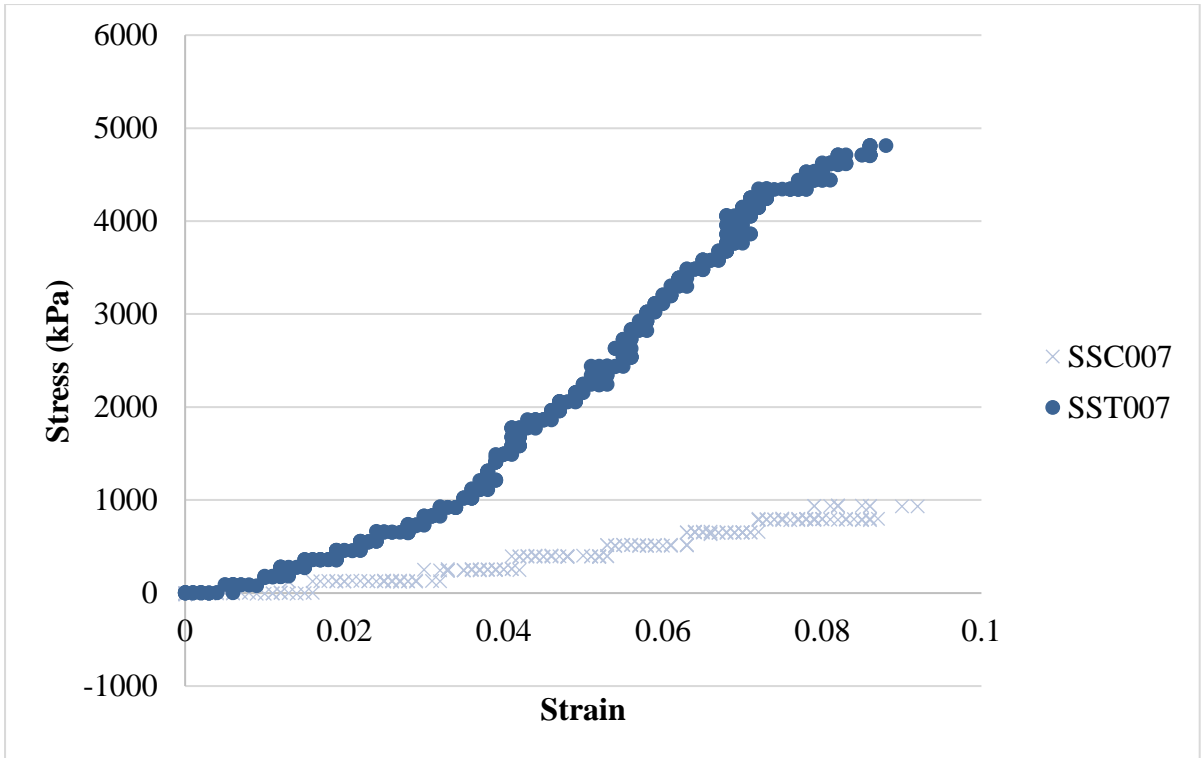


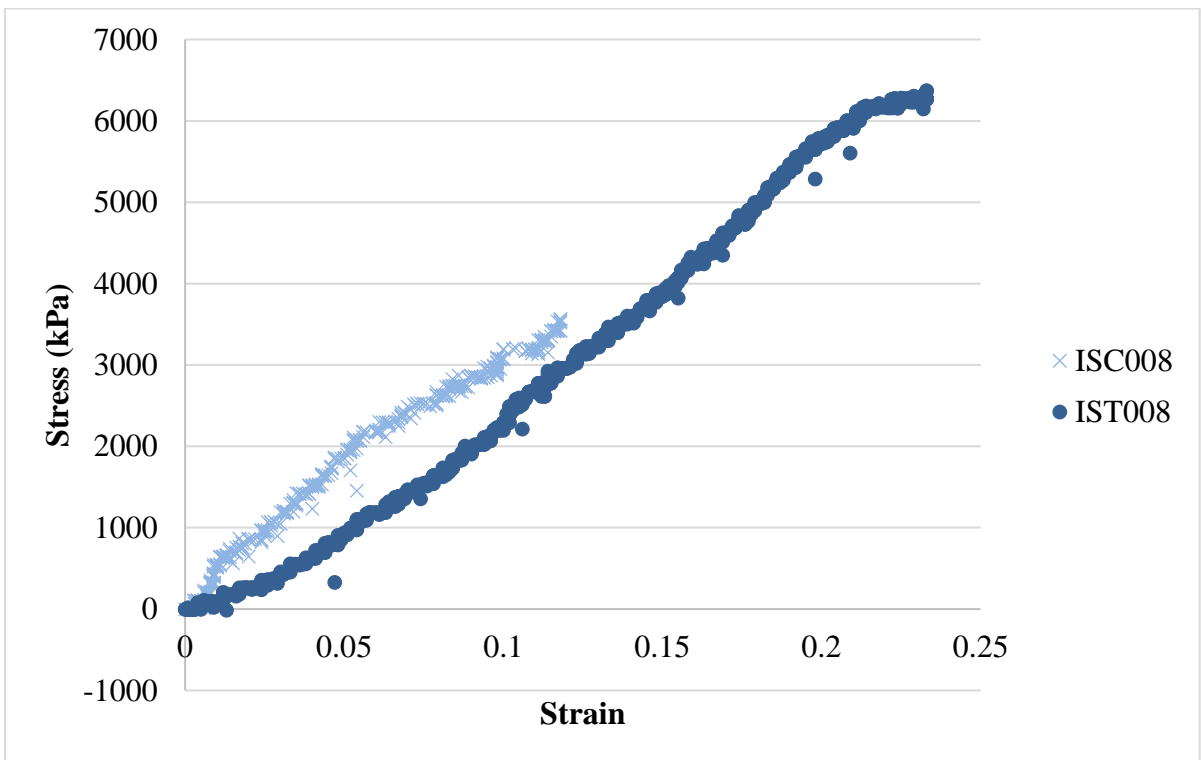
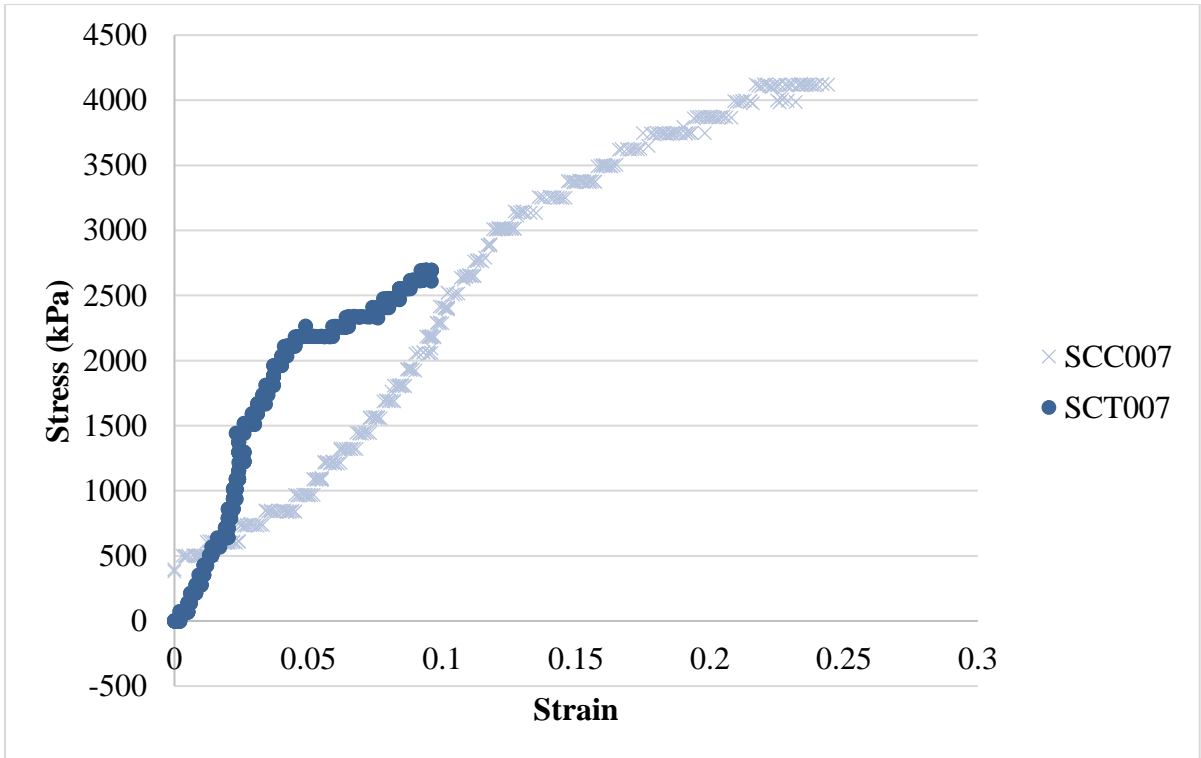


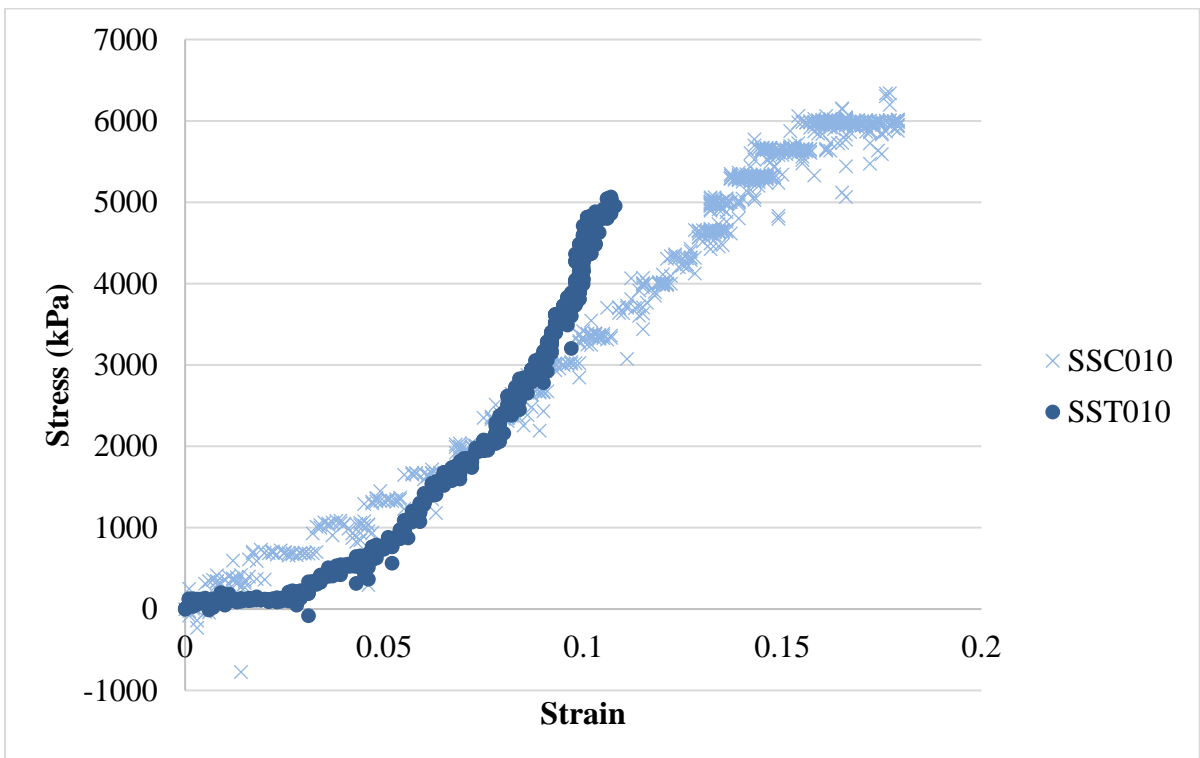
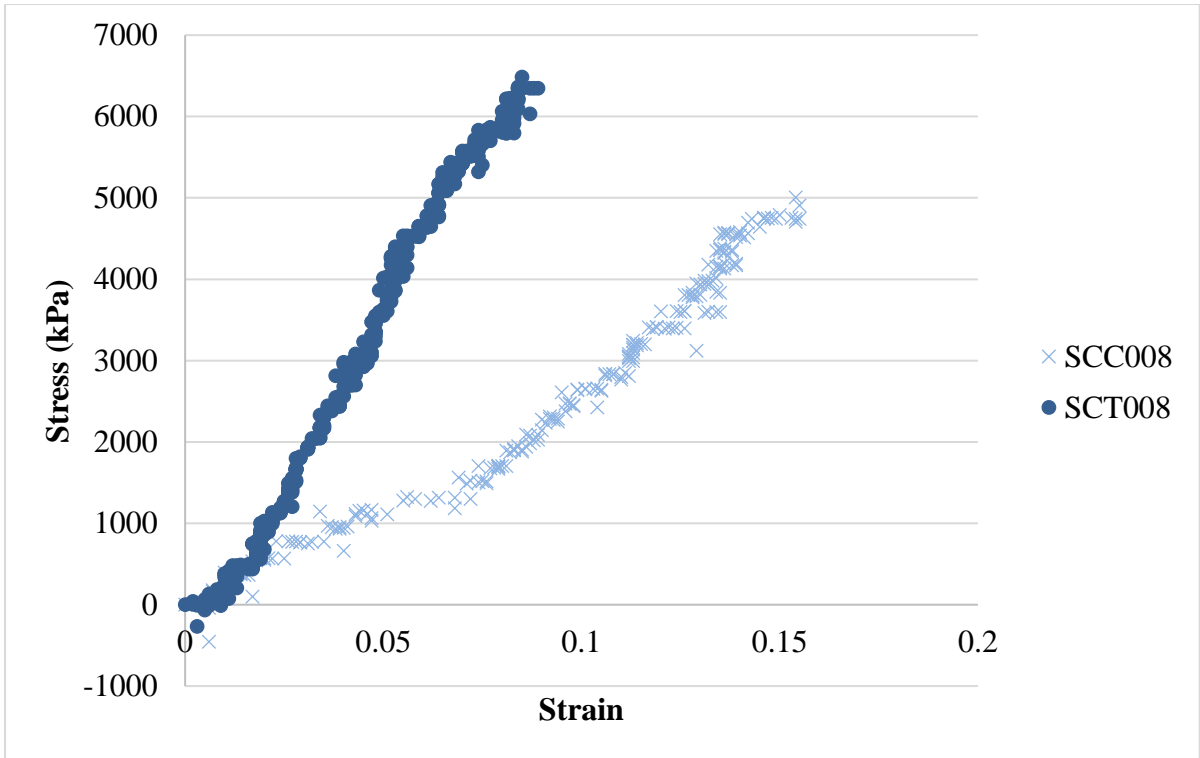
7.6. Annexure 6: Graphic representation for capsular and tendinous comparisons within a sample, in Chapter 4, Section 4.1.4.

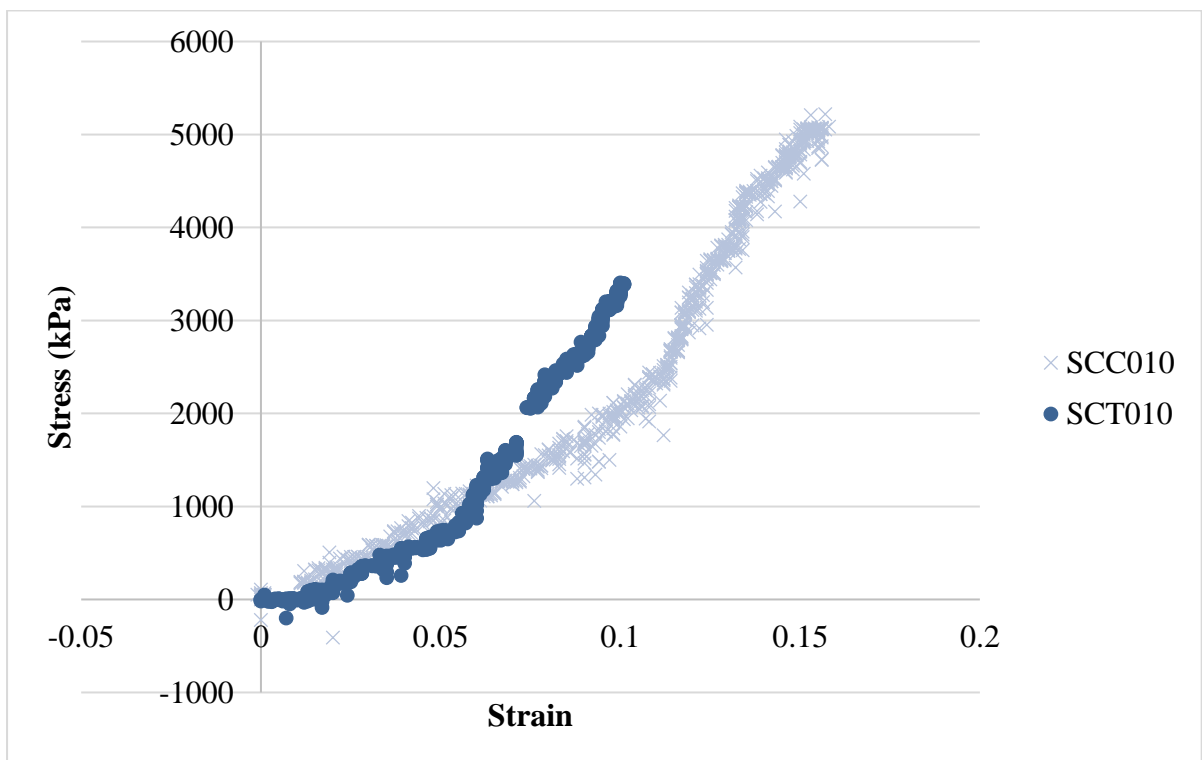
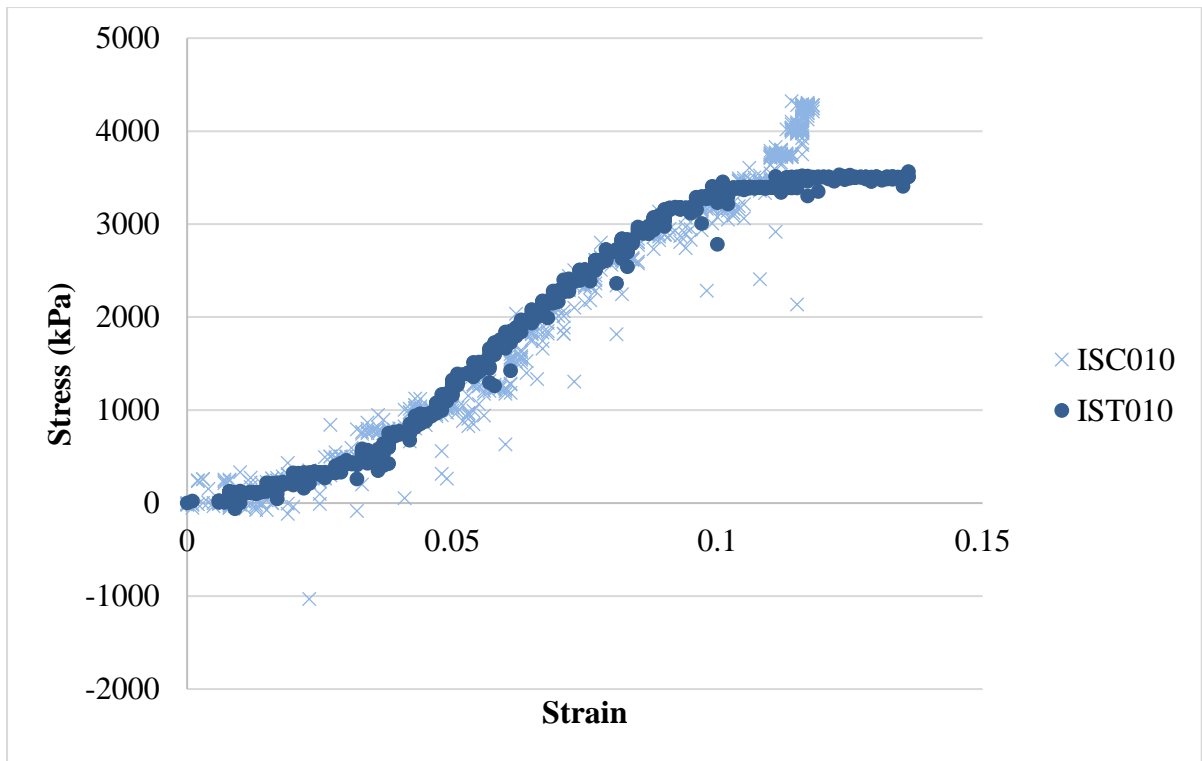


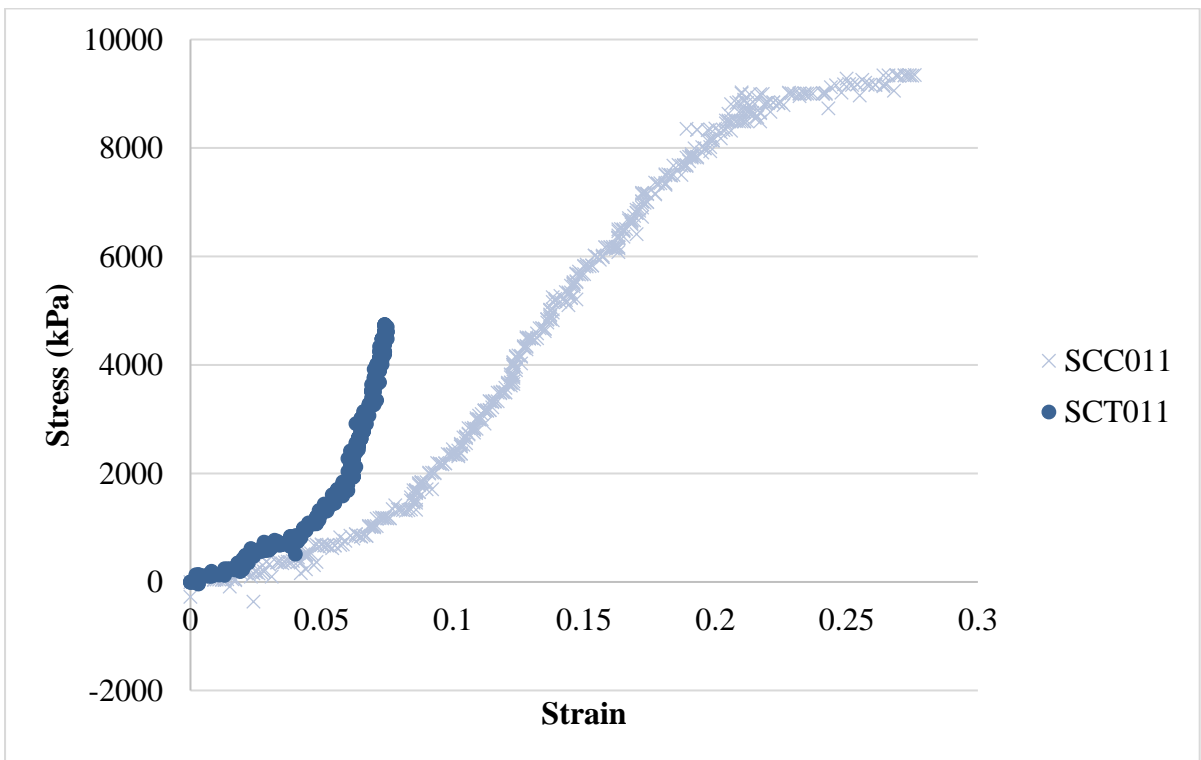
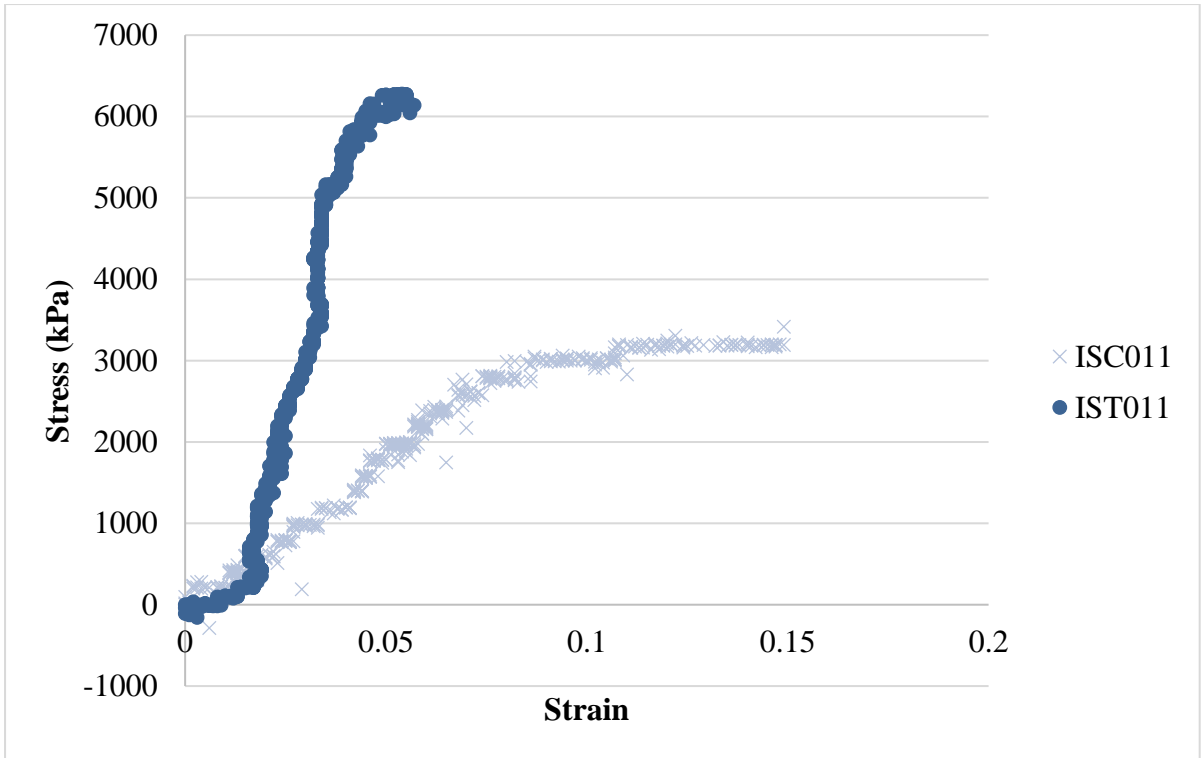


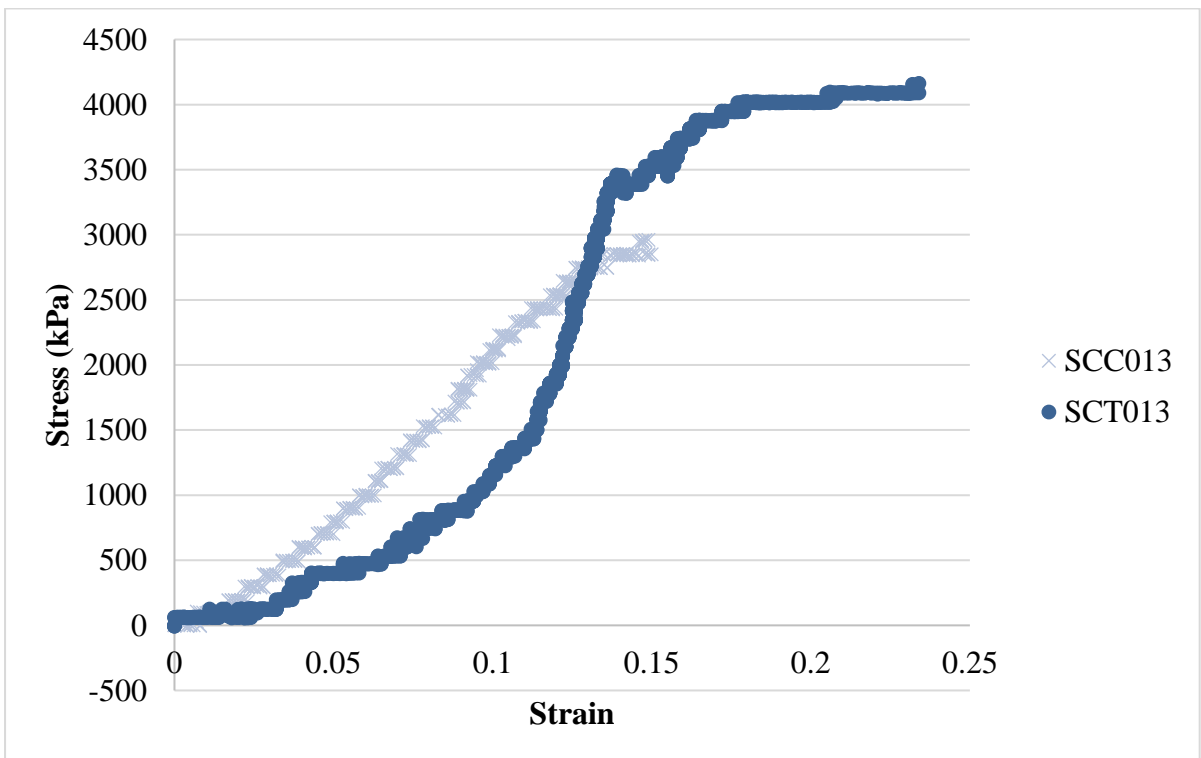
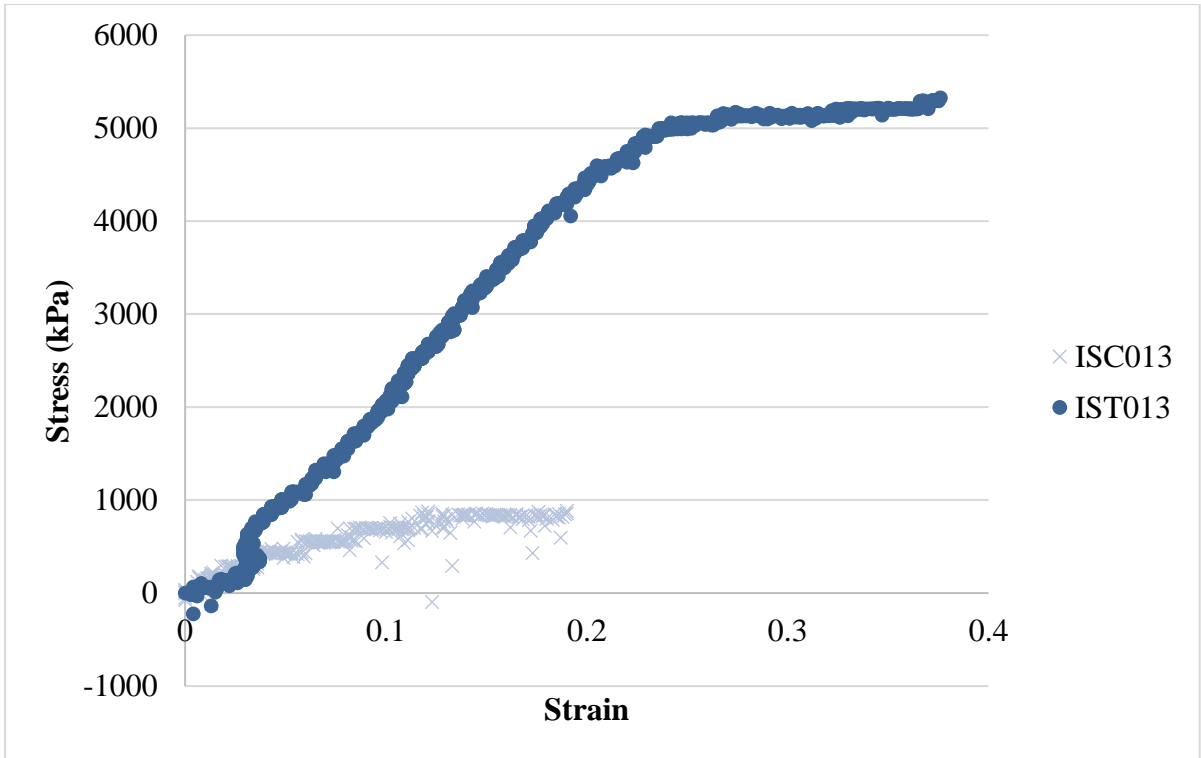


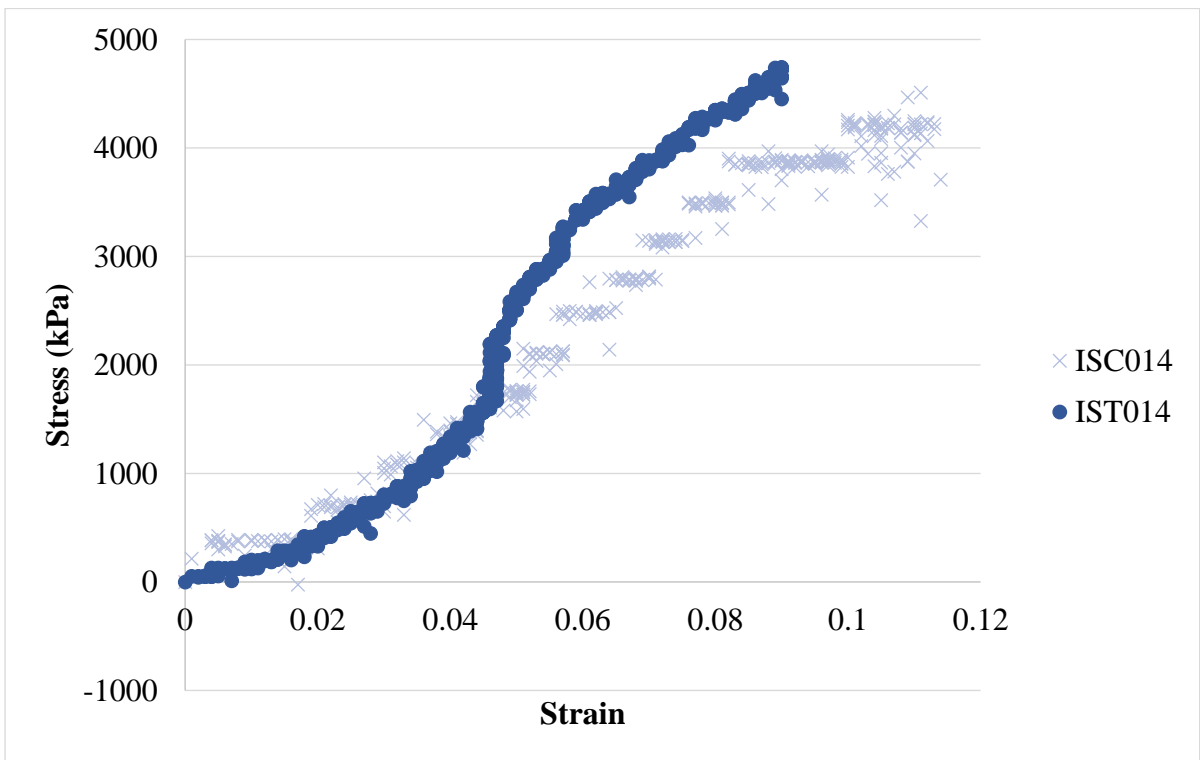
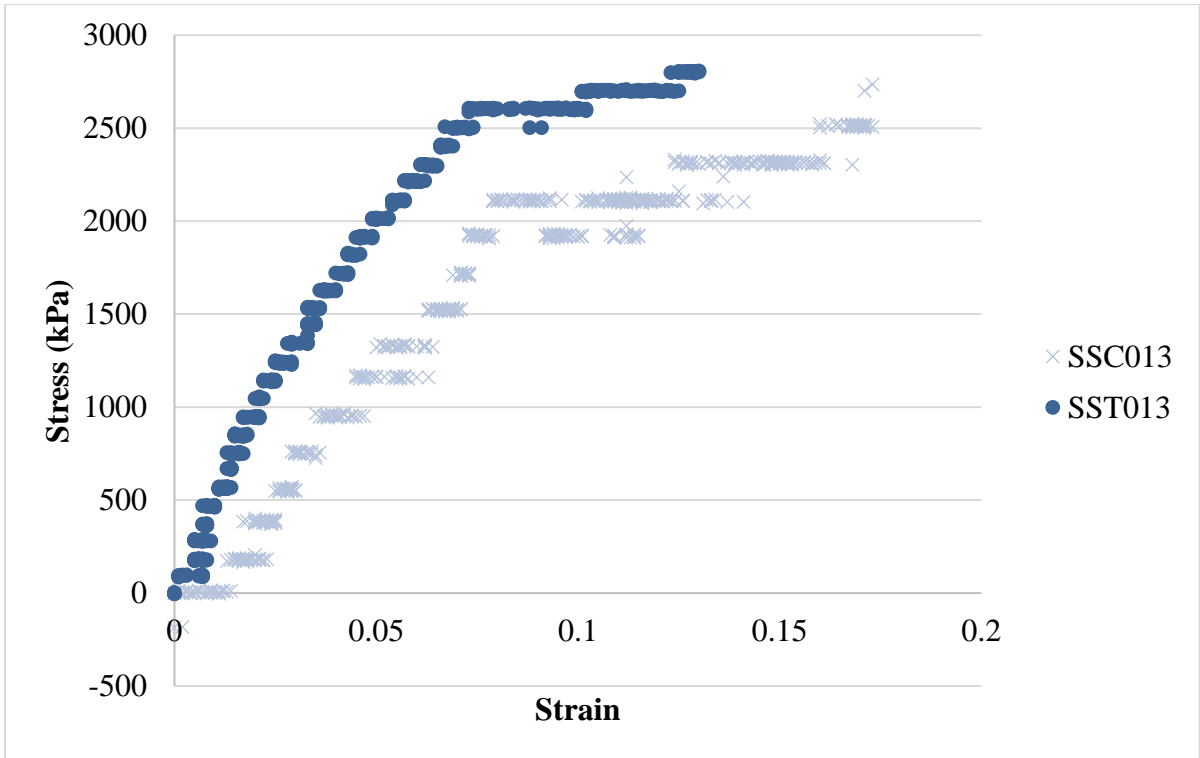


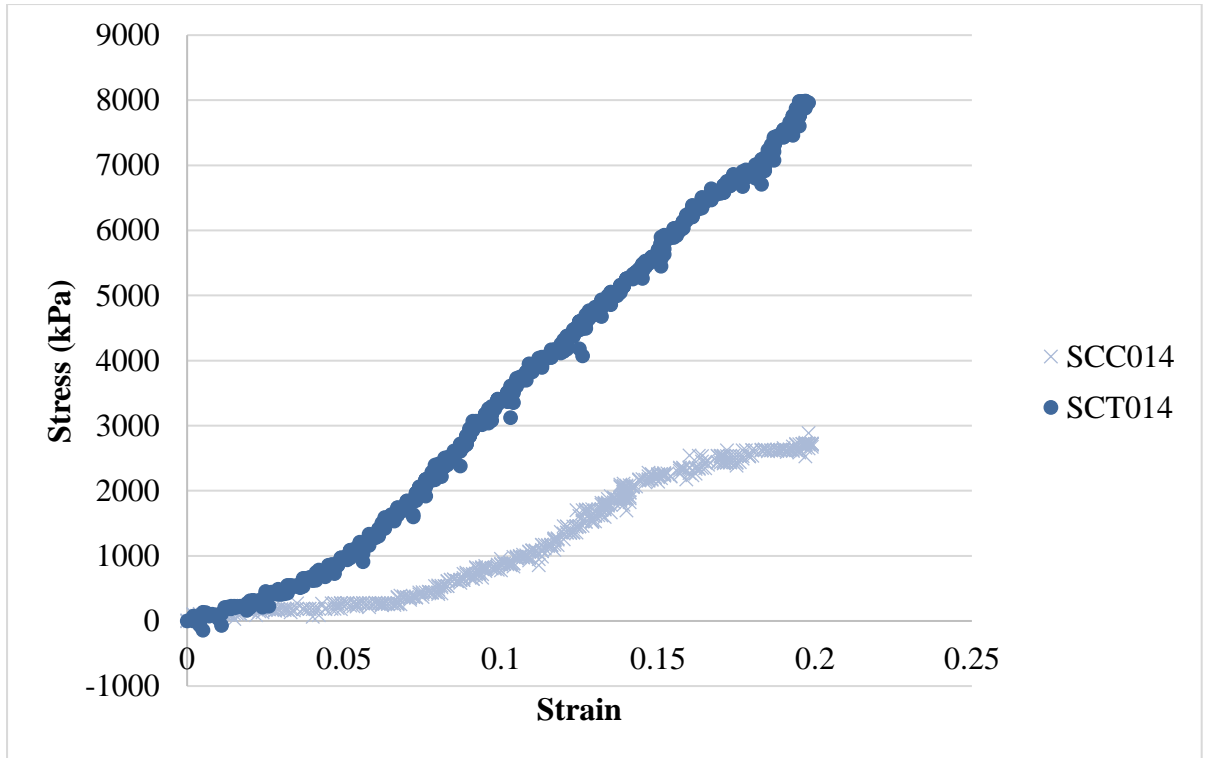












7.7. Annexure 7: Graphic representation for capsular comparisons and tendinous comparisons of single rotator cuff segments, in Chapter 4, Section 4.1.4

